



Democratic and Popular Republic of Algeria
Ministry of Higher Education and Scientific Research
University Mohamed Khider of Biskra



Faculty of Exact Sciences and Science of Nature and Life

Department of Matter Sciences

Ref :

Thesis Presented to obtain the degree of

Doctorate in LMD

Option: Chimie

Specialty: Chemistry of Materials

Entitled:

**Synthesis and characterization of composites:
thermoplastic/lignocellulosic fibers from the
Biskra region**

Presented by:

Nedjla Debabeche

Publicly defended on: 18/11/ 2023

In front of the Jury committee composed of :

Mahmoud Omari	Professor	University of Biskra	President
Oum keltoum Kribaa	Professor	University of Biskra	Supervisor
Omar Ben Mya	Professor	University of El Oued	Examiner
Asma Fettah	M.C.A	University of Biskra	Examiner
Hamida Boussehel	M.C.A	University of Biskra	Co.Supervisor

Acknowledgements

This work results from a collaboration between the Laboratory of Applied Chemistry (LCA), University of Biskra, and the Laboratory of Mechanical Engineering (LGM), University of Biskra.

First, I would like to express my thanks to my thesis director. *Dr. Kribaa Oum Keltoum*, Research Professor at Mohamed Khedr University in Biskra, for supporting me and trusting me during these years with great patience. With her experience in research and teaching and her advice. It is truly a pleasure to work under her supervision. I extend my sincere thanks to *Dr. Boussehel Hamida*, Research Professor at Mohamed Khedr University, Biskra, for her contribution, assistance, and encouragement she gave me during the thesis period.

We sincerely thank all the National Corporation of Cable Industries of Biskra (ENICAB) employees for their welcome and assistance, particularly in developing part of our pilot study and some of the composite properties produced in the company above.

We sincerely thank *Dr. Guerira Belhi*, Head of the Department of Mechanical Engineering at the Faculty of Science and Technology of the University of Biskra, for his presence and valuable assistance in characterizing our developed compounds.

I want to thank the jury members from the bottom of my heart:

- *Pr. Mahmoud Omari*, Professor at the University of Mohamed Khider Biskra finds here the expression of my most sincere thanks for agreeing to chair this thesis.
- *Pr. Omar Ben Mya*, Professor at the University of Eloued for the interest shown in our work and his participation in the jury as an examiner.
- *Dr. Asma Fettah*, Research professor at the University of Mohamed Khider Biskra, for the interest shown in our work and his participation in the jury as an examiner.

With all respect and love I dedicate this work to my dear parents, my family and all my friends

Nedjla Debabeche

Abstract

This study's main goal was to make an eco-friendly composite from palm petiole fibers that could be used as fillers in a linear low-density polyethylene (LLDPE) matrix with a loading of 15–25 wt% and to look into how the composites age naturally. To achieve this main objective, lignocellulosic fibers were prepared using successive treatments on the fiber surface (NaOH, hydrogen peroxide, and acetic anhydride). The NaOH pretreatment aimed to overcome the recalcitrance of lignocellulosic biomass. FTIR showed that pretreatment with NaOH helped the peroxide hydrogen treatment of NaOH-petiole fibers to break down biomass without separating it into different parts. This made it possible to get micrometric-sized lignocellulosic fibers.

These lignocellulosic fibers that have been extracted are hydrophilic, which means that the hydroxyl groups in the fibers interact with water molecules. The hydrophilic nature of these lignocellulosic fibers often results in poor compatibility with hydrophobic polymeric matrices. Surface modification is therefore necessary to make them more hydrophobic and compatible with the hydrophobic matrices. For this reason, we treated the lignocellulosic fibers with acetic anhydride, which is used to modify the surface of the fibers and make them more hydrophobic.

The scanning electron microscopy (SEM) results showed that the enhanced interfacial adhesion between the fibers and the matrix makes treated composites more rigid and more homogeneous, which means that the fibers are distributed more uniformly. The tensile modulus and flexural strength were all enhanced by adding 15-25% of untreated palm petiole fibers, while the tensile strength was decreased. Palm-petiole fiber composites' storage modulus increased, and the acetylated-alkali fiber (FNA) reinforced LLDPE composite showed the highest storage modulus. Loss modulus increased when palm petiole fibers were strengthened. The Tan delta of composites made from palm petiole fibers was low initially but expanded with fiber addition. After exposing the LLDPE/PPF composites to natural aging, we observed, by IRTF, the formation of several oxidation products, an increase in the crystallinity rate, and Young's modulus. Furthermore, the SEM images clearly show that the degradation is severe with aging. We concluded that successive treatments improve the performance of the palm petiole fiber and have the potential to create a new type of sustainable and eco-friendly material for various applications.

Keywords: Palm petiole fibers, Linear low-density polyethylene, Chemical treatment, Natural weathering Morphological, Mechanical, Dynamic mechanical.

المخلص

الهدف الرئيسي لهذه الدراسة هو صنع مركب صديق للبيئة من ألياف أعناق النخيل التي يمكن استخدامها كمواد حشو في مصفوفة البولي إيثيلين الخطي منخفض الكثافة (LLDPE) مع تحميل بنسبة 15-25% بالوزن والنظر في كيفية تقادم المواد المركبة مع مرور الوقت. بطبيعة الحال. ولتحقيق هذا الهدف الرئيسي، تم تحضير الألياف اللجنوسليلوزية باستخدام معالجات متتالية على سطح الألياف (هيدروكسيد الصوديوم، بيروكسيد الهيدروجين، وأنهيدريد الخل). تهدف المعالجة المسبقة لـ NaOH إلى التغلب على عناد الكتلة الحيوية اللجنوسليلوزية. أظهر FTIR أن المعالجة المسبقة باستخدام NaOH ساعدت في معالجة بيروكسيد الهيدروجين على تحطيم الكتلة الحيوية. هذا جعل من الممكن الحصول على ألياف لجنوسليلوزية ذات حجم ميكرومترى. هذه الألياف اللجنوسليلوزية التي تم استخلاصها محبة للماء، مما يعني أن مجموعات الهيدروكسيل الموجودة في الألياف تتفاعل مع جزيئات الماء. غالبًا ما تؤدي الطبيعة المحبة للماء لهذه الألياف اللجنوسليلوزية إلى ضعف التوافق مع المصفوفات البوليمرية الكارهة للماء. لذلك يعد تعديل السطح ضروريًا لجعلها أكثر كارهة للماء ومتوافقة مع المصفوفات الكارهة للماء. لهذا السبب، قمنا بمعالجة الألياف اللجنوسليلوزية بمادة أنهيدريد الخل، والتي تستخدم لتعديل سطح الألياف وجعلها أكثر كارهة للماء.

أظهرت نتائج المجهر الإلكتروني الماسح SEM أن الالتصاق البيني المعزز بين الألياف والمصفوفة يجعل المركبات المعالجة أكثر صلابة وأكثر تجانساً، مما يعني أن الألياف موزعة بشكل أكثر تجانساً. تم تحسين معامل الشد وقوة الإنثناء بإضافة 15-25% من ألياف أعناق النخيل غير المعالجة، بينما انخفضت قوة الشد. زاد معامل تخزين مركبات ألياف أعناق النخيل، وأظهر مركب LLDPE المقوى بالألياف الأسيتيل القلوي FNA أعلى معامل تخزين. يزداد معامل الفقد عندما يتم تقوية ألياف أعناق النخيل. كانت $\tan \delta$ للمواد المركبة المصنوعة من ألياف أعناق النخيل منخفضة في البداية ولكنها توسعت بإضافة الألياف. بعد تعريض مركبات LLDPE/PPF للشيوخة الطبيعية، لاحظنا، بواسطة IRTF، تكوين العديد من منتجات الأكسدة، وزيادة في معدل التبلور، ومعامل يونج. علاوة على ذلك، تظهر صور SEM بوضوح أن التدهور يكون شديداً مع تقدم السن. في الخلاصة توصلنا إلى أن المعالجات المتعاقبة تعمل على تحسين أداء ألياف أعناق النخيل ولديها القدرة على إنشاء نوع جديد من المواد المستدامة والصديقة للبيئة لمختلف التطبيقات.

الكلمات المفتاحية: ألياف أعناق النخيل، البولي إيثيلين الخطي منخفض الكثافة، المعالجة الكيميائية، التجوية الطبيعية، المورفولوجية، الميكانيكية، الميكانيكية الديناميكية.

Table of contents

List of figures	I
List of table	VII

General Introduction

General Introduction	1
Reference	4

Part I: General Review of the Literature

Chapter I : Fibrous Materials

I.1. Generality of lignocellulosic fibers	7
I.2. Morphology of natural cellulosic fibers	7
I.3. Lignocellulosic composition	8
I.4. Date palm	10
I.5. Properties and uses of natural fibers	12
I.6. Lignocellulose modification	13
a. Mechanical treatment	13
b. Chemical treatment	13
c. Chemical functionalization	16
d. Pretreatment combination	17
Reference	19

Chapter II : Composite Materials

II.1. Generality of composite materials 23

II.2. Bio-composite materials 24

II.3. Polyethylenes (PE) 25

II.4. Cellulose fiber-reinforced composite materials 26

II.5. Properties of cellulose fiber-reinforced composites 27

a. Fiber aspect ratio 27

b. Fiber volume fraction 27

c. Fiber orientation 27

d. Fiber dispersion 28

e. Fiber/matrix interface adhesion 28

f. Fibers type 28

II.6. Processes for composite materials 29

a. Extrusion and injection molding 29

b. Compression molding 30

Reference 31

Chapter III : Degradation Of Biocomposite

III.1. Degradation of biocomposites 34

III.2. Natural weathering 34

III.2.1. Visual Changes Due to Natural Weathering 36

III.2.2. Process of water absorption by composites 37

III.2.3. Effect of Natural Weathering on Composite Structure 38

III.2.4. Effect of Natural Weathering on Thermal Properties 38

III.2.5. Effect of Natural Weathering on Mechanical Properties 39

Reference 40

Part II: Experimental Study

Chapter I : Materials and Methods

I.1. Materials 45

I.1.1. Vegetable fibers 45

I.1.2. Resin Linear low-density polyethylene 45

I.2. Methods 46

I.2.1. Preparation of petiole fiber 46

I.2.2. Chemical modification of palm petiole fibers 46

a. 1st Treatment: Alkaline 46

b. 2nd Treatment: Hydrogen peroxide 47

c. 3rd Treatment: Acetylation 48

I.2.3. Mechanical modification of petiole fiber 49

I.2.4. Elaboration of composites 49

a. Extrusion of Linear low-density polyethylene/Petiole fibers 49

b. Compression molding 51

I.2.5. Natural weathering test 52

Reference 53

Chapter II : Techniques of Characterization

II.1. Fourier Transform Infrared Spectrometry (FTIR) 55

II.2. Scanning electron microscopy (SEM)	56
II.3. Differential Scanning Calorimetry (DSC)/Thermogravimetric analysis (TGA)	56
II.4. Dynamic mechanical analysis (DMA)	57
II.5. Tensile test	58
II.6. Three-point bending	60
II.7. Hardness	61
Reference	63

Part III: Results and discussion

Chapter I : Characterization of the Palm Petiole Fibers

I.1. FTIR Spectroscopy	66
I.2. Morphological characterization (SEM)	68
I.3. Thermal analysis	70
I.3.1. Thermogravimetric analysis (ATG/DTG)	70
I.3.2. DSC analysis	73
Reference	75

Chapter II : Characterization of the Composites Elaborates

II.1. Morphological characterization (SEM)	78
a. Load Effect	78
b. Treatment effect	79
II.2. Thermogravimetric analysis (ATG/DTG)	82

Table of contents

a. Load Effect	82
b. Treatment effect	84
II.3. Mechanical Properties	88
II.3.1. Tensile testing	88
II.3.1.1. Tensile strength	88
a. Load Effect	88
b. Treatment effect	89
II.3.1.2. Young's modulus	90
a. Load Effect	90
b. Treatment effect	91
II.3.2. Flexural testing	93
II.3.2.1. Flexural strength	93
a. Load Effect	93
b. Treatment effect	93
II.3.2.2. Flexural modulus	95
a. Load Effect	95
b. Treatment effect	96
II.4. Dynamic mechanical analysis (DMA)	97
II.4.1. Storage modulus (E')	97
a. Load Effect	97
b. Treatment effect	98
II.4.2. Loss modulus (E'')	99
a. Load Effect	99
b. Treatment effect.....	100
II.4.3. Tan Delta.....	101
a. Load Effect	101
b. Treatment effect.....	102

II.5. Hardness..... 104

a. Load Effect 104

b. Treatment effect..... 105

Reference..... 107

Chapter III : Characterization of Composite After Natural Weathering

III.1. Effect of natural weathering on the visual appearance (color)..... 114

III.2. Effect of natural weathering on weight loss 115

III.3. Effect of natural weathering on the morphological structure (SEM) 116

III.4. FTIR Spectroscopy 119

III.5. Effect of natural weathering on the mechanical Properties..... 125

III.5.1. Tensile testing..... 125

III.5.1.1. Tensile strength..... 125

III.5.1.2. Young’s modulus..... 126

Reference..... 127

General Conclusion

General Conclusion 131

Appendices

List of figures

Part I: General Review of the Literature

Chapter I : Fibrous Materials

Figure I.1: Morphology of Natural Cellulosic Fibers	8
Figure I.2 : Lignocellulosic composition	10
Figure I.3 : Date Palm.....	11

Chapter II : Composite Materials

Figure II.1 :Representation of the macromolecular of polyethylene chain.....	25
--	----

Chapter III : Degradation Of Biocomposite

Figure III.1 : Diagram of natural weathering conditions	35
Figure III.2: Wavelength of irradiation waves and UV aging of polymer biocomposites	36
Figure III.3 : Moisture absorption effect on the fiber-matrix interface	37
Figure III.4 : Schematic diagram illustrating the controlling factors contributing to the natural weathering of Biocomposites	38

Part II: Experimental Study

Chapter I : Materials and Methods

Figure I.1 : Palm petiole fibers (PPF)	45
--	----

Figure I.2 : Resin Linear low-density polyethylene (LLDPE)..... 45

Figure I.3 : Preparation of petiole fiber 46

Figure I.4 : Schematic diagram illustrating the chemical modification of palm petiole fibers 46

Figure I.5 : Schematic diagram illustrating the first treatment of petiole fibers with a 10% alkaline solution 47

Figure I.6 : Schematic diagram illustrating the secondary treatment of petiole fibers with a 2.5% hydrogen peroxide solution 47

Figure I.7 : A schematic diagram illustrates the treatment of NaOH-petiole fibers modified with a 10% acetic anhydride solution..... 48

Figure I.8 : A schematic diagram illustrates the treatment of (NaOH/H₂O₂)-petiole fibers modified with a 10% acetic anhydride solution..... 48

Figure I.9 : Mechanical modification of petiole fiber 49

Figure I.10 : Mono-screw extruder machine (Model Polylab QC) 51

Figure I.11 : Hydraulic press schwabenthan polystat (Model 300S) 51

Figure I.12 : Experimental set-up for neat LLDPE, treated and untreated composites on natural weathering test 52

Chapter II : Techniques of Characterization

Figure II.1 : Principle of PerkinElmer Spectrum Two with an ATR-FTIR unit 55

Figure II.2 : Principle of Thermo Scientific Quanta SEM Prisma E electron microscope 56

Figure II.3 : Principle of Thermogravimetric SETARAM Instrumentation LABSYS evo 57

Figure II.4 : Principle of TA instrument DMA Q800 three-point bending machine 58

Figure II.5 : Instron Universal Testing Machine, Instron 5969 59

Figure II.6 : Tensile testing specimens type 1A 60

Figure II.7 : Principe of Flexural three-point according to ISO 178 using Instron Universal Testing
Machine, Instron 5969 61

Figure II.8 : Principe of the Zwick-Roell Durometer 62

Part III: Results and discussion

Chapter I : Characterization of the Palm Petiole Fibers

Figure I.1: FTIR spectra of raw and chemically treated fibers 68

Figure I.2: SEM micrographs of untreated petiole fiber (FU) 69

Figure I.3: SEM micrographs of treated petiole fiber (a) FN and (b) FNH 69

Figure I.4 : SEM micrographs of treated petiole fiber (a) FNA and (b) FNHA 70

Figure I.5: TGA curves of treated and untreated palm petiole fiber 71

Figure I.6 : DTG curves of treated and untreated palm petiole fiber 73

Figure I.7 : DSC curves of treated and untreated palm petiole fiber 73

Chapter II : Characterization of the Composites Elaborates

Figure II.1 : SEM micrographs of (a) LLDPE, untreated composite, (b) LLDPE/FU 15%, and (c)
LLDPE/FU 25% 78

Figure II.2 : SEM micrographs of treated and untreated composite (a-b) LLDPE/FU 15-25%, (c-d)
LLDPE/FN 15-25%, (e-f) LLDPE/FNH 15-25%, (g-h) LLDPE/FNA 15-25%, (j-k)
LLDPE/FNHA 15-25% 82

Figure II.3 : TGA curves of neat LLDPE and untreated composite LLDPE/FU 15-25% 83

Figure II.4 : DTG curves of neat LLDPE and untreated composite LLDPE/FU 15-25% 84

Figure II.5 : ATG curves of treated and untreated composite 15% 85

Figure II.6 : ATG curves of treated and untreated composite 25% 85

Figure II.7 : DTG curves of treated and untreated composite 15% 86

Figure II.8 : DTG curves of treated and untreated composite 25% 86

Figure II.9 : Tensile strength of neat LLDPE and untreated composites 15-25% 88

Figure II.10 : Tensile strength of neat LLDPE, treated and untreated composites 15%..... 89

Figure II.11 : Tensile strength of neat LLDPE, treated and untreated composites 25%..... 89

Figure II.12 : Young's modulus of neat LLDPE and untreated composites 15-25% 91

Figure II.13 : Young's modulus of neat LLDPE, treated and untreated composites 15% 92

Figure II.14 : Young's modulus of neat LLDPE, treated and untreated composites 25% 92

Figure II.15 : Flexural strength of neat LLDPE and untreated composites 15-25%..... 93

Figure II.16 : Flexural strength of neat LLDPE, treated and untreated composites 15% 94

Figure II.17 : Flexural strength of neat LLDPE, treated and untreated composites 25% 94

Figure II.18 : Flexural modulus of neat LLDPE and untreated composites 15-25% 95

Figure II.19 : Flexural modulus of neat LLDPE, treated and untreated composites 15% 96

Figure II.20 : Flexural modulus of neat LLDPE, treated and untreated composites 25% 97

Figure II.21 : Storage modulus of neat LLDPE and untreated composites 15-25% 97

Figure II.22 : Storage modulus of neat LLDPE, treated and untreated composites 15% 98

Figure II.23 : Storage modulus of neat LLDPE, treated and untreated composites 25% 99

Figure II.24 : Loss modulus of neat LLDPE and untreated composites 15-25% 99

Figure II.25 : Loss modulus of neat LLDPE, treated and untreated composites 15% 100

Figure II.26 : Loss modulus of neat LLDPE, treated and untreated composites 25% 101

Figure II.27 : Tan Delta of neat LLDPE and untreated composites 15-25% 102

Figure II.28 : Tan Delta of neat LLDPE, treated and untreated composites 15% 103

Figure II.29 : Tan Delta of neat LLDPE, treated and untreated composites 25% 103

Figure II.30 : Hardness shore A of neat LLDPE and untreated composites 15-25% 104

Figure II.31 : Hardness Shors A of neat LLDPE, treated and untreated composites 15% 106

Figure II.32 : Hardness Shors A of neat LLDPE, treated and untreated composites 25% 106

Chapter III : Characterization of Composite After Natural Weathering

Figure III.1 : Color change evolution of neat LLDPE, treated and untreated composite after 1 year
of natural weathering..... 115

Figure III.2 : Weight loss of neat LLDPE, treated and untreated composite after 6 and 12 months
of natural weathering..... 116

Figure III.3 : SEM micrographs of neat LLDPE, treated and untreated composite (a) LLDPEw, (b)
LLDPE/FUw, (c) LLDPE/FNw, (d) LLDPE/FNHw, (e) LLDPE/FNAw and (f)
LLDPE/FNHAw 118

Figure III.4 : FTIR spectra of neat LLDPE, treated and untreated composite before natural weathering
..... 119

Figure III.5 : FTIR spectra of neat LLDPE, treated and untreated composite after natural weathering
..... 120

Figure III.6 : FTIR spectra of neat LLDPE, treated and untreated composite (a) before natural
weathering and (b) after natural weathering in the 3600-3100 cm⁻¹ region 121

Figure III.7 : FTIR spectra of neat LLDPE, treated and untreated composite (a) before natural weathering and (b) after natural weathering in the 1800-1500 cm^{-1} region **123**

Figure III.8 : FTIR spectra of neat LLDPE, treated and untreated composite (a) before natural weathering and (b) after natural weathering in the 1400-900 cm^{-1} region **124**

Figure III.9: Tensile strength of neat LLDPE and untreated composites before and after natural weathering **125**

Figure III.10 : Young's modulus of neat LLDPE and untreated composites before and after natural weathering **126**

List of table

Part I: General Review of the Literature

Chapter I : Fibrous Materials

Table I.1 : Effects of different pretreatment processes on the compositions and structures of lignocellulosic materials.....	17
---	-----------

Chapter II : Composite Materials

Table II.2 : Principal properties of polyethylenes	25
Table II.3 : Physico-mechanical properties of several natural fibers.....	29

Part II: Experimental Study

Chapter I : Materials and Methods

Table I.4 : Composition of the different formulations	50
Table I.5 : The weather condition data from May 2021 to April 2022 in Biskra, Algeria.....	52

Chapter II : Techniques of Characterization

Table II.6 : Specimen dimensions according to ISO 527-2	60
--	-----------

Chapter I : Characterization of the Palm Petiole Fibers

Table I.7 : Thermal behavior of treated and untreated palm petiole fiber 72

Chapter II : Characterization of the Composites Elaborates

Table II.8 : Thermal parameters of neat LLDPE, treated and untreated composites (15-25%)..... 87

General Introduction

General Introduction

Polymers, or plastics, have existed since the 20th century due to their remarkable properties and a growing demand for this class of materials. These polymers are mainly derived from fossil resources, are non-renewable, poorly non-biodegradable (extremely slow biodegradation kinetics), and hurt the environment [1].

Furthermore, national and international regulatory pressures aimed at reducing the harmful environmental impact of these plastics require substitution solutions for these polymers from petrochemicals. In addition to the gradual disappearance or scarcity, with the increase in the price of petrol in recent years, the market for polymers derived from natural resources, mainly agro-resources, has experienced strong development [2]. The availability, production cost, and price of these agro-resources have made it possible to increase the competitiveness of these biopolymers compared to polymers derived from fossil resources. However, the performance of these biopolymers often needs to be higher than that of heteropolymers [3].

These polymers reinforced via the incorporation of fibers, to development composite materials with polymer matrices, prove to be the future solution. Using natural fibers (palm fibers, hemp, bamboo, and lin) and mainly bio-sourced nano-reinforcements (from these natural fibers) would make it possible to preserve the biodegradable nature of the matrix while reinforcing it [4].

In the valorization of biomass waste from palm cultivation, our study will fundamentally focus on the extraction of fibers lignocellulosic, which can be advantageously used as reinforcements in various applications, as well as on their modification surface for their compatibility with hydrophobic polymers. The applications of these functionalized lignocellulosic as bio-sourced reinforcements in hydrophobic polymer composites will be practical in the future [5].

In recent years, various works have been carried out on the pretreatment of lignocellulosic biomass, the manufacturing or extraction routes of cellulose fibers from different biomasses, and chemical modification.

However, one of the obstacles often highlighted is biocomposites' sensitivity to climatic variations following their exposure to external aggressions such as ultraviolet (UV) rays from the sun, heat, or high humidity. This sensitivity can manifest itself as a loss of mechanical strength. In addition, structural modifications of biocomposites can induce changes in visual appearance. Thus, a quantitative study of the relationships between biocomposites' structure and macroscopic properties would provide elements for understanding their degradation mechanisms and explain the damage caused by external factors [6, 7].

The first consists of the value of agricultural waste, which is the date palms (*Phoenix dactylifera* L.) have an abundance of cellulosic fibers. Date palm trees grow in tropical and subtropical climates, making them the primary source of natural fibers. Both environmental variables and soil quality have an impact on their growth. Algeria is one of the world's largest producers of date palms, and date agriculture generates over 200,000 tons of garbage each year [8]. For this reason, this study was undertaken to take advantage of this waste by developing a composite material based on linear low-density polyethylene loaded with palm petiole fibers. However, the major problem in this type of mixture is the interfacial incompatibility between the matrix and the filler. To solve this problem, These investigations were focused on various combinations of pretreatments on the surface of palm petiole fiber (NaOH, hydrogen peroxide, and acetic anhydride) used as reinforced in LLDPE composites made by a mono-screw extruder machine with a fiber loading of 15–25% by weight. This investigation will help encourage using recycled palm petiole fiber waste and save the environment by substituting synthetic fiber.

This work aims to compare the properties of raw and chemically treated petiole fibers and identify the best chemical treatments and good loading for improving the composite's dynamic, mechanical, and morphological properties. After NaOH and hydrogen peroxide treatments decrease the amount of lignin, acetylation is expected to result in a stronger bond between the palm petiole fibers and LLDPE, making the material stronger.

The second objective aims to enrich and further deepen the results of the study of the durability of composite materials by studying the effects of natural aging, which will be evaluated by determining the physical, mechanical, and morphological properties of the exposed samples.

This thesis will be divided into three parts :

- The first part is a general review of the helpful bibliography for the project. It explores the field of extraction fiber and its derivatives, emphasizing the description and characterization of the constituents of the lignocellulosic raw material, the pretreatment processes, surface modification, and perspectives for improving their properties. Moreover, we will be devoted to generalities on composite materials, in which we will lay the foundations of this work by carrying out advanced knowledge on composite materials based on an organic matrix. It highlights the importance of the fiber-matrix interface of polymers reinforced by plant fibers. Then, we will highlight natural weathering phenomena and the mechanisms involved in aging these materials and their consequences on multi-scale properties.

- The second part corresponds to the description of the material and method, which will present the materials used, the experimental protocols, and the implementation processes for developing LLDPE/palm petiole fiber composites based on a multi-scale approach. This part will describe the techniques and practical methods used to characterize the materials studied and evaluate the effects of natural aging at different scales.
- The third part will discuss the results of the tests on the treated and untreated fibers, discuss the characterization of LLDPE/Palm Petiole Fiber Composites, and address a study of the effect of natural aging on the properties of composites.

In conclusion, this thesis concludes by providing a comprehensive summary of the main findings achieved in this study. It also emphasizes potential research opportunities that can be pursued by the author or other scholars in exploring aspects or dimensions of the research topic that were not addressed in the current research endeavor.

Reference

- [1] R. Yue, C. An, Z. Ye, E. Owens, E. Taylor, and S. Zhao, "Green biomass-derived materials for oil spill response: recent advancements and future perspectives," *Current Opinion in Chemical Engineering*, vol. 36, p. 100767, 2022.
- [2] D. Verma and E. Fortunati, "Biopolymer processing and its composites: an introduction," in *Biomass, Biopolymer-Based Materials, and Bioenergy*, ed: Elsevier, 2019, pp. 3-23.
- [3] N. Shukla, H. Agrawal, I. Srivastava, A. Khan, and G. Devnani, "Natural composites: Vegetable fiber modification," in *Vegetable Fiber Composites and their Technological Applications*, ed: Springer, 2021, pp. 303-325.
- [4] D. K. Rajak, D. D. Pagar, P. L. Menezes, and E. Linul, "Fiber-reinforced polymer composites: Manufacturing, properties, and applications," *Polymers*, vol. 11, p. 1667, 2019.
- [5] G. Rajeshkumar, S. A. Seshadri, G. Devnani, M. Sanjay, S. Siengchin, J. P. Maran, *et al.*, "Environment friendly, renewable and sustainable poly lactic acid (PLA) based natural fiber reinforced composites—A comprehensive review," *J. Clean. Prod.*, vol. 310, p. 127483, 2021.
- [6] P. A. Ling, H. Ismail, and A. Bakar, "Linear low density polyethylene/poly (vinyl alcohol)/kenaf composites: Effect of natural weathering on functional group, weight loss characteristics, tensile, morphological and thermal properties," *Sains Malays*, vol. 47, pp. 571-580, 2018.
- [7] Y. Bellatrache, L. Ziyani, A. Dony, M. Taki, and S. Haddadi, "Effects of the addition of date palm fibers on the physical, rheological and thermal properties of bitumen," *Construction and Building Materials*, vol. 239, p. 117808, 2020.
- [8] R. Khiari and M. N. Belgacem, "Date Palm Nanofibres and Composites," in *Date Palm Fiber Composites*, ed: Springer, 2020, pp. 185-206.

Part I

*General Review of the
Literature*

Chapter I

Fibrous Materials

Chapter I : Fibrous Materials

What are fibrous materials?

Fibrous materials can be classified into two main types: natural and synthetic fibers. Natural fibers are derived from plants, animals, or minerals. Plant fibers include cotton, flax, ramie, jute, and hemp. Animal fibers include silk, wool, and hair. Mineral fibers include asbestos. Synthetic fibers are manufactured from petroleum or other synthetic materials. Regenerated fibers, such as viscose and acetate, are made from the plant material cellulose. Synthetic fibers, such as polyester, polyamides, and polyolefins, are made from petroleum. Inorganic fibers like glass and carbon fibers are made from non-carbon materials [1].

I.1. Generality of lignocellulosic fibers

Lignocellulosic fibers, prevalent in nature, exhibit biodegradability and sustainability, playing a pivotal role in human civilization. These fibrous materials can be naturally derived from various sources, including plants, leaves, seeds, bark, stems, and grasses [2].

Plants provide us with a limitless supply of natural materials rivaling fossil fuels. Lignocellulose fiber, a natural material with exceptional environmental and economic benefits, is one of the most widely studied. However, to use it as a substitute for petroleum-based compounds, we need to thoroughly understand its structure, properties, and how it interacts with other materials of a different nature. Natural fibers such as jute, flax, hemp, sisal, hardwood, softwood, silk, wool, and many others are used as reinforcement in polymer matrices to enhance the composite's qualities [3].

I.2. Morphology of natural cellulosic fibers

At the macroscopic scale, cellulosic fibers all have a cell wall composed of several layers. However, only three of them were identified by electron microscopy: the middle lamella and two concentric walls, primary and secondary. The secondary wall itself consists of three layers (Fig I.1) [4]. Each cell wall layer consists of various polymers with different structures. The middle lamella consists mainly of lignin. The primary wall is a thin layer between 0.1 and 1 μm , formed by an irregular network of microfibrils. The

middle layer of the secondary wall constitutes the central part of the cell wall and thus controls the mechanical properties of the fiber [5].

In addition to cellulose, hemicelluloses, and lignin, the chemical composition of fibers also includes inorganic matter, present in small proportion about the dry mass, water, air, proteins, pectins, waxes, fats, and resins. Microfibrils are almost flexible and attract each other with strong hydrogen bonding at molecular boundaries or between the faces by van der Waals force.

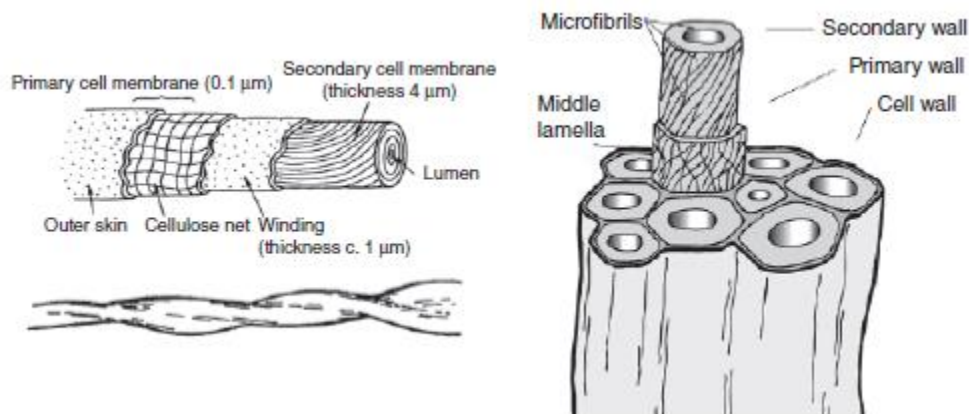


Figure I.1: Morphology of Natural Cellulosic Fibers

I.3. Lignocellulosic composition

Lignocellulosic fibers are an organic material composed of three main elements: carbon (49%), hydrogen (6%), and oxygen (44%), as well as less than 1% nitrogen and inorganic elements (Na, K, Ca, Mg, and Si). Three families of macromolecules mainly constitute lignocellulosic materials: cellulose, hemicellulose, and lignin. It is impossible to define the chemical composition of fibers precisely because it varies with the species and nature of the fibers, the geographical location, the climate, the nature of the soil, and the effect of mechanical or water stress exerted during tree growth [6].

Polysaccharides of fibers (Cellulose and hemicelluloses) are polymers that are part of the carbohydrate family and represent approximately 65 to 70% of the dry matter of fibers.

- **Cellulose**

Cellulose (Fig. I.2), the main component of the plant cell (mainly found in the secondary cell wall), is the most critical biopolymer in biomass (50%). It is a linear homopolymer whose repeating unit is

cellobiose, a dimer of glucose. These units are linked together by β -glucosidic bonds (1-4). Cellulose can be expressed by the molecular formula $(C_6H_{12}O_6)_n$, where n is the degree of polymerization (DP) and varies from 10,000 to 15,000 for native cellulose.

The cellulose chains are linked by intra- and intermolecular hydrogen bridges (Fig I.2) and Van der Waals-type bonds. The association of numerous cellulose macromolecules allows the formation of elementary fibrils; an elementary fibril consists of an average of 36 chains; these elementary fibrils assemble into microfibrils and promote the establishment of a microcrystalline structure. This condensed fibrillar structure is the origin of the remarkable characteristics of cellulose [7].

- **Hemicellulose**

Hemicelluloses are complex polysaccharides of low molecular weight (average degree of polymerization of 150), very hydrophilic and soluble in an alkaline medium, and mainly present at the level of the primary and secondary walls of the plant cell. These polysaccharides can be homopolymers or heteropolymers, and their structures vary according to the nature of the fibers. The monomers of hemicelluloses are represented in (Fig I.2). Compared to cellulose, it has an amorphous structure and comprises several heterogeneous combinations like mannose, glucose, and galactose linked together by β -1,4-glycosidic and β -1,3-glycosidic bonds [8].

- **Lignin**

Lignin is a complex amorphous aromatic polymer in all lignocellulosic materials with a three-dimensional cross-linked structure. It is produced during photosynthesis and is often related to cellulose in cell walls. It remains integrated with cellulose and hemicellulose polymers, which impart high mechanical strength to the plant stalks. In lignocellulosic, the proportion of lignin polymers comprises 10–25% . Due to its complexity, it has no defined structure and may vary from one type of plant to another. It is mainly composed of three phenylpropane units: *p*-coumaryl alcohol (H), coniferyl alcohol (G), and sinapyl alcohol (S). Lignin is formed by cross-linking the three phenylpropane units via the coupling of C-C bonds and C-O bonds as shown in (Fig. I.2); the composition of the monomers depends on the plant species. The variety of components of the monomers and cross-linkage between the units make lignin heterogeneous polymers with cross-linked networks, high molecular weight, polydispersity, and widely varying structures [9].

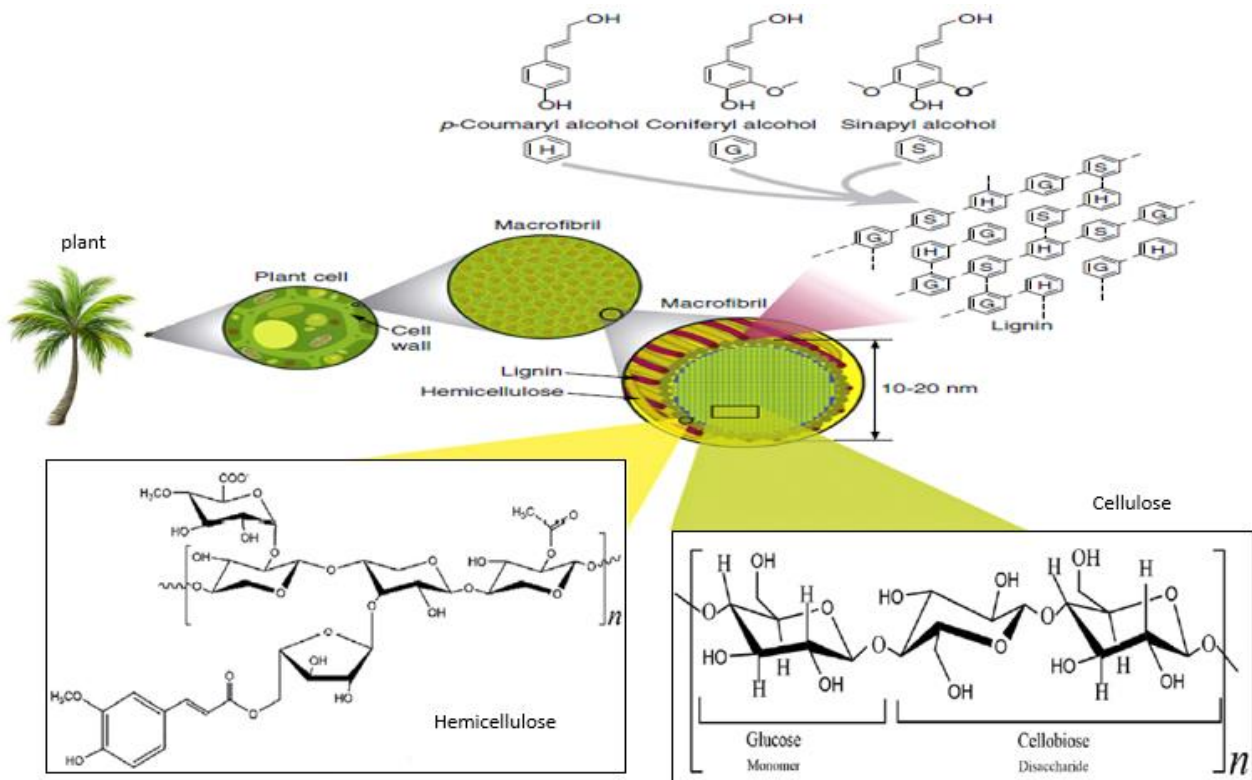


Figure I.2 : Lignocellulosic composition

I.4. Date palm

Date palms are typically cultivated in Saharan oases, but they are also native to North Africa and widely cultivated in Arabia, where they form the characteristic vegetation of oases. They are also grown commercially in the Canary Islands, the northern Mediterranean region, and the southern United States.

Date palms are cold-sensitive plants that can grow on any soil, provided it is fertile and well-drained. In regions with a mild climate, they are grown outdoors in a sunny position. There are over 2,600 species of palm trees, and date palms are dioecious plants, meaning they have separate male and female plants. The palm has a slender trunk, up to 30 meters high, which is visibly covered by the sheaths of fallen leaves. The leaves are pinnate, up to 6 meters long, and are gathered in a sparse apical crown of 20-30 leaves (Fig I.3). The upper leaves are ascending, while the basal leaves are curved downward. The leaves are leathery, linear, rigid, and green [10].

Algeria is a major producer of dates, with over 160,000 hectares of palm groves and 18.6 million date palms. Date agriculture generates over 200,000 tonnes of garbage each year. For reinforced composite applications, date palm tree fibers are extracted from the palm trunk, petiole, rachis, leaflets, and fruit bunches [11].

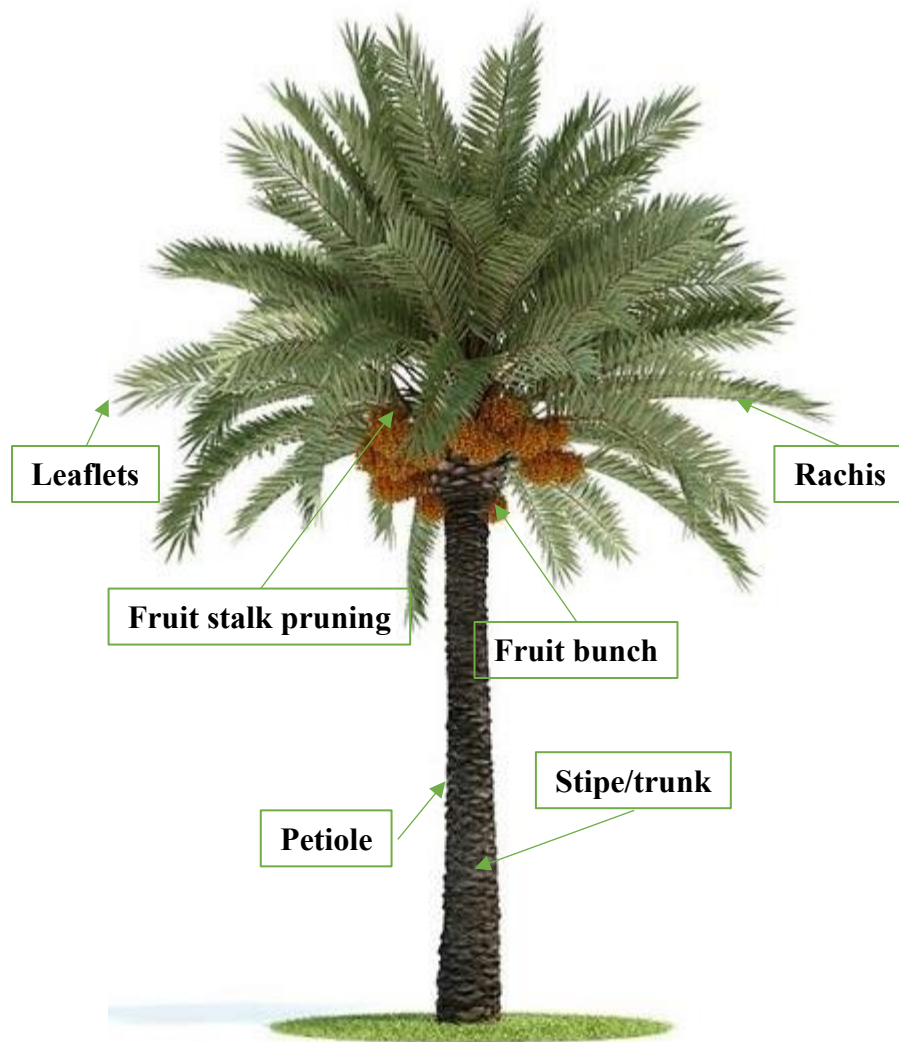


Figure I.3 : Date Palm

The date palm is a versatile tree that provides a wide range of products in addition to its edible fruit. All parts of the tree are used for various purposes. Modern technology and improved communication have expanded the use of date palm products in new industries. Date palm trees are a significant source of fiber, which is used in various applications. The tree's trunk can make furniture, flooring, and fences. The leaves can be used to weave baskets, mats, and roofs. Date palm fiber is also used in industrial products such as ropes, paper, and composites (Fig. I.3). In addition to its fiber, the date palm is a valuable source of other raw materials. The tree's sap can make sugar and vinegar. The seeds can be ground into flour or used to produce oil. Date palm wood is also a valuable resource used in construction and woodworking.

I.5. Properties and uses of natural fibers

A set of parameters governs the properties of these natural fibers:

- the shape factor of the fiber
- the degree of polymerization of the cellulose
- the crystallinity of the cellulose
- the orientation of the cellulose chains
- the chemical composition of the fibers (lignin content, hemicellulose, cellulose)
- defects

The tensile strength and Young's modulus of natural fibers generally increase with the cellulose content of the fibers. The fibers can be used directly after extraction, generally by thermomechanical processes, or after chemical modifications to improve specific properties (hydrophobicity, compatibilization). The main difficulties in developing natural fibers in materials are the harvesting system and storage and transport problems due, in particular, to their sensitivity to degradation by micro-organisms [12].

Natural fibers are historically used in textiles and for papermaking. They can thus be used alone to manufacture geotextiles (soil stabilization, favored germination), filters, or absorbents (activated carbon). In the presence of adhesive, natural fibers are found in building and furniture applications. The main developments concern the combination of natural fibers with other materials; cement and mainly thermoplastic polymers. Indeed, the current interest of industrialists in more CO₂ efficient materials allows natural fibers to find new applications as reinforcement in organic matrices, mainly for the automotive and packaging fields. Good mechanical properties, low density, and low cost make natural fibers a material of choice for preparing organic matrix composites. However, the preparation of these composites could be improved. The hydrophilic nature of natural fibers compared to the use of predominantly hydrophobic polymers and an implementation temperature that is limited due to the risks of thermal degradation of natural fibers are restrictions on the use of natural fibers in composites with polymer matrix. Many studies are being carried out on developing composite materials from natural fibers, particularly on fiber-matrix compatibilization, which depends not only on the fiber used but also on the nature of the matrix [13].

I.6. Lignocellulose modification

The main goal of lignocellulose pretreatment is to overcome the inherent recalcitrance of lignocellulosic materials, which refers to their resistance to enzymatic hydrolysis or microbial degradation. The pretreatment methods aim to disrupt the lignin and hemicellulose components and increase the accessibility of cellulose, the main polysaccharide of interest [14]. There are a number of different pretreatment methods that can be used, including:

a. Mechanical treatment

Mechanical pretreatment methods, such as dry brushing, chipping, grinding, and compression, are often used to break down the crystalline structure and increase the surface area of polysaccharide polymers in the cell wall, making them more susceptible to hydrolysis. Some mechanical pretreatment methods are also necessary to reduce the particle size of the material to an appropriate level before chemical or biological pretreatment can be applied [15].

b. Chemical treatment

Natural fibers are generally induced to various chemical treatments like alkali treatment, silane treatment, isocyanate treatment, and acetylation. To improve the interfacial performance between lignocellulosic fibers and polymer matrices, many technics for the chemical modification of fibers' surfaces have been the subject of numerous citations in the bibliography [16]. Chemical-treated fibers showed higher values of mechanical properties than retting extracted fibers, where the selection of chemical agents for treatment depends on the type of natural fiber and selected the proper concentration and time interval for treatment [17].

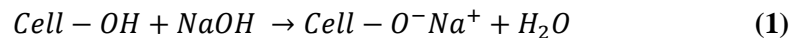
• Alkaline pretreatment

Mercerization is a chemical treatment that uses a fundamental solution to modify lignocellulosic fibers. It is one of the most widely used methods for improving the properties of these fibers. During mercerization, the fibers swell, and the non-cellulosic components, such as hemicellulose, lignin, pectins, and waxy substances, are partially or entirely removed. This leaves behind a purer cellulose fiber with a higher surface area. The increased surface area of the mercerized fibers makes them more reactive and improves their adhesion to other materials. This makes them more suitable for composite materials and other applications where strong fiber-matrix adhesion is essential [18]. Sodium hydroxide

(NaOH), potassium hydroxide (KOH), calcium hydroxide (Ca(OH)₂) are generally used for alkali pretreatment.

The mechanism of mercerization results in the cleavage of acetyl groups from xylan polymers, saponification of intermolecular ester bonds, and alteration of the lignin structure that aids the removal of the lignin compounds [19]. Additionally, these chemicals alter the degree of polymerization, reducing cellulose's crystallinity while increasing surface area [20]. Alkaline pretreatment chemicals diffuse by capillary action to the lumen and subsequent cell layers, reaching the middle lamella and the secondary wall of the LCB. The desired polysaccharides are mainly located in the secondary wall regions, while fewer polysaccharides are present in the middle lamella [21]. For example, (NaOH) is dissociated into (OH⁻) and (Na⁺) ions that attack the ester and ether linkage between lignin-hemicellulose complexes. Additionally, it has the ability to cleave the ester and carbon-carbon bonds in the lignin moieties (ferulic acid) [20]. Other alkaline conditions result in the cleavage of phenolic and non-phenolic β-aryl ether linkages that directly aid in the depolymerization of lignin in lignocelluloses [22].

It should be noted that sodium hydroxide (NaOH) is the most commonly chemical used in this type of treatment. The reaction involved is represented in the following Eq. (1):



The optimization of the parameters influencing the efficiency of this type of treatment such as the concentration of the solution, the temperature and the treatment time contributes to the improvement of the mechanical properties of the lignocellulosic fibers and the composite material [18].

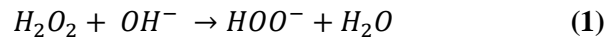
- **Oxidative pretreatment**

Oxidative pretreatment involves oxidation resulting in the cleavage of lignin and the deconstruction of hemicelluloses into their constituents, sugars, and organic acids [23]. The major oxidants used are oxygen, ozone, and hydrogen peroxide, but the mechanism for the deconstruction of biomass varies depending on oxidants and reaction conditions.

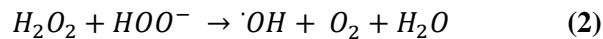
For oxygen delignification, oxygen increases the reaction rate and generation of free radicals at high temperatures and pressure. A phenolate ion is formed when alkali and oxygen react with a phenolic hydroxyl group of lignin, forming a reactive intermediate called hydroperoxide. This intermediate then undergoes fragmentation to form lignin fragments that are mostly water-soluble. The utilization of pure oxygen can improve the reaction rate but with high process cost [24]. Hydrogen peroxide requires alkaline pH for the

production of oxidizing radicals to degrade lignin. The most favorable pH of this pretreatment is 11.5, and increasing or decreasing pH above or below the range of 10–12.5 will result in improper delignification, or it will degrade the sugar molecules. The addition of NaOH can maintain the pH.

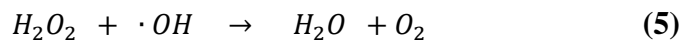
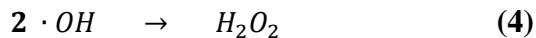
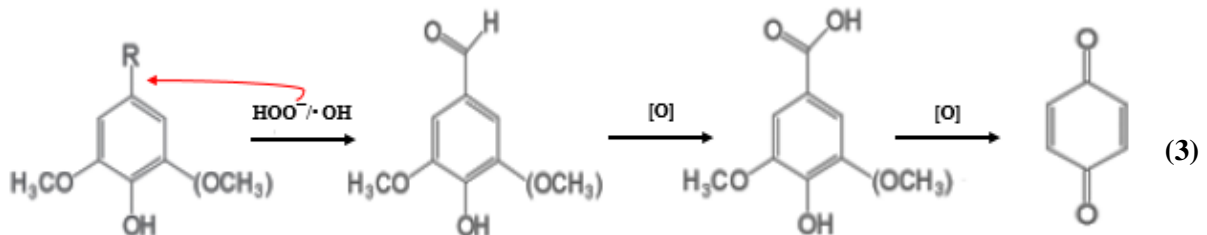
The chemical reactions using hydrogen peroxide as an oxidizing agent in the alkaline liquid medium are depicted. The dissociation of hydrogen peroxide at alkaline pH generates the hydroperoxide anion (HOO^-) through Eq. (1).



The hydroperoxide anion can react with H_2O_2 in the alkaline medium, forming superoxide and hydroxyl radicals, as expressed in Eq. (2).



These radicals are the most potent oxidizers that attack the aryl ether bonds and other linkages under these conditions Eq. (3), and others decomposed to O_2 and H_2O Eq. (4 and 5), influencing oxidation efficiency for hydrogen peroxide. The generation of other compounds is removed by oxidizing phenolic groups into aldehydes and carbonyl compounds [25].



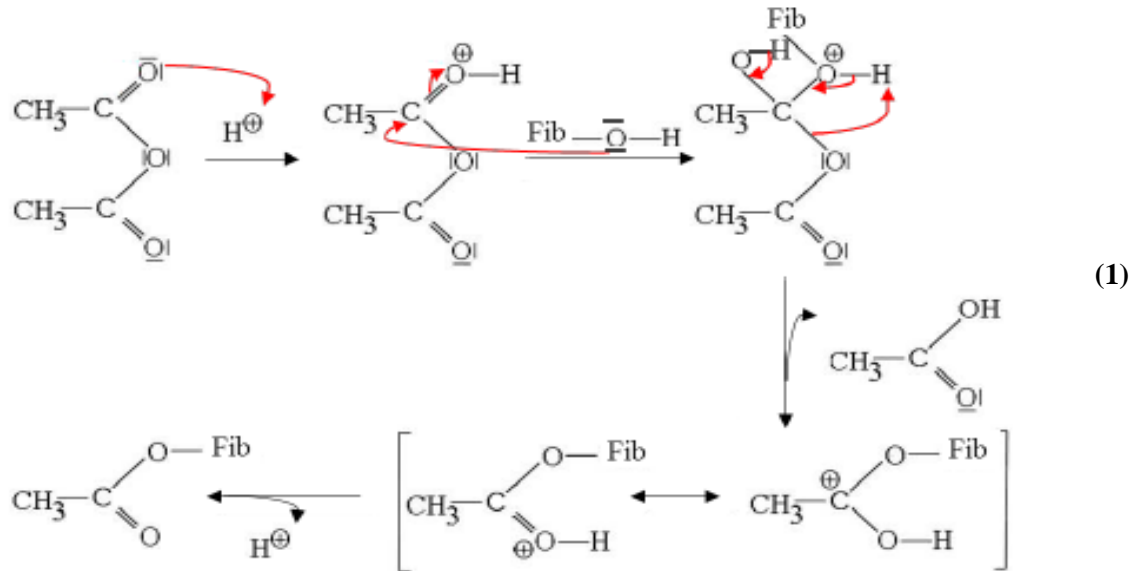
c. Chemical functionalization

The functionalization of cellulosic substrates has been widely exploited, even before determining the polymeric nature of cellulose. Over the years, several ways of chemically treating lignocellulosic fibers have been developed, making it possible to obtain products with varied characteristics depending on the type and uniformity of the distribution of the substituent groups, thus opening up a wide field for the design of new materials. In this regard, many research teams have been particularly interested in improving the compatibility of cellulosic fibers with polymeric matrices through chemical modification. This treatment uses reagents ranging from small molecules, allowing the hydrophilic nature of the cellulosic fiber to be reduced, to macromolecules aimed at creating covalent bonds between the reinforcement and the matrix.

- **Acetylation**

The acetylation of polysaccharides involves replacing available hydrophilic OH groups with more hydrophobic acetyl groups. Today, there are numerous publications on various acetylation methods, resulting in various degrees of substitution and pattern [26]. The most basic reaction to achieve acetylated celluloses is still based on acetic anhydride as the reagent. Different reaction conditions can be used depending on the targeted degree of substitution. In this case, the primary reaction mechanism starts with a nucleophilic attack of the lone electron pair of the alcoholic sugar OH group on the carbonyl carbon atom of the acetic acid anhydride molecule. Due to the consequent split-off of acetic acid, acetylated carbohydrates are formed. This reaction is often performed with acid or base catalysis to the following reaction Eq. (1) [27]:

During acetylation of natural fibers, esterification occurs by reacting acetyl groups (CH_3CO^-) with hydroxyl groups (OH) on the fibers resulting in increased hydrophobicity. This has been shown to improve interfacial bonding, tensile and flexural strength, stiffness, and dimensional and thermal stability. However, over-treatment has been seen to be deleterious to mechanical properties, assumed to be due to the degradation of cellulose and cracking of fibers known to occur with the catalysts used in this process. Acetylation treatment has also been found to reduce the impact strength of the composite. Commonly acetylation is preceded by an alkaline treatment [18, 28, 29].



d. Pretreatment combination

Most pretreatment processes can only partially weaken the factors that limit the hydrolysis of lignocellulosic materials. Thus, combined pretreatment processes are seen as a means of maximizing or improving their digestibility. Concerning the pretreatments described above, we can see that each pretreatment taken individually has a particularly effective action on the lignocellulosic biomass, such as the elimination of hemicelluloses (alkaline pretreatment), the elimination of lignins (oxidative delignification), or the increase of accessible surface or pore volume (grinding). The main effects of these pretreatment processes on the chemical compositions and structures of lignocellulosic materials are summarised and illustrated in Table I.1. [30].

Table I.1: Effects of different pretreatment processes on the compositions and structures of lignocellulosic materials

Processes	Elimination of lignin	Elimination of hemicelluloses	Increase of area surface	Cristallisation of cellulose	Increase the volume of pores
Crusher	-	-	H	H	-
Alkaline	H	H	H	-	H
Acid	M	H	H	-	M
Oxidation	H	-	-	-	F

H: high effect; M: medium effect; F: low effect

These pretreatments can be combined to improve the digestibility of lignocellulosic materials and facilitate the recovery of lignin and hemicelluloses to produce products with high added value. So far, alkaline pretreatments remain the most attractive and cost-effective method for removing lignin and hemicelluloses from lignocellulosic materials.

References

- [1] C. Ge, D. Xu, H. Du, Z. Chen, J. Chen, Z. Shen, *et al.*, "Recent advances in fibrous materials for interfacial solar steam generation," *Advanced Fiber Materials*, vol. 5, pp. 791-818, 2023.
- [2] T. Dele-Afolabi, M. A. Hanim, O. Ojo-Kupoluyi, and E. Atoyebi, "Biobased materials for wastewater treatment," in *Advanced Applications of Biobased Materials*, ed: Elsevier, 2023, pp. 593-624.
- [3] H. Chakhtouna, H. Benzeid, N. Zari, A. e. k. Qaiss, and R. Bouhfid, "Recent advances in eco-friendly composites derived from lignocellulosic biomass for wastewater treatment," *Biomass Conversion and Biorefinery*, pp. 1-27, 2022.
- [4] H. Awais, Y. Nawab, A. Amjad, A. Anjang, H. Md Akil, and M. S. Zainol Abidin, "Environmental benign natural fibre reinforced thermoplastic composites: A review," *Composites Part C: Open Access*, vol. 4, p. 100082, 03/01 2021.
- [5] W. A. Wirawan, M. A. Choiron, E. Siswanto, and T. D. Widodo, "Morphology, structure, and mechanical properties of new natural cellulose fiber reinforcement from waru (*Hibiscus tiliaceus*) bark," *Journal of Natural Fibers*, vol. 19, pp. 12385-12397, 2022.
- [6] K. K. Valladares-Diestra, L. P. de Souza Vandenberghe, V. S. Nishida, and C. R. Soccol, "The potential of imidazole as a new solvent in the pretreatment of agro-industrial lignocellulosic biomass," *Bioresource Technology*, vol. 372, p. 128666, 2023.
- [7] T. Aziz, A. Farid, F. Haq, M. Kiran, A. Ullah, K. Zhang, *et al.*, "A review on the modification of cellulose and its applications," *Polymers*, vol. 14, p. 3206, 2022.
- [8] J. Rao, Z. Lv, G. Chen, and F. Peng, "Hemicellulose: Structure, chemical modification, and application," *Progress in Polymer Science*, p. 101675, 2023.
- [9] C. Huang, Z. Peng, J. Li, X. Li, X. Jiang, and Y. Dong, "Unlocking the role of lignin for preparing the lignin-based wood adhesive: A review," *Industrial Crops and Products*, vol. 187, p. 115388, 2022.
- [10] O. Y. Alothman, H. M. Shaikh, B. A. Alshammari, and M. Jawaid, "Structural, morphological and thermal properties of nano filler produced from date palm-based micro fibers (*Phoenix dactylifera* L.)," *J. Polym. Environ*, vol. 30, pp. 622-630, 2022.
- [11] F. Althoey, I. Y. Hakeem, M. A. Hosen, S. Qaidi, H. F. Isleem, H. Hadidi, *et al.*, "Behavior of concrete reinforced with date palm fibers," *Materials*, vol. 15, p. 7923, 2022.
- [12] R. A. Ilyas, H. A. Aisyah, A. H. Nordin, N. Ngadi, M. Y. M. Zuhri, M. R. M. Asyraf, *et al.*, "Natural-fiber-reinforced chitosan, chitosan blends and their nanocomposites for various advanced applications," *Polymers*, vol. 14, p. 874, 2022.

- [13] N. Shukla, H. Agrawal, I. Srivastava, A. Khan, and G. Devnani, "Natural composites: Vegetable fiber modification," in *Vegetable Fiber Composites and their Technological Applications*, ed: Springer, 2021, pp. 303-325.
- [14] D. P. Maurya, A. Singla, and S. Negi, "An overview of key pretreatment processes for biological conversion of lignocellulosic biomass to bioethanol," *3 Biotech*, vol. 5, pp. 597-609, 2015/10/01 2015.
- [15] B. Kumar, N. Bhardwaj, K. Agrawal, V. Chaturvedi, and P. Verma, "Current perspective on pretreatment technologies using lignocellulosic biomass: An emerging biorefinery concept," *Fuel Processing Technology*, vol. 199, p. 106244, 2020.
- [16] V. Chaudhary and F. Ahmad, "A review on plant fiber reinforced thermoset polymers for structural and frictional composites," *Polymer Testing*, vol. 91, p. 106792, 2020.
- [17] A. Megalingam, M. Kumar, B. Sriram, K. Jeevanantham, and P. Ram Vishnu, "Borassus fruit fiber reinforced composite: A review," *Materials Today: Proceedings*, 2020.
- [18] A. Oushabi, "The pull-out behavior of chemically treated lignocellulosic fibers/polymeric matrix interface (LF/PM): A review," *Composites Part B: Engineering*, vol. 174, p. 107059, 2019/10/01/ 2019.
- [19] D. Kumari and R. Singh, "Pretreatment of lignocellulosic wastes for biofuel production: A critical review," *Renewable and Sustainable Energy Reviews*, vol. 90, pp. 877-891, 2018.
- [20] J. Kim, M. Sunagawa, S. Kobayashi, T. Shin, and C. Takayama, "Developmental localization of calcitonin gene-related peptide in dorsal sensory axons and ventral motor neurons of mouse cervical spinal cord," *Neuroscience Research*, vol. 105, pp. 42-48, 2016.
- [21] F. Gu, L. Yang, Y. Jin, Q. Han, H.-m. Chang, H. Jameel, *et al.*, "Green liquor pretreatment for improving enzymatic hydrolysis of corn stover," *Bioresource Technology*, vol. 124, pp. 299-305, 2012/11/01/ 2012.
- [22] Y. Sewsynker-Sukai, A. Naomi David, and E. B. Gueguim Kana, "Recent developments in the application of kraft pulping alkaline chemicals for lignocellulosic pretreatment: Potential beneficiation of green liquor dregs waste," *Bioresource Technology*, vol. 306, p. 123225, 2020/06/01/ 2020.
- [23] A. T. W. M. Hendriks and G. Zeeman, "Pretreatments to enhance the digestibility of lignocellulosic biomass," *Bioresource Technology*, vol. 100, pp. 10-18, 2009.
- [24] W. Den, V. K. Sharma, M. Lee, G. Nadadur, and R. S. Varma, "Lignocellulosic biomass transformations via greener oxidative pretreatment processes: access to energy and value-added chemicals," *Frontiers in chemistry*, vol. 6, p. 141, 2018.
- [25] S. Niju and M. Swathika, "Delignification of sugarcane bagasse using pretreatment strategies for bioethanol production," *Biocatalysis and Agricultural Biotechnology*, vol. 20, p. 101263, 2019.
- [26] J. R. Martins, "Sugarcane bagasse xylan acetylation and its effect on bioplastic formulation, properties and biodegradation," 2022.

- [27] X. Li, L. G. Tabil, and S. Panigrahi, "Chemical treatments of natural fiber for use in natural fiber-reinforced composites: a review," *Journal of Polymers and the Environment*, vol. 15, pp. 25-33, 2007.
- [28] A. Bledzki, A. Mamun, M. Lucka-Gabor, and V. Gutowski, "The effects of acetylation on properties of flax fibre and its polypropylene composites," *Express Polymer Letters*, vol. 2, pp. 413-422, 2008.
- [29] V. Tserki, N. Zafeiropoulos, F. Simon, and C. Panayiotou, "A study of the effect of acetylation and propionylation surface treatments on natural fibres," *Composites Part A: applied science and manufacturing*, vol. 36, pp. 1110-1118, 2005.
- [30] Y. Zheng, J. Shi, M. Tu, and Y.-S. Cheng, "Principles and Development of Lignocellulosic Biomass Pretreatment for Biofuels," in *Advances in Bioenergy*. vol. 2, Y. Li and X. Ge, Eds., ed: Elsevier, 2017, pp. 1-68.

Chapter II

Composite Materials

Chapter II : Composite Materials

What is the composite materials ?

A composite material is defined as an assembly of at least two immiscible constituents, each with high adaptability. The respective qualities of the constituents complement each other to form a material with improved mechanical, thermal, and physicochemical performance. It is possible to modulate the properties of a composite according to a specified need. The adaptability of these materials makes them a significant asset and places them in a competitive position with traditional materials (metals, alloys) [1].

II.1. Generality of composite materials

A composite material consists of a reinforcement and a binder, commonly called a matrix. The reinforcement, as its name suggests, will ensure the mechanical strength of the composite. The matrix ensures cohesion between the different elements and manages the flow of forces while guaranteeing resistance to the environment and temperature. Different types of composite materials depend on the chosen reinforcement or matrix couple [2]. Among the fibrous reinforcements commonly used, we can mention:

- Glass fibers are currently the most widely used.
- Carbon fibers are used for structural applications.
- Aramid fibers are used for more targeted applications, such as ballistic protection.
- natural fibers are rapidly emerging due to their low cost and positive environmental impact.

There are also different types of matrices, and there are three main families: organic matrices, ceramic matrices, and metallic matrices. Among the organic matrices, three categories of polymers can be used:

- Thermoplastic polymers.
- Thermosetting polymers.
- Elastomers.

The significant diversity of reinforcement and matrix makes it possible to shape composite materials according to the expressed need. Improving the physico-mechanical characteristics of these materials is one of the keys to their industrial development [3].

II.2. Bio-composite materials

In recent years, research on developing new materials with high performance and affordable cost has been expanding. With the emancipation of environmental consciousness, this research has mainly focused on environmentally friendly materials, the terms "renewable," "recyclable," and "sustainable" are in tune with the times. This highlights the emergence of a new type of material, renewable and easily degradable, biocomposites.

A material will be "bio-composite" if it has at least one biodegradable element among its matrix and reinforcement. We will therefore make the difference between a fully biodegradable bio-composite material, consisting of a biodegradable reinforcement and a biodegradable matrix, and a partially biodegradable composite, having either a biodegradable matrix or a biodegradable reinforcement. Therefore, two critical themes emerge on bio-composite materials; the first aims to develop 100% biodegradable materials, while the second is interested in replacing synthetic reinforcements with natural fibers [4].

The development of fully biodegradable composite materials can be achieved by using cellulose fibers or starch as reinforcement and biodegradable polymer matrices such as polylactic acid (PLA) or polyhydroxy butyrate (PHB). These composites have the advantage of being environmentally friendly, durable, and biodegradable. At the end of the cycle, they can be recycled or composted without causing environmental toxicity. In general, adding fibers makes it possible to significantly increase the rigidity of the composite and its mechanical resistance. These composites are beginning to be used in the automotive field to make floor mats and canvas roofs.

The second central research theme applied to bio-composite materials concerns the replacement of synthetic fibers used as reinforcement for composite materials. Despite their excellent mechanical properties, synthetic fibers have several significant drawbacks. We can cite, for example, glass fibers, their non-recyclable nature, which requires their incineration at the end of their life. Glass fibers are also very irritating to the respiratory tract, hence the need for significant precautions when handling them. Finally, their abrasive nature leads to premature equipment wear, resulting in frequent replacement of the latter. Cellulose fibers are excellent candidates for replacing glass fibers because of their natural origin and

desirable strength/weight ratio. However, using cellulose fibers leads to composites that are dark in color and sensitive to humidity, representing a significant obstacle to their development on an industrial scale [5].

II.3. Polyethylenes (PE)

As part of this project, we were particularly interested in thermoplastic matrices and, more specifically, in polyethylenes. PE is a generic name used to describe polyolefins resulting from the polymerization of ethylene (C₂H₄)_n where n is the number of repeat units, leading to macromolecules composed by the repetition of the motif (CH₂), (Fig II.1).

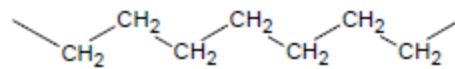



Figure II.1 :Representation of the macromolecular of polyethylene chain

In 2008, the quantity of synthetic plastics produced was 245 million tons. Polyethylene alone accounts for a quarter of this production due to its low manufacturing cost and good physical and mechanical properties. In addition, this polymer generally allows easy shaping, such as extrusion or injection. It also has excellent electrical insulation, impact resistance properties, and outstanding chemical and biological inertness (food contact). These are the most commonly used polymers to manufacture plastic bags, packaging bottles, and toys. There are many types, but these are generally classified into two large families, which are defined according to their density [6]. The (table II.1) below presents the main characteristics of polyethylene [7].

Table II.1: Principal properties of polyethylenes

Properties	Density (g/cm ³)	Crystallinity (%)	Melting (°C)	Stress (MPa)	Elongation (%)	Impact resistance (J/m)	Elastic modulus (MPa)	shore D
HDPE	0.941-0.965	± 86	± 132	18	20 - 100	27 - 160	960 - 1000	63-67
Typical chain branching								
LDPE	0.910-0.925	± 35	100-115	7 - 17	100 - 700	0.67 - 21	102 - 240	41- 46
Typical chain branching								

LLDPE	0.919-0.925	± 53	± 124	14-21	200-1200	-	100-200	50- 56
Typical chain branching								

II.4. Cellulose fiber-reinforced composite materials

Composite materials prepared using natural fibers are popular scientifically, ecologically, and socially. Indeed, as many renewable materials come from agricultural production, this is a vector of non-food economic development for the rural areas of developing countries. During the 20th century, the emergence of synthetic polymers based on petroleum-derived raw materials relegated natural polymers to a spectator role. However, over the past two decades, increasing attention has again been paid to the use of these compounds for various reasons:

- The desire to reduce the environmental impact.
- The limited quantity of petroleum sources decreases dependence on petroleum products.
- The improvement of databases concerning the properties and morphologies of natural materials.

Cellulose fibers have unique advantages such as abundance, non-toxicity, non-irritability, and non-corrosive properties for equipment, in addition to a renewable character. Composites using cellulose fibers as reinforcement have received much attention because of their potential to serve as an alternative to synthetic reinforcements. Cellulose fibers have a lower cost and lower production energy than glass fibers or carbon fibers. In addition, the lower weight (20 to 30% of the total mass) and the greater volume of cellulosic fibers compared to synthetic fibers offer a desirable strength-to-weight ratio. In the automotive industry, using composite materials based on cellulose fibers makes it possible, in particular, to reduce the quantity of non-renewable energy and polluting emissions while reducing the fuel consumption of vehicles. Cellulose fibers, therefore, have several properties superior to those of synthetic fibers, which arouses the interest of researchers, as evidenced by the number of publications in recent years on composites reinforced with cellulose fibers. Replacing synthetic fibers with natural fibers is more relevant than ever. Biobased composite materials can compete with petroleum-based products and obtain marketplaces currently dominated by them [8, 9].

II.5. Properties of cellulose fiber-reinforced composites

Different parameters govern the properties of composites based on cellulose fibers: the aspect ratio of the fibers, their volume fraction, their orientation, their dispersion, and the fiber/matrix adhesion. Each of these parameters will have a direct link to the performance of the composite, so it is essential to understand these mechanisms to maximize their effects fully.

a. Fiber aspect ratio

The mechanical strength of composites depends on how well the stress is distributed throughout the material. The matrix is the first to be affected when a composite is stressed. It then transfers the focus to the reinforcement. The more efficiently the stress is transferred from the matrix to the reinforcement, the better the mechanical properties of the composite will be. Maximizing the fiber/matrix interactions and improving the adhesion quality between the two are necessary to optimize stress distribution. It has been shown that the higher the aspect ratio (length/diameter) of the fibers, the better the transfer of stress flows within the composite material. Cellulose fibers have an excellent aspect ratio and a large specific surface area, making them an effective reinforcement for composites [8].

b. Fiber volume fraction

The volume fraction of fibers is a crucial factor in determining the mechanical properties of a composite material. As a general rule, higher fiber content results in better mechanical properties. However, the length of the fibers must also be considered. Using tiny fibers to maintain a high volume fraction increases the number of fiber ends, which can weaken the composite. Conversely, using too-long fibers (i.e., > 9–10 mm) can cause them to fold and roll up on themselves during mixing, weakening the composite. In all cases, an excessive volume fraction of fibers will deteriorate the mechanical properties of the composite. Beyond a specific value, the fibers tend to agglomerate, resulting in poor dispersion. The choice of formulation route is also essential, especially when the fiber content is high. The shearing forces induced during mixing must be sufficiently high and repeated to allow optimal mixing of the various constituents [10].

c. Fiber orientation

Fiber orientation has a significant effect on the mechanical properties of composite materials. Indeed, it is reported that Young's modulus and the tensile strength of materials decrease according to the degree of orientation of the fibers. Cellulose fibers have significant lengthwise strength. This is much lower in the

other directions, hence the need to align the fibers as much as possible lengthwise when formulating composites.

d. Fiber dispersion

Cellulose fiber dispersion in polymer matrices is crucial. Due to their polar nature, cellulose fibers clump together when mixed with apolar matrices. This creates uneven composites with areas rich in cellulose fibers and others rich in matrix, which harms performance. Therefore, good cellulose fiber dispersion is essential. Fibers must be well-separated and coated by the matrix. Fiber-to-fiber interactions, such as hydrogen bonding and fiber length, directly affect fiber dispersion. Longer fibers and stronger fiber-fiber interactions cause fibers to entangle and clump together. The choice of formulation is essential to limiting this phenomenon. Higher shear forces and mixing times improve dispersion. Classically, mono or twin-screw extruders provide the best results. Physicochemical treatments and chemical modifications of cellulose fibers are also effective and commonly used methods [11].

e. Fiber/matrix interface adhesion

Cellulose fiber-reinforced composites rely on strong fiber/matrix adhesion for their mechanical properties. Good fiber/matrix adhesion improves stress transfer within the composite. Cellulose fibers are polar and hydrophilic, while thermoplastic matrices such as polyethylene are apolar and hydrophobic. This incompatibility weakens the fiber/matrix interface. To improve fiber/matrix adhesion, surface treatments can be used to modify the surface energy of the fibers. Another approach is to add a coupling agent with intermediate properties to the two phases [12].

f. Fibers type

The type of fiber used in a composite material significantly impacts all of the parameters mentioned previously, such as the aspect ratio, orientation, dispersion, and fiber adhesion. This is because the intrinsic properties of the fiber, such as its mechanical properties, composition, water content, and dimensions, all play a decisive role in the performance of the composite material. As a result, the nature of the fibers used determines the physico-mechanical properties of the composite material (Table II.2.) [13].

Table II.2: Physico-mechanical properties of several natural fibers

Fiber	Tensile strength (MPa)	Young's modulus (GPa)	Elongation at break (%)	Density (g/cm ³)
Abaca	400	12	3-10	1,5
Bagasse	290	17	-	1,25
Bamboo	140-230	11-17	-	0,6-1,1
Linen	345-1035	27,6	2,7-3,2	1,5
Hemp	690	70	1,6	1,48
Jute	393-773	26,5	1,5-1,8	1,3
Kenaf	930	53	1,6	-
Sisal	511-635	9,4-22	2,0-2,5	1,5
Ramie	560	24,5	2,5	1,5
Palm	248	3,2	25	0,7-1,55
Ananas	400-627	1,44	14,5	0,8-1,6
Coconut	175	4-6	30	1,2
Curaua	500-1150	11,8	3,7-4,3	1,4

II.6. Processes for composite materials

Different formulation methods can be used. These operations will allow the assembly of the different phases to obtain the most homogeneous material possible. During the development of composite materials based on cellulose fibers, the low dispersion of the fibers within the matrix does not allow for obtaining perfectly homogeneous materials. The choice of the formulation route and the operating conditions will directly impact the mechanical properties of the composite produced [14].

a. Extrusion and injection molding

Extrusion and injection molding are the main techniques used in plastic processing. *Extrusion* is the transformation of a thermoplastic material (powder or granulate) into a continuous product with a given profile by forcing through a die of said material previously softened by heat. The different constituents are introduced at one end of the extruder, mixed, and forced by one or more rotating screws through the gradually heated tooling. A hot and deformable extrusion emerges at the other end, which must be maintained and cooled during its final shaping. The production of composites reinforced with cellulose fibers by extrusion makes it possible to optimize the mixing of the reinforcement within the matrix while mainly orienting the fibers in the direction of the length. Injection molding makes obtaining the material in the desired shape possible. The assembly can be connected to the outlet of the extruder in order to directly inject the hot extrudate inside the heated mold without having to cool it.

b. Compression molding

Compression molding makes it possible to obtain parts by deformation and distribution of the material between two molds. This method is widely used on an industrial scale due to its high reproducibility and the short time required for its implementation. A mixing step can be carried out beforehand to optimize the composite's homogeneity; an extruder or a hot roller mixer is required.

References

- [1] M. Y. Khalid, Z. U. Arif, W. Ahmed, and H. Arshad, "Recent trends in recycling and reusing techniques of different plastic polymers and their composite materials," *Sustainable Materials and Technologies*, vol. 31, p. e00382, 2022.
- [2] V. Chaudhary and F. Ahmad, "A review on plant fiber reinforced thermoset polymers for structural and frictional composites," *Polymer Testing*, vol. 91, p. 106792, 2020.
- [3] D. Verma and E. Fortunati, "Biopolymer processing and its composites: an introduction," in *Biomass, Biopolymer-Based Materials, and Bioenergy*, ed: Elsevier, 2019, pp. 3-23.
- [4] R. D. S. G. Campilho, "Recent innovations in biocomposite products," in *Biocomposites for High-Performance Applications*, D. Ray, Ed., ed: Woodhead Publishing, 2017, pp. 275-306.
- [5] C. Wang, S. S. Kelley, and R. A. Venditti, "Lignin-based thermoplastic materials," *ChemSusChem*, vol. 9, pp. 770-783, 2016.
- [6] Z. Yao, H. J. Seong, and Y.-S. Jang, "Environmental toxicity and decomposition of polyethylene," *Ecotoxicology and Environmental Safety*, vol. 242, p. 113933, 2022.
- [7] A. Zhang, Y. Hou, Q. Wang, and Y. Wang, "Characteristics and polyethylene biodegradation function of a novel cold-adapted bacterial laccase from Antarctic sea ice psychrophile *Psychrobacter* sp. NJ228," *Journal of Hazardous Materials*, vol. 439, p. 129656, 2022.
- [8] S. M. Rangappa, S. Siengchin, J. Parameswaranpillai, M. Jawaid, and T. Ozbakkaloglu, "Lignocellulosic fiber reinforced composites: Progress, performance, properties, applications, and future perspectives," *Polymer Composites*, vol. 43, pp. 645-691, 2022.
- [9] R. Yue, C. An, Z. Ye, E. Owens, E. Taylor, and S. Zhao, "Green biomass-derived materials for oil spill response: recent advancements and future perspectives," *Current Opinion in Chemical Engineering*, vol. 36, p. 100767, 2022.

- [10] A. Arbelaz, J. Ibarbia, B. Imaz, and L. Soto, "Natural Fiber–Reinforced Cement Mortar Composite Physicomechanical Properties: From Cellulose Microfibers to Nanocellulose," *Journal of Materials in Civil Engineering*, vol. 35, p. 04023094, 2023.
- [11] S. A. Stel'makh, E. M. Shcherban', A. Beskopylny, L. R. Mailyan, B. Meskhi, and V. Varavka, "Quantitative and qualitative aspects of composite action of concrete and dispersion-reinforcing fiber," *Polymers*, vol. 14, p. 682, 2022.
- [12] H. Sharma, A. Kumar, S. Rana, N. G. Sahoo, M. Jamil, R. Kumar, *et al.*, "Critical review on advancements on the fiber-reinforced composites: Role of fiber/matrix modification on the performance of the fibrous composites," *Journal of Materials Research and Technology*, 2023.
- [13] D.-Y. Yoo and N. Banthia, "Impact resistance of fiber-reinforced concrete—A review," *Cement and Concrete Composites*, vol. 104, p. 103389, 2019.
- [14] C. Vanheusden, P. Samyn, B. Goderis, M. Hamid, N. Reddy, A. Ethirajan, *et al.*, "Extrusion and Injection Molding of Poly (3-Hydroxybutyrate-Co-3-Hydroxyhexanoate)(Phbhx): Influence of Processing Conditions on Mechanical Properties and Microstructure," *Polymers*, vol. 13, p. 4012, 2021.

Chapter III

Degradation Of

Biocomposite

Chapter III : Degradation Of Biocomposite

III.1. Degradation of biocomposites

The behavior of biobased composites in the face of various environmental and microbiological aggressions is treated. It is, therefore, essential to first recall the notion of durability applied to composite materials. Defines the lifetime of a material as "the time during which the material, or more precisely one of its properties, will maintain its functionality under well-defined conditions." In the case of composites, the author specifies that "aging can act on each of the constituents individually or in combination, but also at the interface between the fibers and the matrix, which is very often a privileged place of degradation." Assessing the behavior of biobased composites over time also requires addressing the issue of their colonization by microorganisms. Colonization can lead to changes in the material's chemical, physical or mechanical properties, grouped under the terms "biodegradation" and "biodeterioration." Depending on the medium, aging can act on the fibers, matrix, and interface [1].

III.2. Natural weathering

The aging carried out in the laboratory does not make it possible to simulate all the external parameters likely to alter the properties of the biocomposites during their life cycle. Indeed, acid rain, external pollution, or the development of bacteria can catalyze the kinetics of degradation (Fig III.1). As a result, natural aging is more reliable in representing actual conditions. However, this type of aging needs to be reported in the literature [2, 3]. Indeed, a very long exposure time is often necessary to detect an effective degradation of the material.

Furthermore, it can be noted that work on the exterior aging of biocomposites mainly includes surface properties such as chemical composition and visual appearance (color, gloss). Among these studies, many concern the behavior of composite materials in the outdoor environment, which their main outdoor application can explain. Most polymers exposed to the exterior are susceptible to degradation due to temperature, solar radiation, humidity, rain, oxygen in the air, and atmospheric pollutants [4-6]. The consequences of such degradation are reduced mechanical properties, discoloration, embrittlement, and erosion of the material's surface.

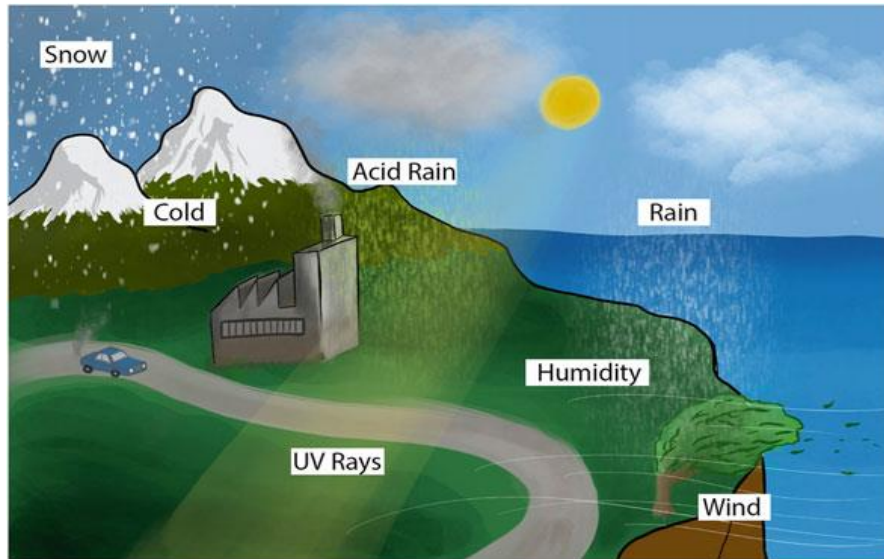


Figure III.1 : Diagram of natural weathering conditions

The study of the natural aging of HDPE composites 50% by weight of wood flour for 2000 h was carried out by Nicole M. Stark et al [7]. The results indicate that the surface oxidation produced immediately after exposure to the composites is greater than that of virgin HDPE. This suggests that adding wood flour to the HDPE matrix accelerates oxidation. The results also show that pure HDPE can undergo cross-linking in the initial stages of aging; the wood flour in the composite can impair the physical ability of HDPE to cross-link, which carries the risk of causing chain scissions of the HDPE. Calculations of oxidized and non-oxidized carbon content show that HDPE/FB composites experienced a dramatic increase in oxidized carbon content compared to virgin HDPE (80% versus 5%, respectively). This proves the detrimental effect of adding wood to the HDPE matrix, which effectively increases composite samples' surface oxidation after weathering exposure.

By FTIR spectroscopy, the study's results showed an increase in the carbonyl index due to increased scission reactions of the polymer chains. The vinyl index remained constant after 250 h of exposure; after that, it grew until 1000 h, then reached a plateau for all samples. The concentration of vinyl groups was much higher for virgin HDPE than for HDPE/FB composites, suggesting that vinyl formation occurs mainly in the composite's polymer component [8].

HDPE composites reinforced with 60 wt% bamboo fiber compression molded showed a higher crystallinity rate than in the unaged state, even after three years of exposure in Taichung (Taiwan) [9]. This is due to stabilizing the crystallinity rate after four months of increase, after which the proportion of the crystalline phase was certainly unaffected. The degradation was indeed manifested by cross-linking of the

macromolecular chains of the PE. Furthermore, the artificial aging carried out in enclosures can be correlated with natural aging. Variations in visual appearance, such as color, can, in particular, be monitored to compare the degradation mechanisms involved during the two types of aging to assess the representativeness of natural aging conditions in enclosures [10].

III.2.1. Visual changes due to natural weathering

The fatigue resistance of composites reinforced with natural fibers is predominantly affected by weathering conditions, specifically ultraviolet radiation. UV irradiation can significantly alter the physical and chemical properties of a substance. Therefore, material selection is significant. UV aging is caused primarily by solar radiation and less frequently by UV light generated artificially. UV irradiation can cause surface discoloration and molecular deterioration in composites; these reactions are photolysis, photo-oxidation, and photocatalysis. Photoaging diminishes the mechanical performance of composites due to the material's chain scission after protracted radiation exposure. In such instances, UV stabilizers are frequently applied during manufacturing to increase composites' durability. Fig III.2 depicts the wavelength of UV irradiation and photooxidative senescence on polymer biocomposites [11].

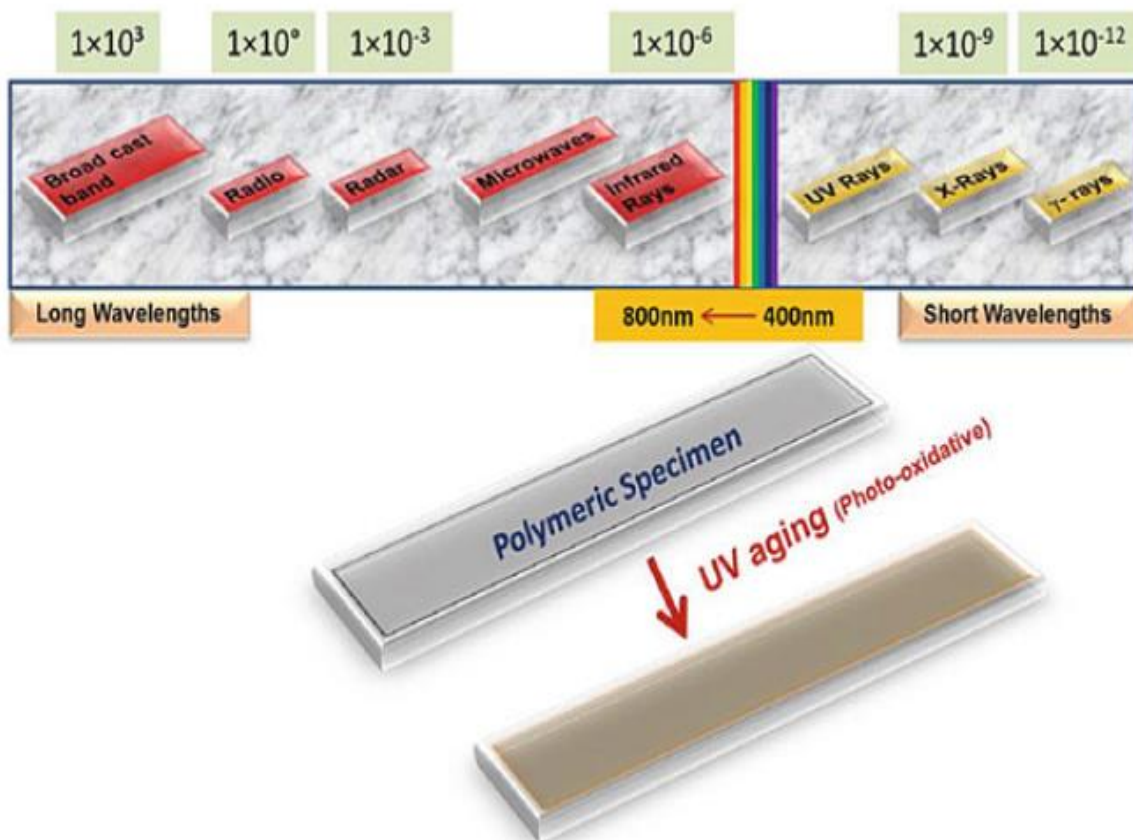


Figure III.2: Wavelength of irradiation waves and UV aging of polymer biocomposites

III.2.2. Process of water absorption by composites

Contact between a hydrophilic material and water molecules leads to water absorption by the surfaces and then in the fabric volume according to the diffusion laws. According to various authors, the diffusion of water in bio-sourced composites with an organic matrix is governed by different and successive mechanisms, as shown in Fig III.3 [12].

Water molecules can penetrate fiber by capillary action between the polymer chains of the fiber and at the fiber/matrix interface. This is often due to poor adhesion during the composite processing steps. The water molecules then form hydrogen bonds with the hydroxyl groups of cellulose and hemicelluloses. The water molecules then diffuse at the interface and into the matrix. Some fiber components can also be hydrolyzed at this level, leading to decohesion at the fiber/matrix interface. This can reduce the functional properties of the composite [13]. Fibers are susceptible to humid environments due to the numerous hydroxyl groups in the molecules constituting them. The hydroxyl groups of the fibers can absorb water directly or indirectly. Directly, the water molecules would be easily absorbed by the hydroxyls present on the surface of the fibers or the hydroxyls of the amorphous zones. This "free" water would quickly evaporate. Water molecules would also be absorbed on the inner surface of the voids. They could thereby be trapped and bound to the fiber skeleton. These water molecules would be inserted between the cellulose chains, thus promoting their sliding relative to each other and causing the fibers to swell. This "bound" water corresponds to slower absorption and desorption processes than "free" water. In addition, other water molecules can also combine with the water already bound to the fiber (Fig III.3.). The hygroscopic behavior varies from component to component for compounds such as hemicelluloses, lignin, and pectins. Hemicelluloses are very hydrophilic due to their many hydroxyl groups and long branched chains, in which water can more easily diffuse; lignin is less hydrophilic, allowing it to exert a water barrier effect [14].

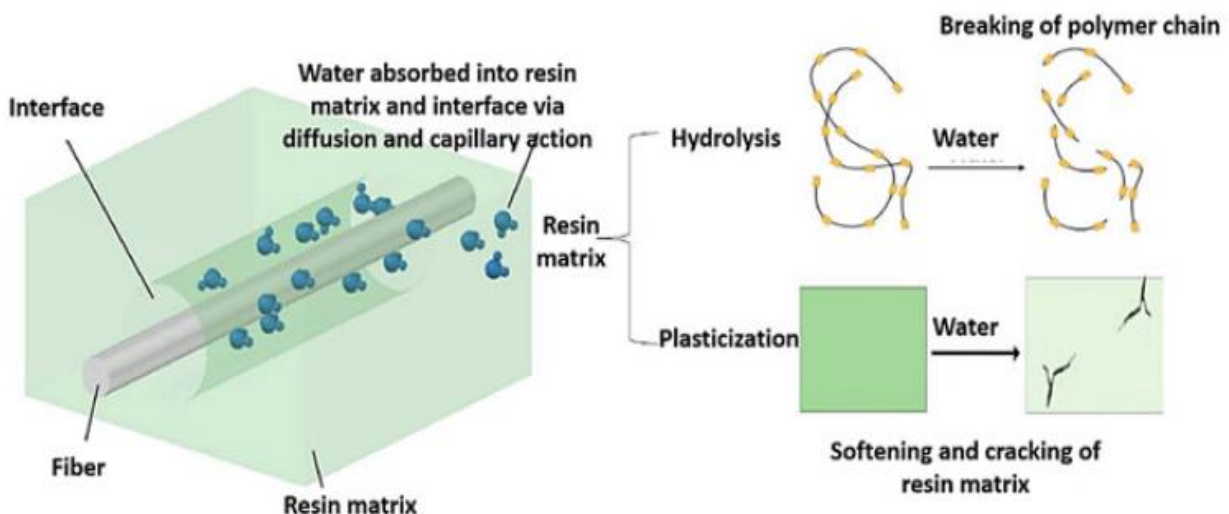


Figure III.3 : Moisture absorption effect on the fiber-matrix interface

III.2.3. Effect of natural weathering on composite structure

Surface roughness and bulk macrostructure are essential factors in determining the durability of biocomposites under natural weathering conditions. In addition to the aesthetic changes outlined in (Fig. III.4), natural weathering exposure significantly degrades the surface of entirely biodegradable composites, regardless of the polymer matrix or fiber combination. Moisture is absorbed from rainfall through the surface of the composite, primarily through the hygroscopic fibers. The diffusion of moisture into the polymer matrix is then prolonged. In simpler terms, the surface of biocomposites is severely damaged when exposed to natural weathering, such as rainfall and sunlight. Biocomposites are hygroscopic, meaning they absorb moisture from the air. The moisture then diffuses into the polymer matrix, which can lead to the degradation of the composite. [6, 15].

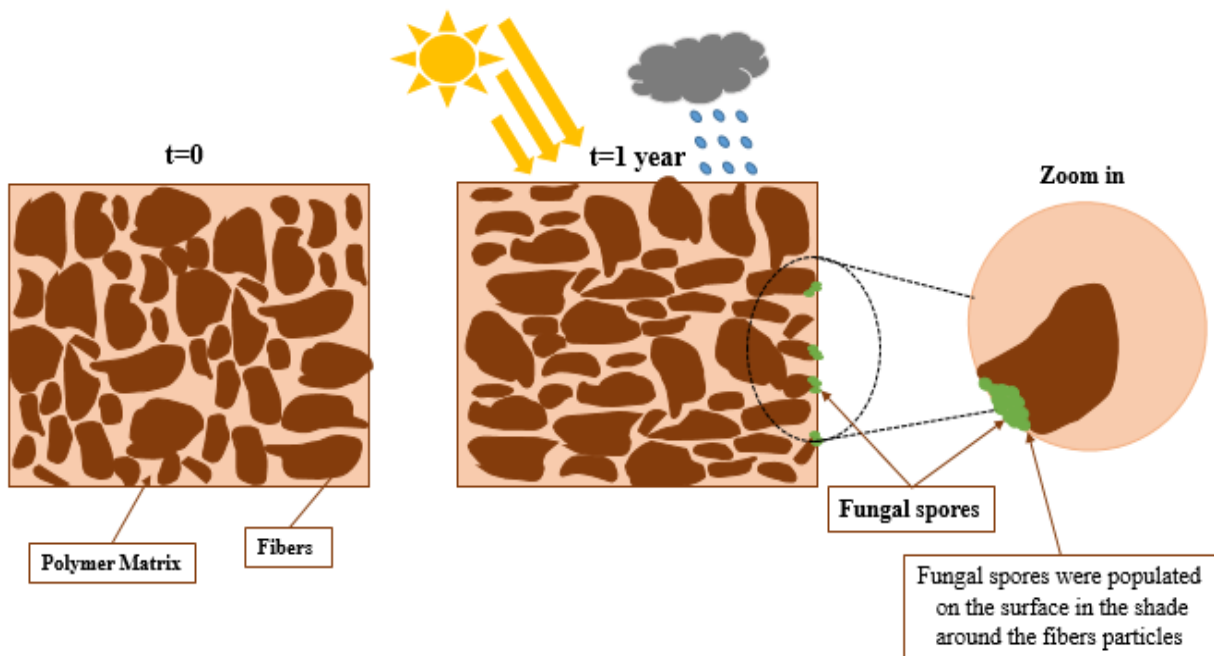


Figure III.4 : Schematic diagram illustrating the controlling factors contributing to the natural weathering of Biocomposites

III.2.4. Effect of natural weathering on thermal properties

The thermal properties of biopolymers are altered by natural weathering, specifically the crystallization of semi-crystalline polymers. In composites, natural fibers promote crystal growth of the polymer matrix, resulting in increased crystallinity and fewer crystal globules. Therefore, these filaments can affect the thermal properties of the deterioration process. When composites are exposed to such environmental conditions, their mechanical performance degrades due to chain scission, molecular weight reduction, and

embrittlement. Composite fatigue efficacy is affected by the type of resin, fiber, and fiber content [16, 17]. analyzed the strong relationship between time and temperature in composite fatigue performance in order to develop a streamlined testing procedure. The arrangement of molecular chains, filler–matrix interfacial adhesion, activation energy, degree of crystallinity, and enthalpic relaxation are modified by thermal aging.

III.2.5. Effect of natural weathering on mechanical properties

The capacity of materials to withstand natural outdoor degradation is one of the essential factors to consider when evaluating the durability of biocomposites for outdoor applications. Mechanical degradation occurs when composites are subjected to constant dynamic and static loads. Typically, pigment variations are observed due to the aging of materials. In addition, aging causes brittleness due to chain scission and crosslinking; increasing mechanical modulus is a creep; "plastic deformation of a material over specified duration." The effect of creep on composites is not solely dependent on stress level or duration but also depends significantly on composition type [18].

Reference

- [1] M. E. González-López, A. S. M. del Campo, J. R. Robledo-Ortíz, M. Arellano, and A. A. Pérez-Fonseca, "Accelerated weathering of poly (lactic acid) and its biocomposites: A review," *Polymer Degradation and Stability*, vol. 179, p. 109290, 2020.
- [2] Z. Wang, C. An, X. Chen, K. Lee, B. Zhang, and Q. Feng, "Disposable masks release microplastics to the aqueous environment with exacerbation by natural weathering," *Journal of hazardous materials*, vol. 417, p. 126036, 2021.
- [3] K. G. Satyanarayana, G. G. Arizaga, and F. Wypych, "Biodegradable composites based on lignocellulosic fibers—An overview," *Progress in polymer science*, vol. 34, pp. 982-1021, 2009.
- [4] T. Sang, C. J. Wallis, G. Hill, and G. J. Britovsek, "Polyethylene terephthalate degradation under natural and accelerated weathering conditions," *European polymer journal*, vol. 136, p. 109873, 2020.
- [5] M. U. Rashid, "Experimental investigation on durability characteristics of steel and polypropylene fiber reinforced concrete exposed to natural weathering action," *Construction and Building Materials*, vol. 250, p. 118910, 2020.
- [6] M. S. S. Hosen, M. E. Hoque, M. Z. Rahman, and S. Sagadevan, "Aging effects on mechanical properties of biocomposites with recycled polymers," in *Aging Effects on Natural Fiber-Reinforced Polymer Composites: Durability and Life Prediction*, ed: Springer, 2022, pp. 317-333.
- [7] N. M. Stark and L. M. Matuana, "Surface chemistry changes of weathered HDPE/wood-flour composites studied by XPS and FTIR spectroscopy," *Polymer Degradation and Stability*, vol. 86, pp. 1-9, 2004/10/01/ 2004.
- [8] L. Küpper, J. Gulmine, P. Janissek, and H. Heise, "Attenuated total reflection infrared spectroscopy for micro-domain analysis of polyethylene samples after accelerated ageing within weathering chambers," *Vibrational Spectroscopy*, vol. 34, pp. 63-72, 01/16 2004.

- [9] S. Mohanty and S. Nayak, "Short Bamboo Fiber-reinforced HDPE Composites: Influence of Fiber Content and Modification on Strength of the Composite," *Journal of Reinforced Plastics and Composites - J REINF PLAST COMPOSITE*, vol. 29, pp. 2199-2210, 07/12 2010.
- [10] C. H. Lee, A. Khalina, and S. H. Lee, "Importance of interfacial adhesion condition on characterization of plant-fiber-reinforced polymer composites: A review," *Polymers*, vol. 13, p. 438, 2021.
- [11] B. P. Chang, A. K. Mohanty, and M. Misra, "Studies on durability of sustainable biobased composites: a review," *RSC advances*, vol. 10, pp. 17955-17999, 2020.
- [12] S. Dinesh, P. Kumaran, S. Mohanamurugan, R. Vijay, D. L. Singaravelu, A. Vinod, *et al.*, "Influence of wood dust fillers on the mechanical, thermal, water absorption and biodegradation characteristics of jute fiber epoxy composites," *Journal of Polymer Research*, vol. 27, pp. 1-13, 2020.
- [13] J.-W. Park, T.-H. Lee, J.-H. Back, S.-W. Jang, H.-J. Kim, and M. Skrifvars, "Phenyl silane treatment and carding process to improve the mechanical, thermal, and water-absorption properties of regenerated cellulose lyocell/polylactic acid bio-composites," *Composites Part B: Engineering*, vol. 167, pp. 387-395, 2019.
- [14] K. Yorseng, S. M. Rangappa, H. Pulikkalparambil, S. Siengchin, and J. Parameswaranpillai, "Accelerated weathering studies of kenaf/sisal fiber fabric reinforced fully biobased hybrid bioepoxy composites for semi-structural applications: Morphology, thermo-mechanical, water absorption behavior and surface hydrophobicity," *Construction and Building Materials*, vol. 235, p. 117464, 2020.
- [15] D. Friedrich, "Effects from natural weathering on long-term structural performance of wood-polymer composite cladding in the building envelope," *Journal of Building Engineering*, vol. 23, pp. 68-76, 2019.
- [16] M. Ahmad Sawpan, M. R. Islam, M. D. H. Beg, and K. Pickering, "Effect of accelerated weathering on physico-mechanical properties of polylactide bio-composites," *Journal of Polymers and the Environment*, vol. 27, pp. 942-955, 2019.

- [17] C. Chastre, P. Faria, J. Neves, M. Ludovico-Marques, H. Biscaia, and L. Nunes, "Testing Durability on Construction Materials," in *Advances on Testing and Experimentation in Civil Engineering: Materials, Structures and Buildings*, ed: Springer, 2023, pp. 29-51.

- [18] A. Vedrtam, S. Kumar, and S. Chaturvedi, "Experimental study on mechanical behavior, biodegradability, and resistance to natural weathering and ultraviolet radiation of wood-plastic composites," *Composites Part B: Engineering*, vol. 176, p. 107282, 2019.

Part II

Experimental Study

Chapter I

Materials and Methods

Chapter I : Materials and Methods

I.1. Materials

I.1.1. Vegetable fibers

Palm petiole fibers (PPF) were gathered through the yearly pruning process of date palm trees (Fig I.1) in the oasis of Biskra (south of Algeria).



Figure I.1: Palm petiole fibers (PPF)

I.1.2. Resin Linear low-density polyethylene

Linear low-density polyethylene resin type (LLDPE 3505 U) used as a matrix was purchased from the Plastic & Consultations Center (Alamirya Alexandria, Egypt). According to the manufacturer, this resin can be used in an extrusion machine or a rotational molding machine. LLDPE 3505 U is known to be a white powder with a particle size of 500 m (Fig I.2.), an actual density of 0.935 g/cm³, a bulk density of 0.37 g/cm³, and a melting flow rate of 5 g/10 min (129 °C, 2.16 kg) according to ISO 1872/1 and ASTM D 1895, ISO 1133, respectively.



Figure I.2: Resin Linear low-density polyethylene (LLDPE)

I.2. Methods

I.2.1. Preparation of petiole fiber

The palm petiole was wash with cold water to remove impurities soluble in cold water, rinse with hot water to remove impurities soluble in hot water, and dry in the air for four days. The petiole was ground using an electric mill and sieving to 250 μm as shown in fig I.3.



Figure I.3 : Preparation of petiole fiber

I.2.2. Chemical modification of palm petiole fibers

In This study, the petiole fibers (PF) were treated with three successive chemical treatments as shown in Fig. I.4.

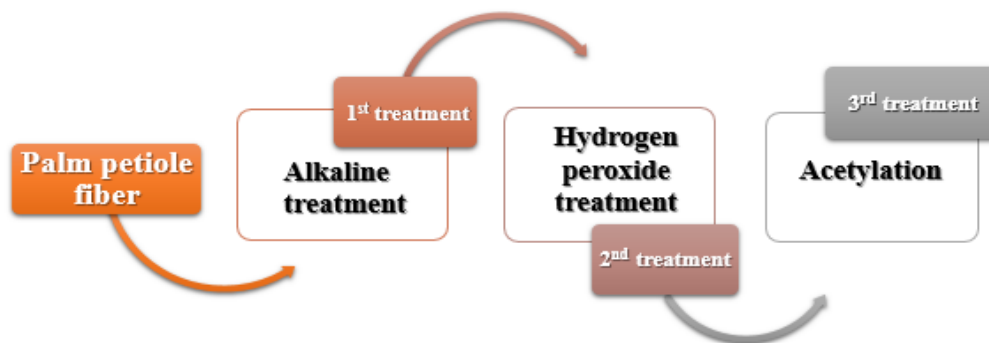


Figure I.4 : Schematic diagram illustrating the chemical modification of palm petiole fibers

a. 1st Treatment: Alkaline

The first treatment is carried out by an alkaline solution, which means intending to extract the maximum amount of hemicellulose and a part of the lignin, the pectins, waxy substances, and natural impurities covering the external surface of the wall of the fiber. The sample is placed in a beaker containing 1L of a 10% soda solution for 72 hours. The whole takes on a dark brown color very quickly. After 72 hours of treatment, the fibers are rinsed several times with distilled water containing 10^{-2} mol/l of hydrochloric acid

HCl to neutralize the excess sodium hydroxide, as shown in Fig I.5. They are finally washed with distilled water until they have a neutral pH. The fibers are then placed in an oven at 80°C for 24 hours.

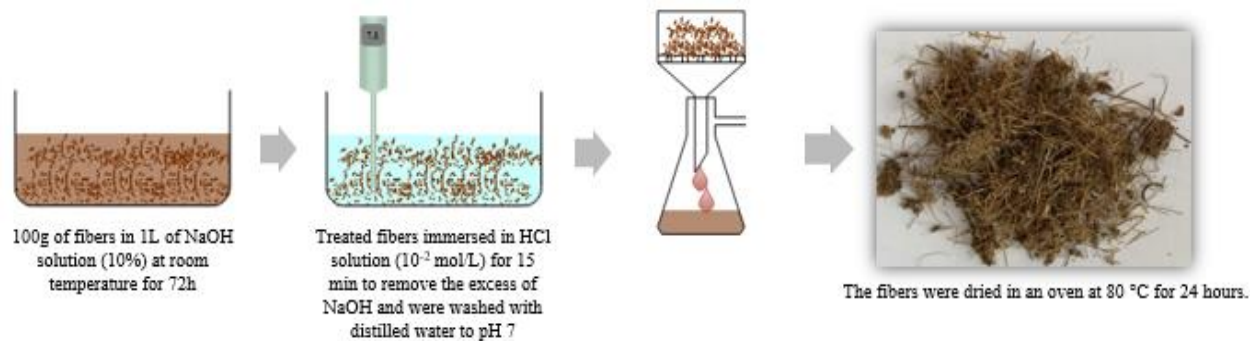


Figure I.5 : Schematic diagram illustrating the first treatment of petiole fibers with a 10% alkaline solution

b. 2nd Treatment: Hydrogen peroxide

Secondary treatment has as its primary objective the elimination of lignin and hemicellulose remaining at the end of the immediate treatment. At the same time, The bleaching of fibers using hydrogen peroxide in an alkaline medium because it allows for obtaining the highest level of whiteness.

The fiber obtained after extraction with soda has a brown color, due to chromophore groups (unsaturated or conjugated bonds). During bleaching, proteins and phenolic molecules are oxidized, solubilized, and removed by filtration. This treatment was carried out in a buffered medium at 25°C to avoid significant degradation of the cellulose. The fibers were bleached at room temperature with hydrogen peroxide (2.5%) and sodium hydroxide at a high pH of 11.5. After 72 hours of treatment, the fibers are filtered and washed with plenty of water until the medium is neutralized. In the end, the fibers are then placed in an oven at 80°C for 24 hours as shown in Fig I.6.

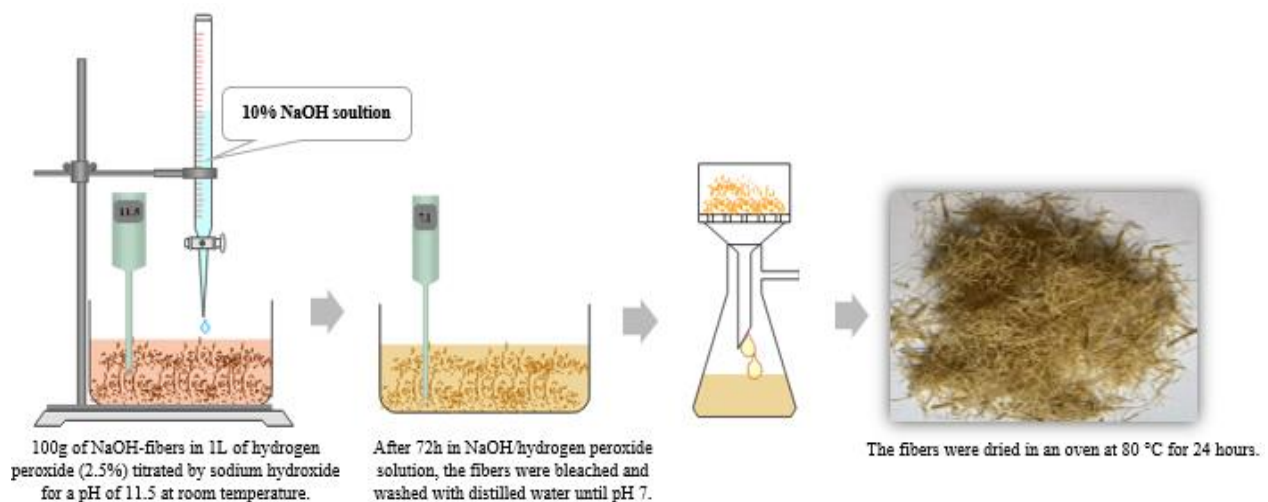


Figure I.6 : Schematic diagram illustrating the secondary treatment of petiole fibers with a 2.5% hydrogen peroxide solution

c. 3rd Treatment: Acetylation

The third treatment aims to replace available hydrophilic OH groups of cellulose extracted with hydrophobic acetyl groups. The sample previously extracted with NaOH and H₂O₂ was acetylated by acetic anhydride in bulk and under the catalytic action of sulfuric acid. The reagent/catalyst ratio used in the present study was proposed by Olaru et al. [1]. Acetic anhydride (10%) was mixed manually with sulfuric acid (5 ml) in a wide-diameter beaker. After adding 100 g of fiber to the reaction medium, the beaker was covered with an aluminum film to minimize the hydrolysis of the acetic anhydride under the effect of the surrounding humidity. The acetylation was carried out at room temperature for 72 h. At the end of the reaction, the fibers underwent a series of washings and filtrations with demineralized water until neutral pH. After washing, the modified fibers were dried at 80 °C for 24 hours as shown in Fig I.7 and I.8.

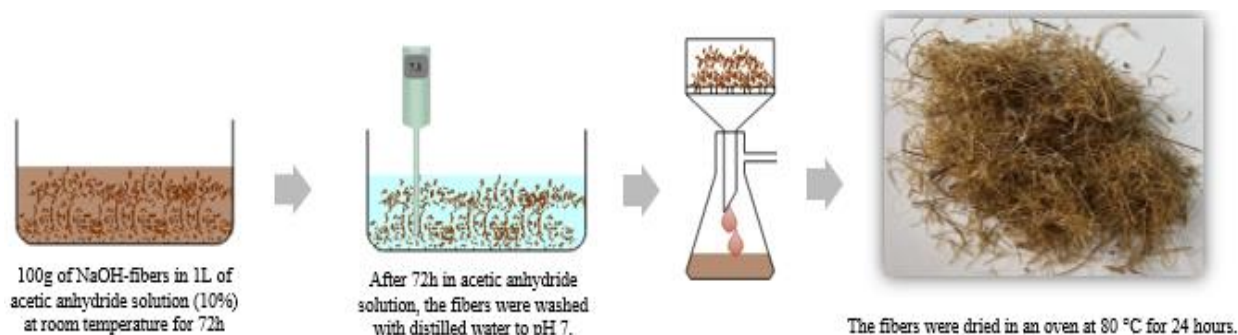


Figure I.7 : A schematic diagram illustrates the treatment of NaOH-petiole fibers modified with a 10% acetic anhydride solution.

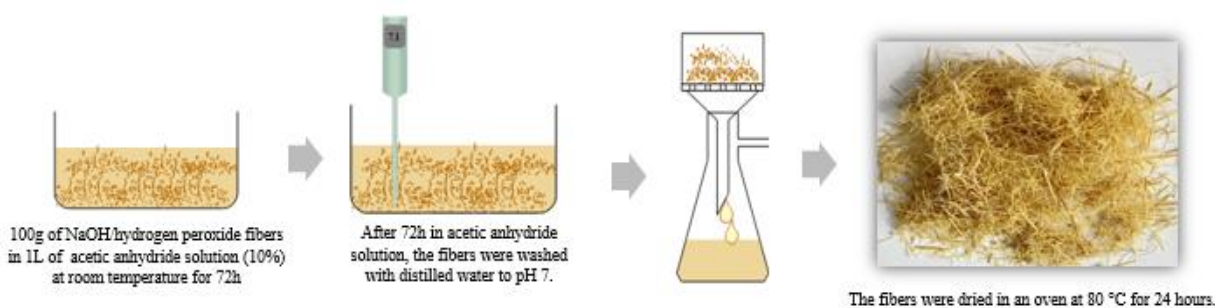


Figure I.8 : A schematic diagram illustrates the treatment of (NaOH/H₂O₂)-petiole fibers modified with a 10% acetic anhydride solution

The fibers samples were referred to by the method of modification they had been subjected to:

- **FU**: unmodified fibers.
- **FN**: NaOH-modified fibers.
- **FNH**: 1-NaOH, 2-hydrogen peroxide-modified fibers.

- **FNA:** 1-NaOH, 2-acetic anhydride-modified fibers.
- **FNHA:** 1-NaOH, 2-hydrogen peroxide, 3-acetic anhydride-modified fibers.

I.2.3. Mechanical modification of petiole fiber

The humidity character of the fibers leads to the formation of agglomerations during mixing in the molten state with the granules of the thermoplastic matrix by a mono-screw extruder, where the agglomerates are considered breaking points that cause the embrittlement of the composite plates. The objective of mechanical treatment is to reduce the petiole's size and eliminate the bulky fibers using a succession of increasingly fine grids. The dried fibers were crushed into smaller sizes by the mortar grinder (Make: Retsch, Model: RM 200, Germany) and sieved to a granulometry of 38 μm by the sieve shaker (Make: Retsch, Model: AS 200, Germany) as shown in Fig. I.9.



Figure I.9 : Mechanical modification of petiole fiber

I.2.4. Elaboration of composites

a. Extrusion of Linear low-density polyethylene/Petiole fibers

The different mass proportions of each of the powders of Linear low-density polyethylene and the petiole fibers that go into each formulation have been mixed for about 10 minutes to ensure that the maximum possible homogeneous mixtures are obtained and where the LLDPE/palm petiole fibers composite was prepared with different formulations listed in Table I.1, with a co-rotating mono-screw

extruder machine (Make: Thermo Scientific, Model: Polylab QC, Germany) equipped with four heating zones.

Table I.1: Composition of the different formulations

Formulation	Composition %	
	LLDPE	Fibers
LLDPE	100	0
LLDPE/FU 15%	85	15
LLDPE/FU 25%	75	25
LLDPE/FN 15%	85	15
LLDPE/FN 25%	75	25
LLDPE/FNH 15%	85	15
LLDPE/FNH 25%	75	25
LLDPE/FNA 15%	85	15
LLDPE/FNA 25%	75	25
LLDPE/FNHA 15%	85	15
LLDPE/FNHA 25%	75	25

Initially, the cylinder of the extruder must be cleaned with polyethylene, and the screw speed of the cylinder is adjusted to 2 rpm; the temperature of four zones was set at 100, 120, 125, and 130 °C along the extruder. Then, The material moves along the screw; it's exposed to heat generated by external heaters or internal heating elements within the barrel. The heat softens and melts the material, converting it into a dense molten state. The rotation of the screw also helps to mix and homogenize the molten material, ensuring uniform composition.

As the material progresses along the screw, it enters the compression zone. Here, the channel depth of the screw decreases, leading to increased pressure within the barrel. This pressure buildup helps to refine the material's homogeneity and eliminate air bubbles. Depending on the desired product, the extruder may be equipped with various types of dies, including round or flat. The molten material passes through the mold, which shapes it into the desired form. Cooling systems may rapidly cool and solidify the extruded material as it exits the mold. Cutting mechanisms such as rotating blades or guillotine cutters are employed at the exit of the mold. This step ensures consistent product dimensions as shown in Fig I.10.

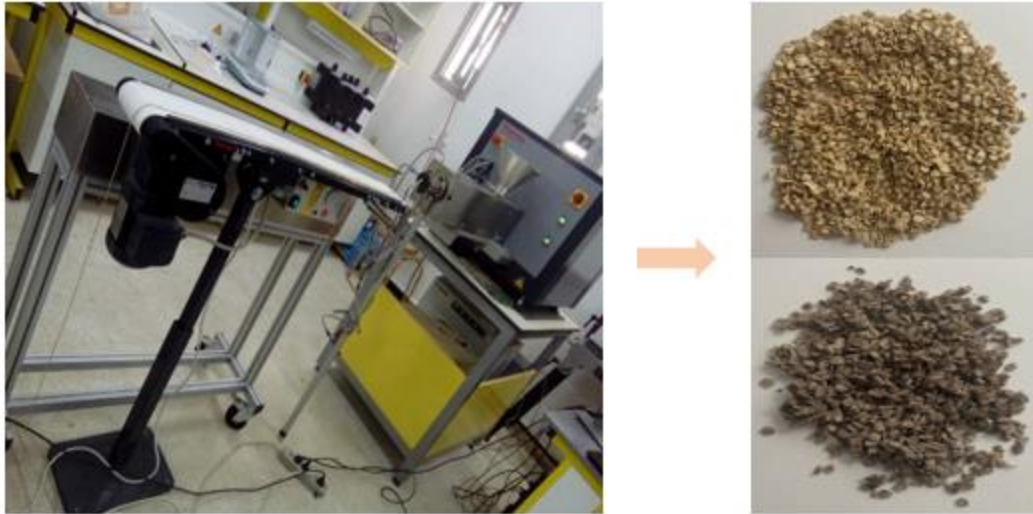


Figure I.10 : Mono-screw extruder machine (Model Polylab QC)

b. Compression molding

The extruded composites were compressed with a hydraulic press machine (Make: schwabenthan polystat, Model: 300S, Germany), Fig I.11. The press is turned on and left in a warm-up state until its temperature reaches 140°C. The small pieces obtained are placed in a mold between two sheets of aluminum under the following conditions:

The temperature is 140° C, under a pressure of 300 bars and for a residence time of 3 min and the plates require 50g weight for each mix. A preheating is carried out until a preliminary melting of the mixture to avoid the presence of air bubbles; a degassing is carried out before applying the final pressure.



Figure I.11 : Hydraulic press Schwabenthan polystat (Model 300S)

I.2.5. Natural weathering test

This test was carried out for 12 months by direct exposure of LLDPE/PPF composite to natural weathering. The specimens were suspended in an iron wire facing the sun, as shown in Fig I.12.

The weather condition data were collected from May 2021 to April 2022 in Biskra, Algeria, and are summarized in Table I.2. The average temperature range was 26.16667 °C, the average relative humidity was 42.5 %, the total rainfall was 1.391667 mm, and the entire duration of sunlight was 282.6083 h. The composite samples were referred after natural weathering with :

- LLDPEw, LLDPE/FUw, LLDPE/FNw, LLDPE/FNHw, LLDPE/FNAw and LLDPE/FNHAw



Figure I.12 : Experimental set-up for neat LLDPE, treated and untreated composites on natural weathering test

Table I.2: The weather condition data from May 2021 to April 2022 in Biskra, Algeria

Month	May	June	July	Aug	Sept	Oct	Nov	Dec	Janu	Feb	Mar	Apr
T (°C)	27	31	37	36	33	32	36	15	11	14	17	25
Humidity %	45	40	35	30	35	40	45	50	55	50	45	40
UV indice	5-10	10-11	11-12	12-13	11-12	10-11	8-10	6-8	4-6	5-7	6-8	6-10
Sunlight (h)	322.5	348.3	362.9	354.1	314.2	279.2	239.2	206.6	201.8	217.9	250.1	294.5
Rainfall (mm)	1.2	0.1	0.1	1.5	1.7	1.9	1.8	1.3	3.2	1.2	1.2	1.5

Reference

- [1] N. Olaru, L. Olaru, C. Vasile, and P. Ander, "Surface modified cellulose obtained by acetylation without solvents of bleached and unbleached kraft pulps," *Polimery*, vol. 56, pp. 834-840, 2011.

Chapter II

Techniques of

Characterization

Chapter II : Techniques of Characterization

To demonstrate the chemical modification of the palm petiole fibers and the performance of the composite materials developed, different tests were used, namely:

II.1. Fourier Transform Infrared Spectrometry (FTIR)

An infrared spectrometer makes it possible to know the chemical nature of a product by identifying specific absorption bands present on the spectrum. Each absorption band corresponds to a chemical bond vibration pattern between two atoms. It provides information about the molecular structure of a particular compound by detecting the presence of functional groups in that compound [1]. We acquired the infrared spectra with a PerkinElmer Spectrum Two with an ATR-FTIR unit, (Fig II.1.) although several IR is available, the most common ones are made of synthetic diamonds. Diamond is both chemically inert and IR-transparent but is also complex and, as a result, can withstand high pressures. At the diamond sample interface, the IR light penetrates the sample only a few micrometers and analyzes the characteristic peaks of palm petiole fibers before and after treatments. The fiber was placed on a diamond crystal with a resolution of 2 cm^{-1} and analyzed in a spectral range of $400\text{--}4000\text{ cm}^{-1}$.

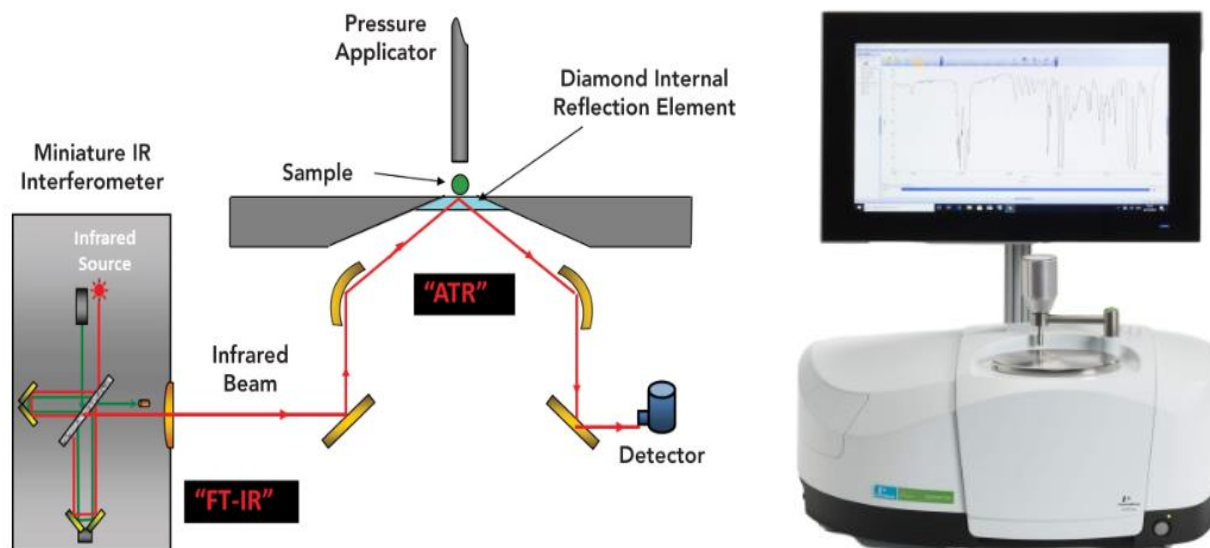


Figure II.1 : Principle of PerkinElmer Spectrum Two with an ATR-FTIR unit

II.2. Scanning electron microscopy (SEM)

Scanning electron microscopy (SEM) is an electron microscopy technique based on the principle of electron-matter interactions, capable of producing high-resolution images of the surface of a sample. The principle of SEM consists of an electron beam scanning the surface of the sample to be analyzed, in response, re-emits certain particles which are analyzed by different detectors, thus making it possible to reconstruct a virtual image of the object observed by SEM in three dimensions from the surface [2].

The images were taken by a Thermo Scientific Quanta SEM Prisma E electron microscope made in the USA (Fig II.2.) Image resolution can be up to 3 nm at 30 kV to 7 nm at 3 kV. The image obtained gives a topographic view of the surface with a much greater depth of field than in optical microscopy. An accelerating voltage of 10-15 kV was used to avoid the degradation of the sample, which would take place if the speed of impact of the incident electrons on the object was too great.

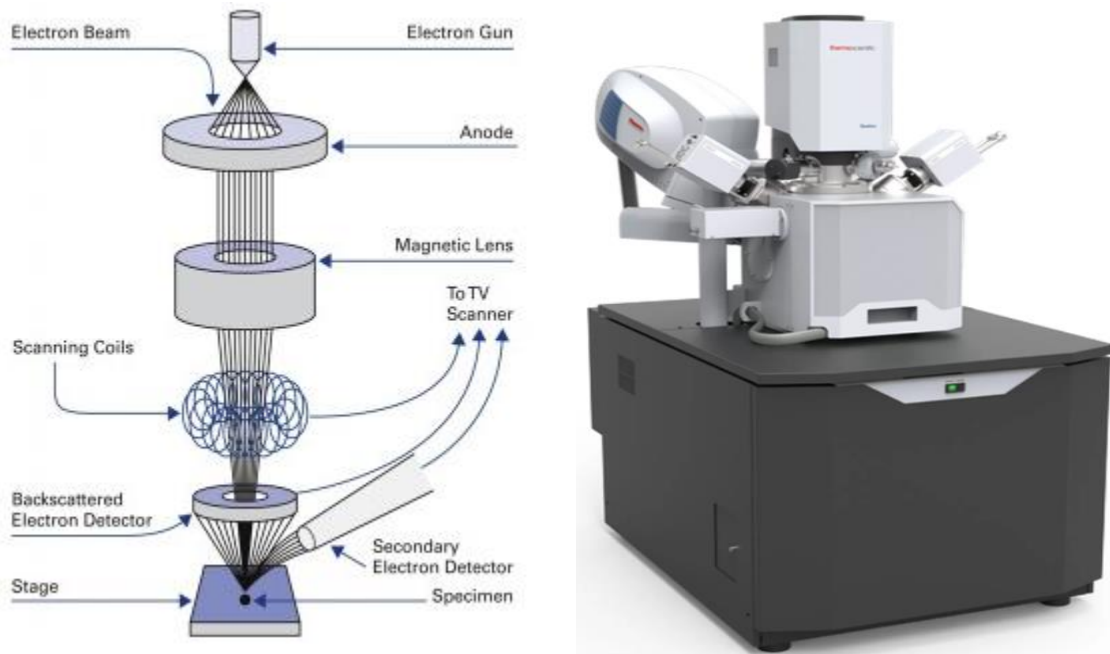


Figure II.2 : Principle of Thermo Scientific Quanta SEM Prisma E electron microscope

II.3. Differential Scanning Calorimetry (DSC)/Thermogravimetric analysis (TGA)

Differential Scanning Calorimetry (DSC) is a technique used to study the behavior of polymers when heated. This involves recording the exo or endothermic effects caused by physical or chemical modifications of the materials. In contrast, the Thermogravimetric analysis (TGA) is a thermal analysis technique that allows for measuring the amount and rate of change in mass of a sample as a function of temperature and

time. It makes it possible to evaluate any group or phase variations lost when the material decomposes, dehydrates, or oxidizes and determine the degradation area [3].

The coupled thermogravimetric analyzer (TGA/DSC) device is a SETARAM Instrumentation LABSYS evo (Fig II.3). The test portion varies between 20 and 70 mg of sample, and the heating rate is 5°C/min under a standard atmosphere. The results of a TGA measurement are usually displayed as a curve in which mass or mass percentage varies with temperature or time. The results can also be presented as variations of the TGA curve's first derivative as a temperature or time function. This derivative tells us about the rate at which mass change occurs and is known as the differential thermogravimetric or DTG curve. The difference in mass occurs when the sample loses material or reacts with the surrounding atmosphere; different phenomena can cause weight loss or gain, and the glass transition temperature T_g is taken at the "ONSET" point from the DSC thermogram, and the polymerization reaction's exothermic heat (ΔH) is calculated from the exothermic peak limited by the baseline.

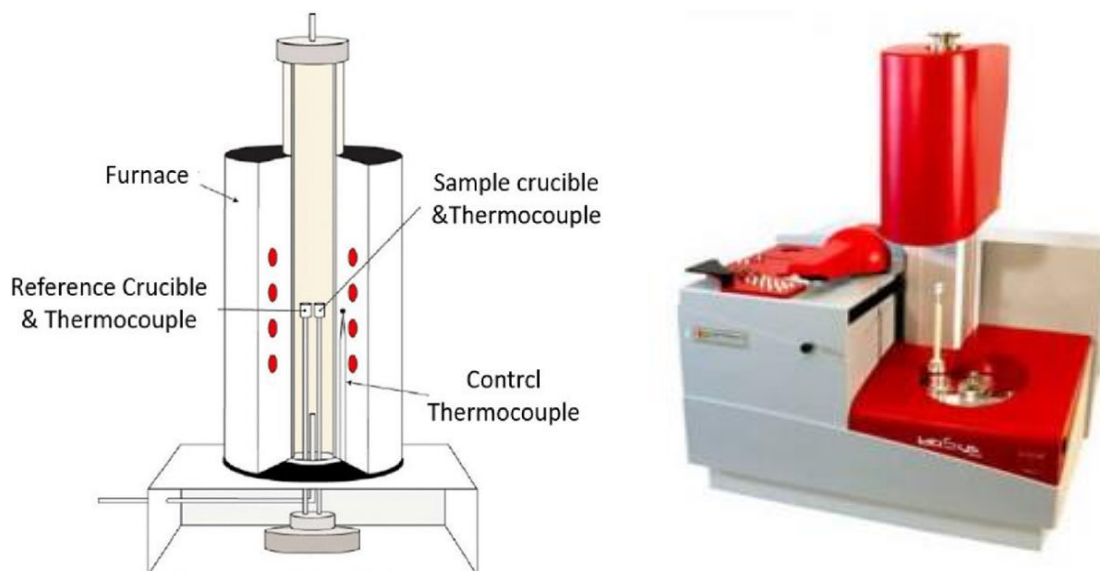


Figure II.3 : Principle of Thermogravimetric SETARAM Instrumentation LABSYS evo

II.4. Dynamic mechanical analysis (DMA)

Dynamic mechanical analysis consists of measuring the response of a material following dynamic stress as a function of frequency and temperature. It gives valuable information on the moduli of conservation (E') and loss (E'') and the tangent of the angle of loss $\tan \delta$.

- E' is the component of the modulus in phase with the deformation, which corresponds to the energy accumulated in elastic form and is known under the modulus of conservation or elastic modulus.

- E'' represents the viscous component of the material. Viscosity reflects its ability to dissipate mechanical energy. This phenomenon is associated with the friction of the chains of molecules and their flow, and it is called the loss modulus.
- The ratio between the loss modulus and the storage modulus defines the tangent of the loss angle ($\tan \delta = E''/E'$). This quantity represents the proportion of energy dissipated compared to the elastic energy stored during a deformation cycle [4].

The composites were analyzed using the TA instrument DMA Q800 three-point bending machine (Fig II.4). The tests were conducted by subjecting rectangular samples, with an estimated size of $59.70 \times 12.80 \times 3.18$ mm, to a strain of 1 mm at a frequency of 1 Hz. The temperature was gradually increased from 20 to 80 °C at a heating rate of 2 °C/min to avoid thermal gradients in the sample as shown in Fig II.4.

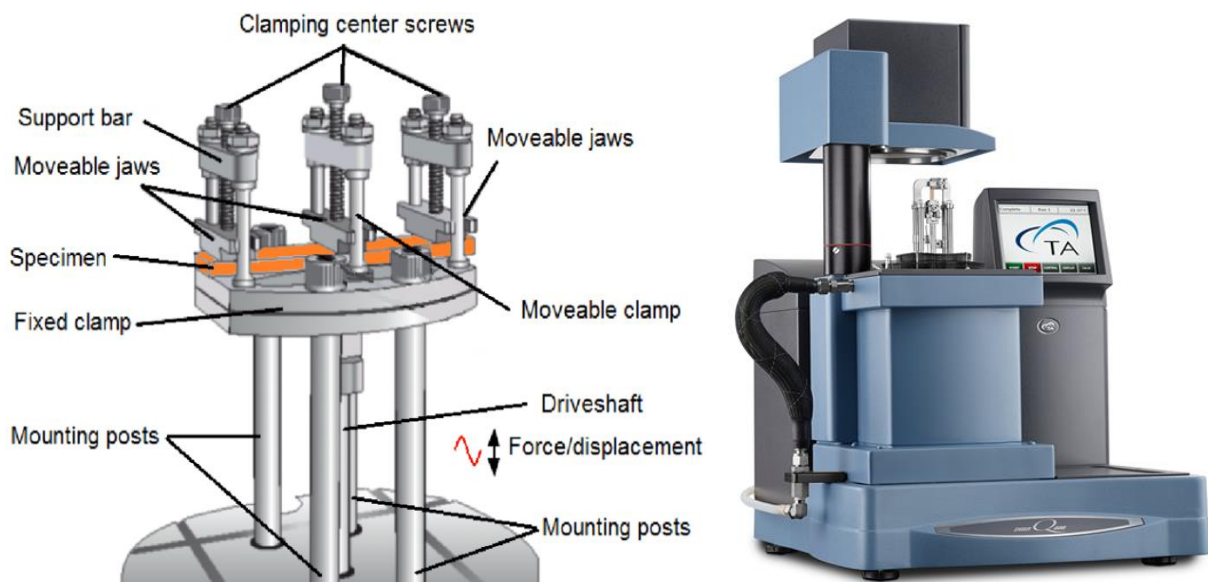


Figure II.4 : Principle of TA instrument DMA Q800 three-point bending machine

II.5. Tensile test

The tensile test is used most to evaluate fiber-matrix interactions within composite materials. The principle of this test consists in fixing the two ends of a composite specimen in the jaws of the tensile machine. The machine then applies a tensile force, causing the specimen to lengthen until it breaks gradually. During a tensile test, the force applied to the specimen and the elongation of the test piece is measured simultaneously. The force applied was measured by the testing machine, and the elongation was measured using an extensometer. The recorded data makes it possible to establish a stress-strain curve.

Initially, the composite's elastic deformation is characterized by a linear relationship between stress and strain. In this zone, the mechanical behavior of the composite is characterized by a modulus of elasticity which represents the slope of the stress-strain curve. Beyond the linear zone, the deformation of the material is irreversible, the material crosses the barrier of elasticity, and there is a plastic deformation that continues until the specimen breaks [5].

We used an Instron Universal Testing Machine, Instron 5969 (Fig II.5), controlled by Bluehill3 software. The test was conducted at room temperature with cells having a maximum capacity of 5 kN, and the test was carried out at a 5 mm/min speed. The tensile testing specimens were prepared according to (ISO 527-2, geometry type 1A) specific dimensions. The samples used in ISO 527-2 are rectangular and have a standardized length, width, and thickness. The parameters are listed in Table II.1, and the specimens' measurements are given in Fig II.6.



Figure II.5 : Instron Universal Testing Machine, Instron 5969

Table II.1: Specimen dimensions according to ISO 527-2

l₁	30.0 ± 0.05 mm
l₂	58 ± 2 mm
l₃	75 mm
L₀	25.0 ± 0.5 mm
L	12 ± 2 mm
h	2 mm
r	30 mm
b₁	5.0 ± 0.5 mm
b₂	10.0 ± 0.5 mm

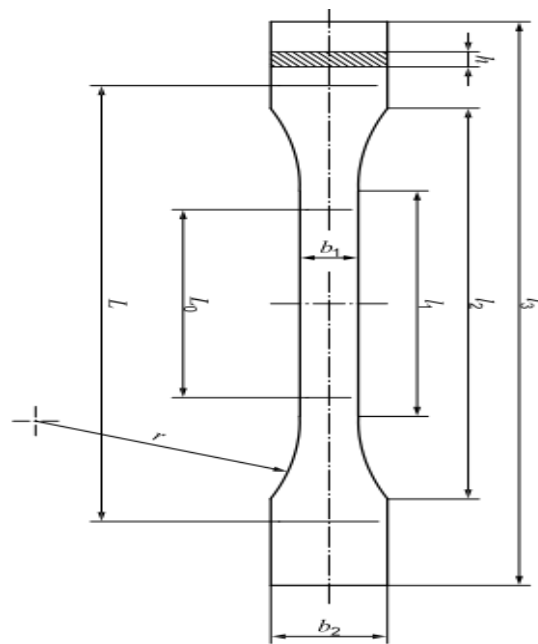


Figure II.6 : Tensile testing specimens type 1A

II.6. Three-point bending

Three-point bending is a test method used to measure the mechanical properties of composite materials. The specimen is placed between two supports, and a force is applied in the middle of the specimen. The force causes a deformation of the specimen, which is measured. The material's mechanical properties, such as flexural strength, modulus of elasticity, and yield strength, can be calculated from the deformation of the specimen [6].

Flexural tests were done in the three-point bending mode according to ISO 178 using Instron Universal Testing Machine, Instron 5969. The prescribed size for the specimens used in the test is a length of 80 mm, a width of 10 mm, and a thickness between 2 and 4 mm, as shown in Fig II.7.

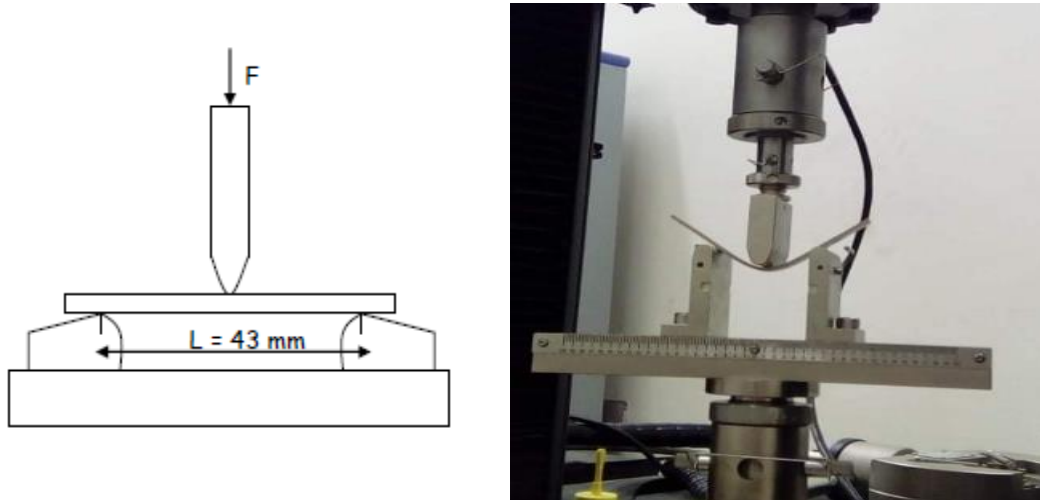


Figure II.7 : Principle of flexural three-point according to ISO 178 using Instron Universal Testing Machine, Instron 5969

II.7. Hardness

The shore hardness of a composite material is a measure of a material's resistance to penetration by an indenter. Shore hardness is measured on a scale of 0 to 100, where 0 is the softest and 100 is the hardest. There are two Shore hardness scales: Shore A and Shore D. The Shore A scale is used for soft materials, while the Shore D scale is used for hard materials. Many factors, such as the type of matrix, reinforcement, the matrix/reinforcement ratio, and the manufacturing process, influence the shore hardness of composite material [7]. Shore hardness is an important parameter when designing composite structures, as it affects the material's deformation resistance, fatigue resistance, and fracture toughness. Shore hardness is expressed as follows:

$$\text{Hard Shore } X = M$$

X: being the lure corresponding to the type of Shore durometer used: A or D.

M: Calculated average value.

The test specimen may have any shape (square, rectangular, or disk) provided that the dimensions allow obtaining at least five measurements at different locations spaced apart from each other by at least 6 mm and from the edges of the specimen of at least 12 mm. The face of the specimen on which the measurement is to be made must be as flat as possible. Using specimens with two parallel faces is preferable to have the

test face flat and horizontal. The durometer used in the shore A hardness measurements of the composites studied is of the Zwick Roell type according to the ASTM D 2240 standard (Fig II.8).

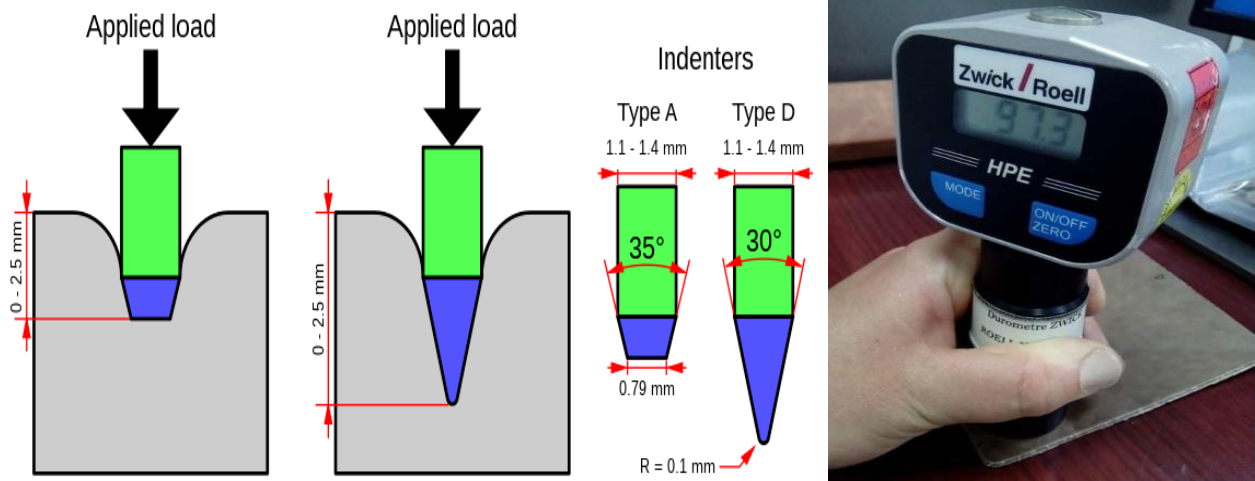


Figure II.8 : Principe of the Zwick-Roell Durometer

Reference

- [1] S. Veerasingam, M. Ranjani, R. Venkatachalapathy, A. Bagaev, V. Mukhanov, D. Litvinyuk, *et al.*, "Contributions of Fourier transform infrared spectroscopy in microplastic pollution research: A review," *Critical Reviews in Environmental Science and Technology*, vol. 51, pp. 2681-2743, 2021.
- [2] N. Ural, "The significance of scanning electron microscopy (SEM) analysis on the microstructure of improved clay: An overview," *Open Geosciences*, vol. 13, pp. 197-218, 2021.
- [3] C. Leyva-Porras, P. Cruz-Alcantar, V. Espinosa-Solís, E. Martínez-Guerra, C. I. Piñón-Balderrama, I. Compean Martínez, *et al.*, "Application of differential scanning calorimetry (DSC) and modulated differential scanning calorimetry (MDSC) in food and drug industries," *Polymers*, vol. 12, p. 5, 2019.
- [4] M. A. Bashir, "Use of dynamic mechanical analysis (DMA) for characterizing interfacial interactions in filled polymers," *Solids*, vol. 2, pp. 108-120, 2021.
- [5] A. Sola, W. J. Chong, D. P. Simunec, Y. Li, A. Trinchi, I. L. Kyratzis, *et al.*, "Open challenges in tensile testing of additively manufactured polymers: A literature survey and a case study in fused filament fabrication," *Polymer Testing*, p. 107859, 2022.
- [6] S. Cao, G. Xue, and E. Yilmaz, "Flexural behavior of fiber reinforced cemented tailings backfill under three-point bending," *IEEE Access*, vol. 7, pp. 139317-139328, 2019.
- [7] G. Pintaude, "Hardness as an indicator of material strength: A critical review," *Critical Reviews in Solid State and Materials Sciences*, vol. 48, pp. 623-641, 2023.

Part III

Results and discussion

Chapter I

Characterization of the

Palm Petiole Fibers

Chapter I : Characterization of the Palm Petiole Fibers

This study aims to characterize treated and untreated petiole fibers (NaOH sodium, hydrogen peroxide, and acetic anhydride). The identification of functional groups resulting from the chemical treatments was demonstrated by FTIR spectroscopic analysis, and the effect of the modification on thermal and morphological properties was also examined by ATG/DTG and DSC thermal analysis and scanning electron microscopy (SEM).

I.1. FTIR Spectroscopy

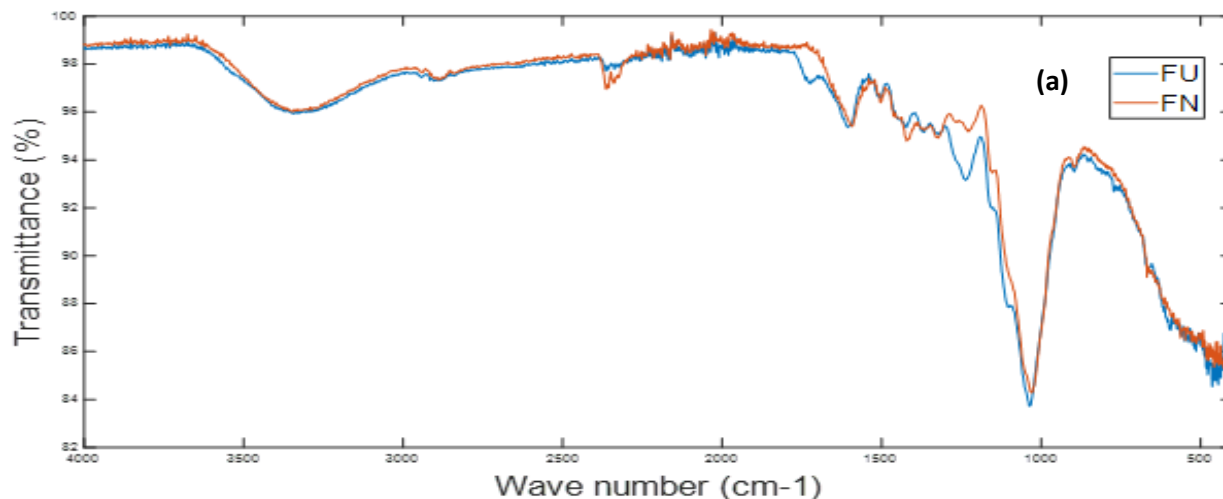
The infrared spectra of palm petiole fibers before and after three pretreatments are shown in Fig I.1. The fibers have been modified to remove impurities and waxes, all while minimizing the absorption of water. The peak at 3340 cm^{-1} corresponds to the O-H stretching of hydrogen bonds. The decreased intensity of the peak at 3340 cm^{-1} after alkali treatment is due to the extraction of lignin, hemicellulose, and other constituents from the fiber surface, resulting in a large number of exposed O-H groups. As a result, the fibers become more hydrophilic. The peaks at 1723 cm^{-1} are attributed to C=O stretching vibration in the carboxylic acid in lignin or ester groups of hemicellulose and pectin for untreated fibers.

The intensity of those peaks is reduced by 10% when palm petiole fibers are treated with NaOH. The carbonyl groups of lignin have a wavenumber of roughly 1598 cm^{-1} . This peak appears in FU, but the intensity of those peaks in FN has decreased, which indicates that lignin has been reduced by NaOH treatment. The peak at 1224 cm^{-1} is responsible for the C–O stretching of acetyl lignin and it was removed by 10% in FN. The C–H bending deformation of hemicellulose is attributed at 1367 cm^{-1} in FU. This intensity was removed by the NaOH treatment [1]. The intensity of the peak at 1103 cm^{-1} also notes the decrease, which is attributed to the elongation of the C-O-C ether groups of lignin. This reduction is due to the solubilization of lignin, hemicellulose, waxes, and pectins in sodium hydroxide [2].

After the double pretreatment with NaOH/H₂O₂ solution, the large quantities of hemicelluloses and lignins can be removed, and the hard structure can be broken. Increasing cellulose solubility caused the peak at 3340 cm^{-1} to grow stronger due to the breaking of the hydrogen bond. The peak at 1723 cm^{-1} , attributed to C=O, became weaker because hemicelluloses and lignin are soluble in NaOH and H₂O₂.

During NaOH/ H₂O₂ treatment, the peak at 1650 cm⁻¹ attributed to H-O-H bending or aromatic C=C stretching was significantly reduced [3]. The decreases in peaks assigned to hemicellulose and lignin show that bleaching could eliminate part of the hemicellulose and lignin in the fibers. As shown in Fig. I.1, the intensities of the C=C stretching of aromatic lignin and the symmetric bending of CH₂ in hemicellulose at 1505 cm⁻¹ and 1422 cm⁻¹ respectively [4] in the spectra of FNH were clearly higher than those in the spectra of FN. When compared to NaOH treatment, this indicates that bleaching with NaOH/ H₂O₂ is substantially more effective at removing lignin.

On the other hand, the advantage of the acetylation process with acetic anhydride is that it creates chemical bonds with the structure of the fibers, which allows the creation of a coating that protects against moisture [5]. The appearance of the peaks in the regions of 1723 cm⁻¹ and 1238 cm⁻¹ was attributed to the axial deformation of (C=O)-O and C=O from acetyl groups, respectively, (Fig I.1), and confirmed the incorporation of the acetyl groups into the palm petiole fibers molecule. Both peaks were characterized by strong peaks in FNA when compared with FN. The peak of the C-H stretching in the acetyl group is observed at 1367 cm⁻¹ [6]. The presence of impurities, wax, and lignin on the surface, and the hydrophilic characteristics, are the variables that contribute to poor fiber-polymer matrix adhesion. For this reason, we modified the surface of the fiber to improve the adhesion interfacial.



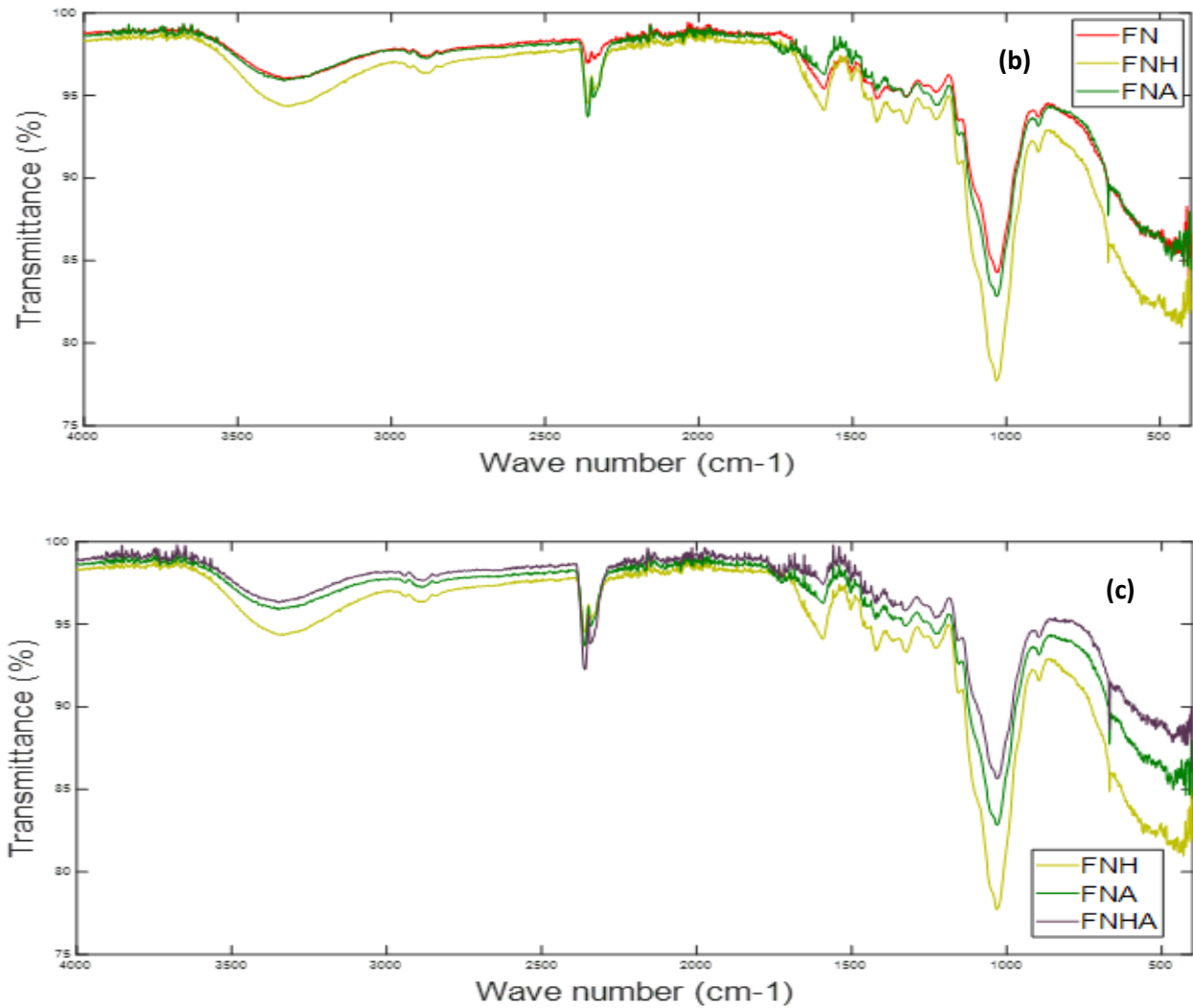


Figure I.1: FTIR spectra of raw and chemically treated fibers.

I.2. Morphological characterization (SEM)

The morphological study investigated the characteristic morphology of the size, appearance, and topography of treated and untreated palm petiole fibers (PPF).

As shown in Fig I.2. Untreated fibers are long and have a unique morphology characterized by their high aspect ratio (length to diameter ratio) gives them high tensile strength and modulus; this makes them well-suited for applications where high strength and stiffness are required, such as in structural composites.

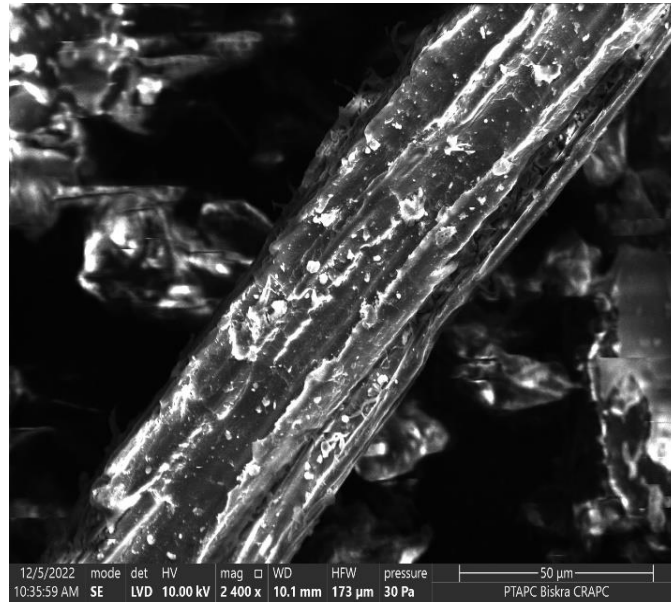


Figure I.2: SEM micrographs of untreated petiole fiber (FU)

As shown in Fig I.3 (a). The alkaline treatment removes impurities such as hemicellulose, lignin, and pectin, enhancing the adhesion to the polymer matrix; the treatment also causes the fiber to swell and become more flexible. Removing impurities exposes the underlying cellulose fibers, which are the most vital component of the fiber, where the swelling of the fiber increases its surface area and flexibility [7].

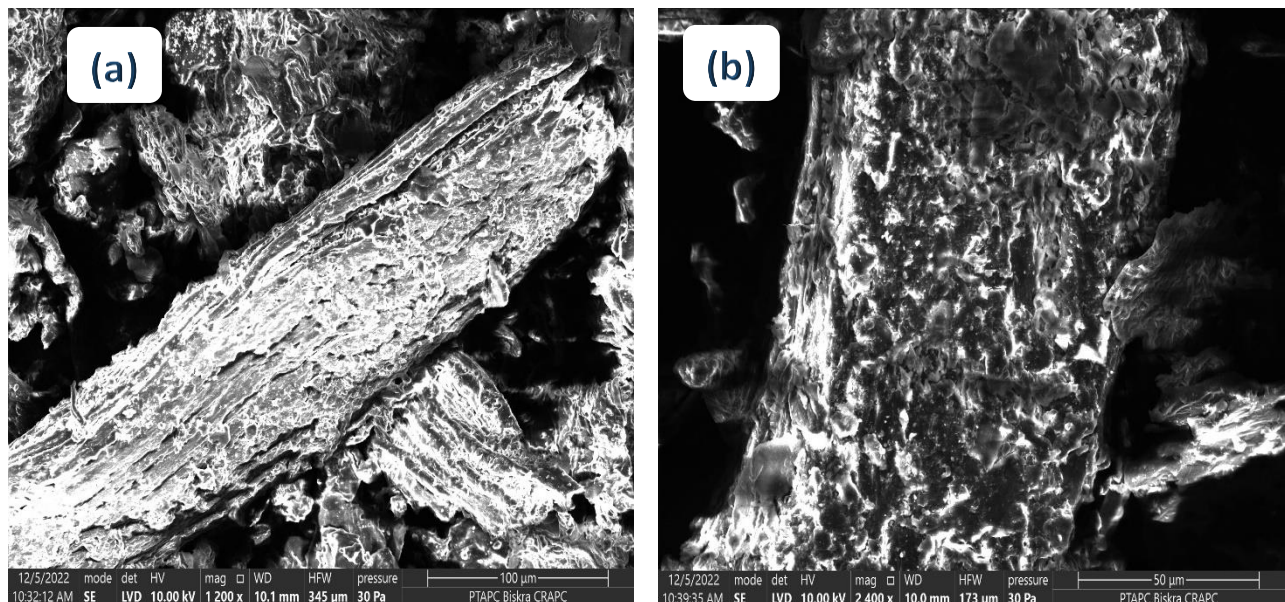


Figure I.3: SEM micrographs of treated petiole fiber (a) FN and (b) FNH

The difference in the fiber surface morphology after hydrogen peroxide/alkaline treatment is due to the cuticle's removal and the lumen's opening, as shown in Fig I.3 (b).

The cuticle is a waxy layer that covers the surface of plant fibers and protects them from moisture and abrasion. The alkaline solution then opens the fibers' lumen, allowing water and other molecules to penetrate the fibers. The treatment results in a decrease in fiber diameter, an increase in fiber length, and a change in the fiber surface morphology. The reduction in fiber diameter is due to removing more lignin and hemicellulose from the fiber surface. The increase in fiber length is due to the separation of the fiber bundles between as [8].

The acetylation process modifies the PPF surface by replacing the hydroxyl groups' hydrogen atoms in the fiber cell membrane with acetyl groups. This reduces the fiber's polarity, removes waxy material from the surface, and causes the fiber diameter to increase slightly due to the deposition of acetyl groups on the fiber surface and also reduces the roughness of the fiber surface due to the removal of waxy material, as shown in Fig I.4 (a) and I.4 (b). Acetylation treatment also increases the fiber's crystallinity due to the cellulose molecules' cross-linking [9].

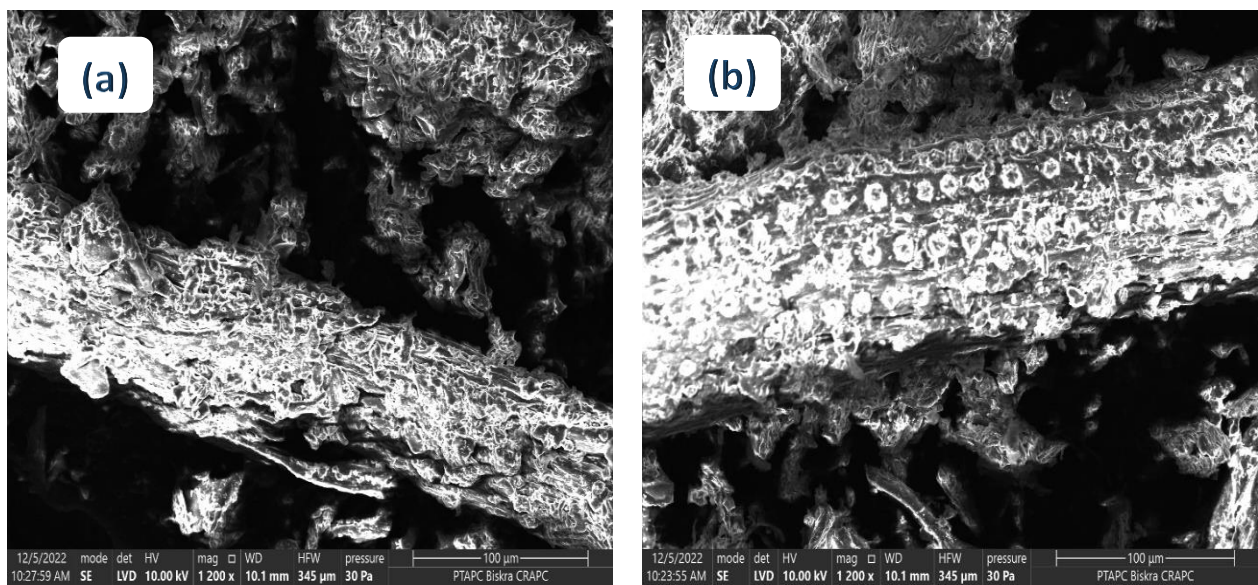


Figure I.4 : SEM micrographs of treated petiole fiber (a) FNA and (b) FNHA

I.3. Thermal analysis

I.3.1. Thermogravimetric analysis (ATG/DTG)

Thermal stability is commonly evaluated by determining the onset temperature of thermal decomposition and was used to measure the weight loss of composites as a function of rising temperature. Higher decomposition temperatures give greater thermal stability.

Fig I.5. shows the fibers' thermal degradation curves as a function of the chemical treatment of palm petiole fibers. All fibers presented two stages: a first stage with a slight weight loss in the range of (30-180 °C), due to the release of humidity retained in the fiber component, and a second stage where hemicellulose and lignin degradation happened (200-310 °C), while another loss of mass at (310-450 °C), is related to the degradation of the cellulose. The release of noncombustible gases, such as carbon dioxide can explain it, and carbon monoxide is present in the samples containing high cellulose content [10]. The final process is around (450-700 °C), which produces a reactive coal residue. Table I.1, indicates the degradation stages.

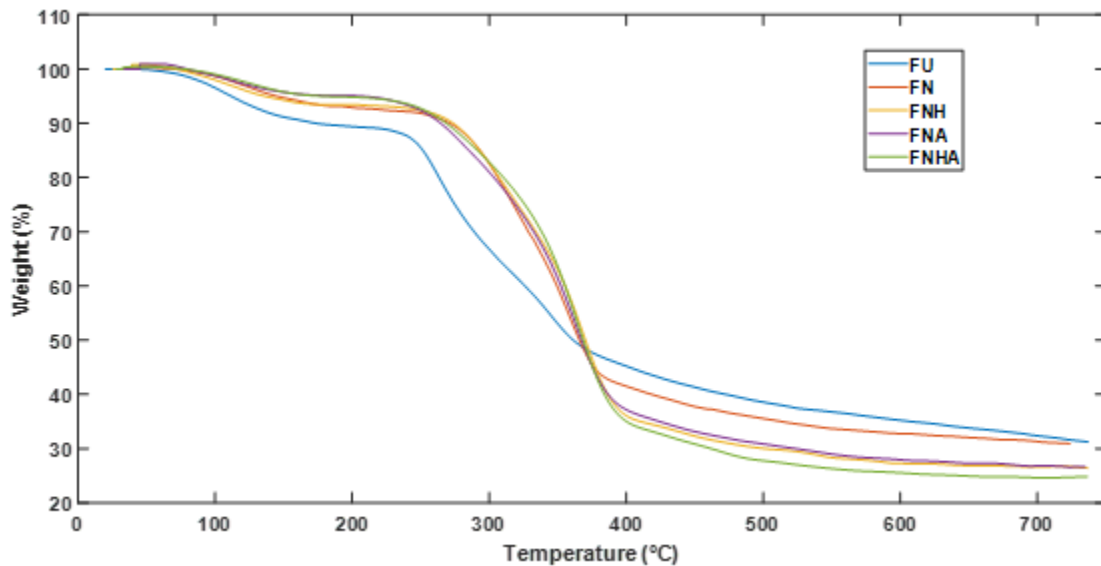


Figure I.5: TGA curves of treated and untreated palm petiole fiber

After treatment with the alkali solution, the initial temperature of decomposition of the fiber (FN) increased to 255.5 °C, compared to the untreated fiber (FU) at 221.8 °C. This indicates that the alkali solution treatment improved the thermal stability of the petiole fiber [11]. This is possibility due to the fact that the relative content of lignin and hemicellulose in the petiole fiber decreased after the alkali treatment.

The TGA curve for FNH shows that the NaOH/H₂O₂ treatment was the most thermally stable, at 260 °C, compared to the other treatments, but in the middle of the process, the mixed treatment showed a behavior similar to or slightly superior to the alkali. Consequently, from the thermal analysis, it is revealed that NaOH/H₂O₂ is more effective in the removal of non-cellulosic materials than conventional NaOH treatment, resulting in better thermal stability according to [12].

From these thermograms Fig. I.5. We can infer that acetylated petiole fiber (FNA) exhibits higher thermal stability compared to untreated fiber (FU). This may be attributed to the substitution of OH groups by more voluminous ones, thereby the stability of hemicellulose has been increased during acetylation [13]. It is also partially due to the fact that some components of the fiber, such as lignocellulose, which degrade at a lower temperature, may be extracted during alkali treatment. For acetylated petiole fiber the residue left at 700 °C (26.8%) is less than that of untreated material (32.4%), which indicates that the acetylated material is lost with volatile products and does not contribute to char formation.

The TGA curve of FNHA acetylated (NaOH and NaOH/H₂O₂ pretreated) fibers shows that the degradation behaviors for all the treated fibers were similar to each other. This can be attributed to the further purification of the fibers that took place due to the treatment. From table I.1, it was observed that, in all cases, the degradation temperatures of lignin, hemicelluloses, and cellulosic constituents for acetylated fibers were higher than those for untreated and alkalized- acetylated fibers. As a result, it can be deduced that FNHA fibers were more thermally stable than the untreated (FU) and (FNA) fibers.

Table I.1: Thermal behavior of treated and untreated palm petiole fiber.

Sample	IDT (°C)	MDR (%/min)	MDT (°C)	Residue (%) at 700 (°C)
FU	221.8	93.46	339.7	32.4
FN	255.5	87.44	355.1	31.33
FNH	260	86.09	366	26.63
FNA	222.1	85.71	361.5	26.8
FNHA	230	84.93	363.5	24.63

IDT: initial decomposition temperature, **MDR:** Maximum degradation rate, **MDT:** Maximum decomposition temperature.

Other researchers [14, 15], who studied the chemical structure of different parts of the date palm tree, also reported similar observations. They found that the hemicellulose, cellulose, and lignin decomposed in the temperature ranges of (260-340 °C) for hemicellulose, (320-380 °C) for cellulose, and (300-580 °C) for lignin, showing their overlapping decomposition processes. Moreover, the degree of crystallinity also influences the thermal stability of natural fibers (Fig I.6). Overall, the analysis results revealed that FNH and FNHA fibers have good thermal stability and might be applied in the industrial manufacture of composites, which require high resistance to elevated temperatures.

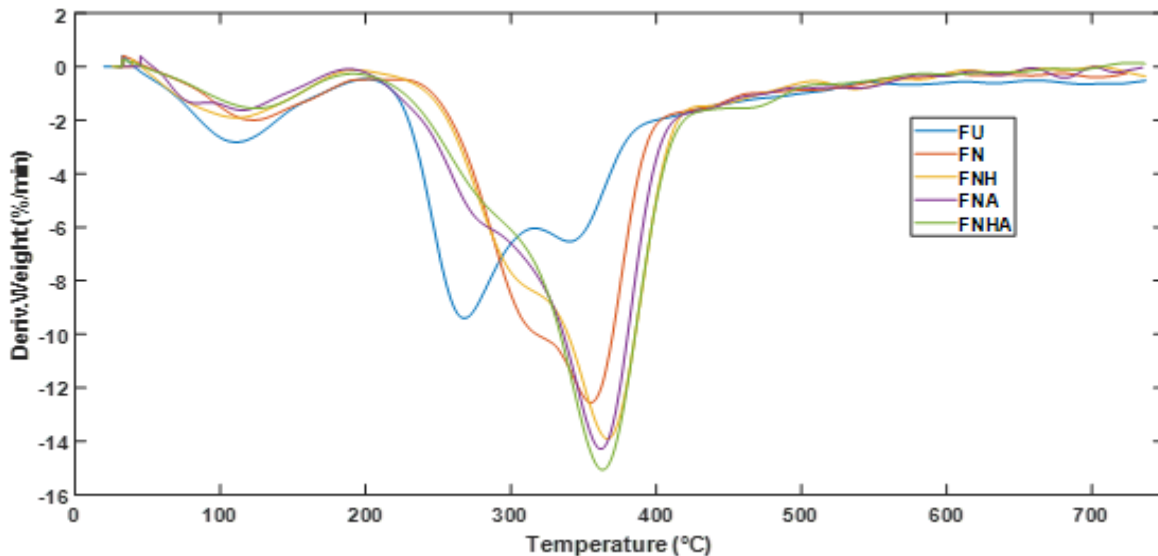


Figure I.6 : DTG curves of treated and untreated palm petiole fiber

I.3.2. DSC analysis

As for DSC analysis (Fig. I.7), all samples showed broad exotherms extending from 70 to 140 °C, which correlated to water vaporization. The heat flow from untreated fibers is remarkably more significant than the other samples. This showcased that the untreated fibers required higher heat energy for evaporating more extensive water content, in line with the weight loss shown in the TGA curve.

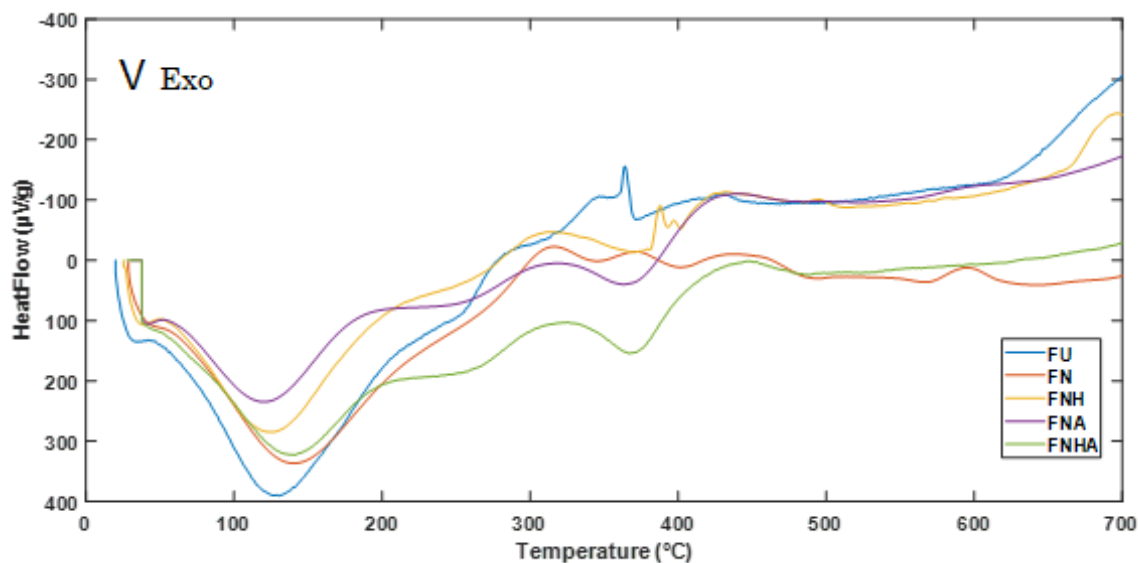


Figure I.7 : DSC curves of treated and untreated palm petiole fiber

The exothermic peak corresponds to the decomposition of lignin, hemicelluloses, and fiber cellulose. For the untreated fiber (FU), the exothermic peak is observed in the 200 - 475 °C. While the fibers treated with soda (FN) and treated with hydrogen peroxide (FNH) exhibit an exothermic peak between 250 °C and 480 °C. This is probably due to the partial removal of lignin, hemicellulose, and cellulose from the fiber [16]. As a result, the thermal stability of FN is increased compared to untreated fiber.

Besides this, the acetylated fiber FNA and FNHA revealed a third-wide exotherm at around 370 °C, correlating to the energy required to decompose cellulose-based compounds. This was possibly due to the milling effect that had gradually decreased the fiber compactness of fibers after numerous treatment cycles and subsequently reduced its thermal resistance withstanding high temperatures. Beyond this point, both curves rise to likely form an exothermic band for heat release to break down the bonds of cellulose and hemicellulose components. Thus, the analyzed DSC results herein agreed well with the TGA curves [17].

Reference

- [1] A. E. Bekele, H. G. Lemu, and M. G. Jiru, "Experimental study of physical, chemical and mechanical properties of enset and sisal fibers," *Polym. Test.*, vol. 106, p. 107453, 2022.
- [2] G. Rajeshkumar, S. A. Seshadri, G. Devnani, M. Sanjay, S. Siengchin, J. P. Maran, *et al.*, "Environment friendly, renewable and sustainable poly lactic acid (PLA) based natural fiber reinforced composites—A comprehensive review," *J. Clean. Prod.*, vol. 310, p. 127483, 2021.
- [3] W. Wang, M. Xu, J. Lou, and A. Dong, "Changes in physicochemical properties and structures of jute fibers after tetraacetylenediamine activated hydrogen peroxide treatment," *J. Mater. Res. Technol.*, vol. 9, pp. 15412-15420, 2020.
- [4] Y. Liu, H. Liu, J. Xiong, A. Li, R. Wang, L. Wang, *et al.*, "Bioinspired design of electrospun nanofiber based aerogel for efficient and cost-effective solar vapor generation," *J. Chem. Eng.*, vol. 427, p. 131539, 2022.
- [5] M. Barczewski, D. Matykiewicz, and M. Szostak, "The effect of two-step surface treatment by hydrogen peroxide and silanization of flax/cotton fabrics on epoxy-based laminates thermomechanical properties and structure," *J. Mater. Res. Technol.*, vol. 9, pp. 13813-13824, 2020.
- [6] J. Bartz, J. T. Goebel, M. A. Giovanaz, E. da Rosa Zavareze, M. A. Schirmer, and A. R. G. Dias, "Acetylation of barnyardgrass starch with acetic anhydride under iodine catalysis," *Food Chem.*, vol. 178, pp. 236-242, 2015.
- [7] M. D. Alotaibi, B. A. Alshammari, N. Saba, O. Y. Alothman, M. Sanjay, Z. Almutairi, *et al.*, "Characterization of natural fiber obtained from different parts of date palm tree (*Phoenix dactylifera* L.)," *International journal of biological macromolecules*, vol. 135, pp. 69-76, 2019.
- [8] A. M. Adel, A. M. El-Shafei, A. A. Ibrahim, and M. T. Al-Shemy, "Chitosan/nanocrystalline cellulose biocomposites based on date palm (*Phoenix dactylifera* L.) sheath fibers," *Journal of Renewable Materials*, vol. 7, p. 567, 2019.
- [9] M. A. H. Alharbi, S. Hirai, H. A. Tuan, S. Akioka, and W. Shoji, "Effects of chemical composition, mild alkaline pretreatment and particle size on mechanical, thermal, and structural properties of

- binderless lignocellulosic biopolymers prepared by hot-pressing raw microfibrillated Phoenix dactylifera and Cocos nucifera fibers and leaves," *Polymer Testing*, vol. 84, p. 106384, 2020.
- [10] A. F. Tarchoun, D. Trache, and T. M. Klapötke, "Microcrystalline cellulose from Posidonia oceanica brown algae: Extraction and characterization," *International journal of biological macromolecules*, vol. 138, pp. 837-845, 2019.
- [11] S. Krishnasamy, S. M. K. Thiagamani, C. M. Kumar, R. Nagarajan, R. Shahroze, S. Siengchin, *et al.*, "Recent advances in thermal properties of hybrid cellulosic fiber reinforced polymer composites," *International journal of biological macromolecules*, vol. 141, pp. 1-13, 2019.
- [12] E. V. Bachtiar, K. Kurkowiak, L. Yan, B. Kasal, and T. Kolb, "Thermal stability, fire performance, and mechanical properties of natural fibre fabric-reinforced polymer composites with different fire retardants," *Polymers*, vol. 11, p. 699, 2019.
- [13] H. U. Zaman and R. A. Khan, "Acetylation used for natural fiber/polymer composites," *J. Thermoplast. Compos. Mater.*, vol. 34, pp. 3-23, 2021.
- [14] M. Asim, M. Jawaaid, H. Fouad, and O. Alothman, "Effect of surface modified date palm fibre loading on mechanical, thermal properties of date palm reinforced phenolic composites," *Composite Structures*, vol. 267, p. 113913, 2021.
- [15] M. Beroual, D. Trache, O. Mehelli, L. Boumaza, A. F. Tarchoun, M. Derradji, *et al.*, "Effect of the delignification process on the physicochemical properties and thermal stability of microcrystalline cellulose extracted from date palm fronds," *Waste and Biomass Valorization*, vol. 12, pp. 2779-2793, 2021.
- [16] K. H. Reddy, R. M. Reddy, M. Ramesh, D. M. Krishnu, B. M. Reddy, and H. R. Rao, "Impact of alkali treatment on characterization of tarsi (sterculia urens) natural bark fiber reinforced polymer composites," *Journal of Natural Fibers*, 2019.
- [17] C. H. Lee, A. Khalina, and S. H. Lee, "Importance of interfacial adhesion condition on characterization of plant-fiber-reinforced polymer composites: A review," *Polymers*, vol. 13, p. 438, 2021.

Chapter II

Characterization of the Composites Elaborates

Chapter II : Characterization of the Composites Elaborates

This chapter is devoted to characterizing composites that combine the linear low-density polyethylene (LLDPE) matrix and a fibrous filler (15-25% Petiole fiber). We studied the properties of the composite materials formed: morphological properties, thermal, mechanics, and dynamic mechanics properties.

II.1. Morphological characterization (SEM)

a. Load Effect

Scanning Electron Microscopy (SEM) was carried out to investigate fiber pull-out and fiber/matrix interaction. The effect of loading fibers on the interface of composites was examined by examining the fractured surfaces of LLDPE, LLDPE/FU 15%, and LLDPE/FU 25% composites; the images obtained are shown in Fig II.1 (a,b and c).

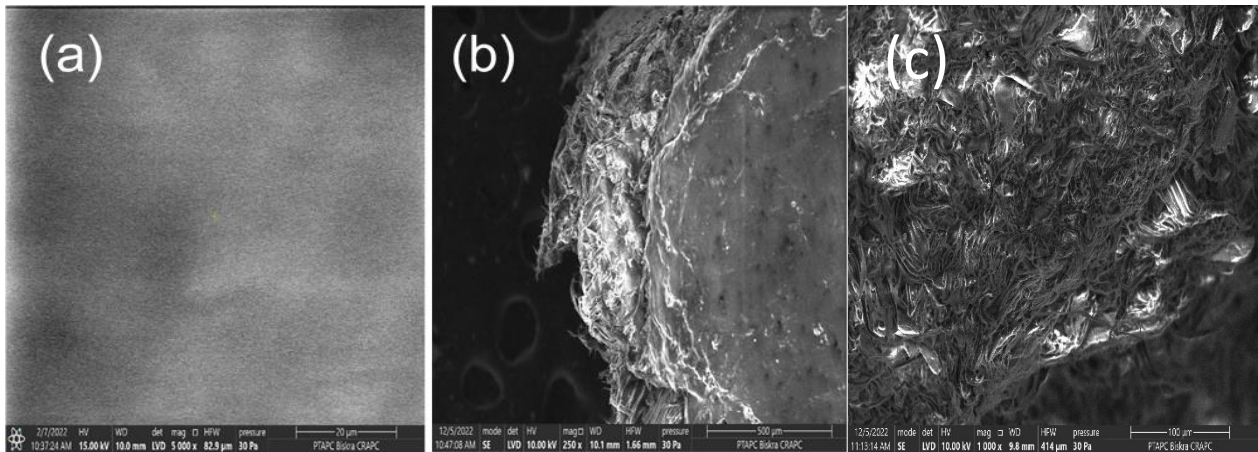


Figure II.1: SEM micrographs of (a) LLDPE, untreated composite, (b) LLDPE/FU 15%, and (c) LLDPE/FU 25%

Fig II.1 (a) neat LLDPE shows smooth and homogeneous surfaces on the cross-section. On the other hand, for the untreated composites Fig II.1 (b and c), we observe a rough, irregular, and heterogeneous surface, and the presence of micro-voids and cavities on the surface due to the loosening of the load from the PE matrix during the fracture; fiber pullout and fiber breakage were also detected [1]. These microvoids become more pronounced as the load rate increases in LLDPE/FU 25% composites, highlighting the incompatibility of the two phases due to poor interfacial adhesion and differences in the polarities of the

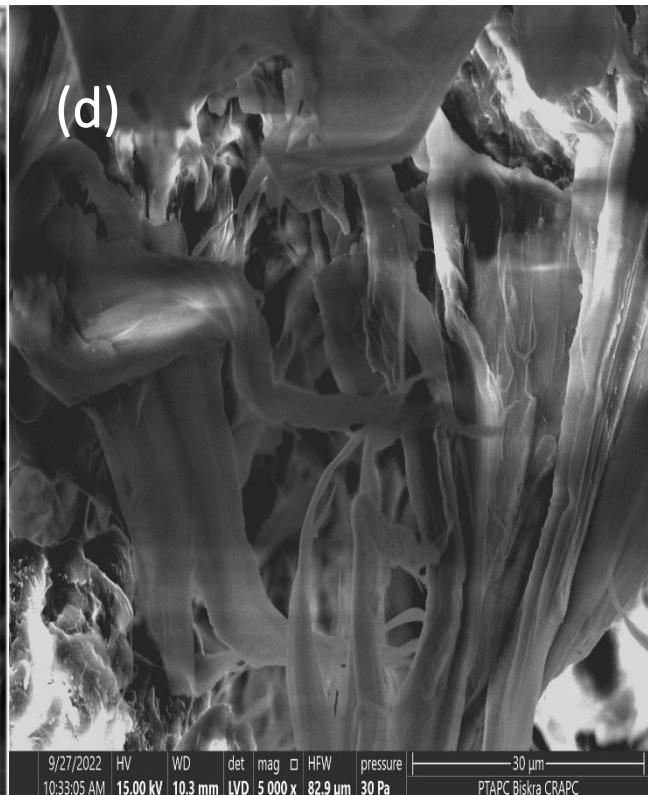
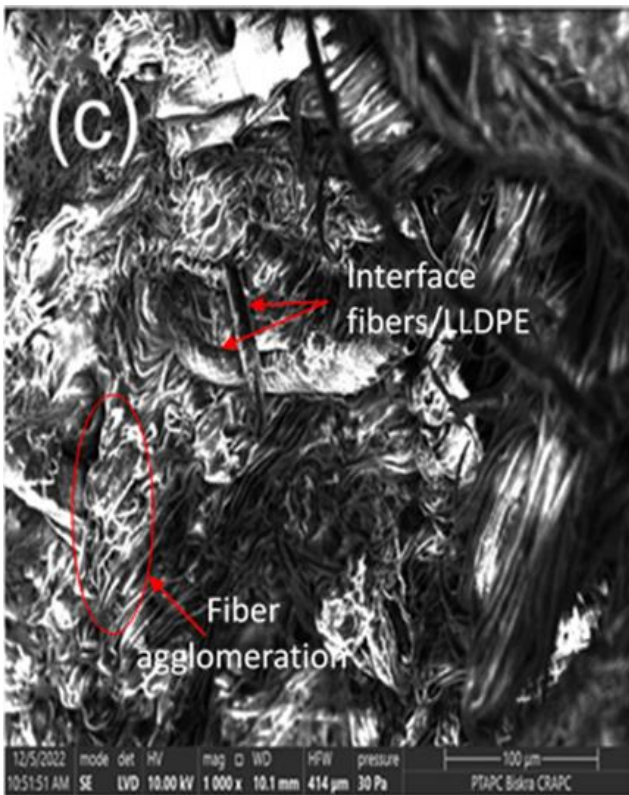
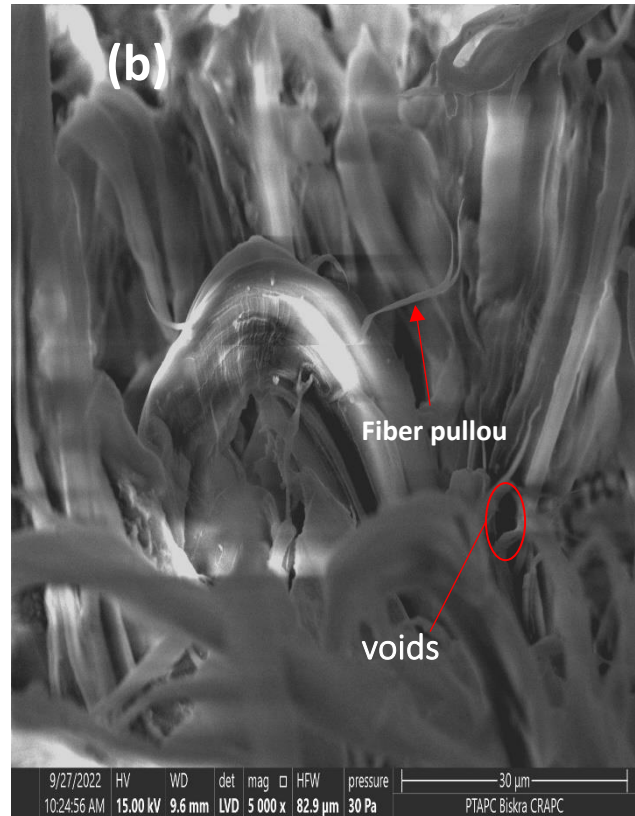
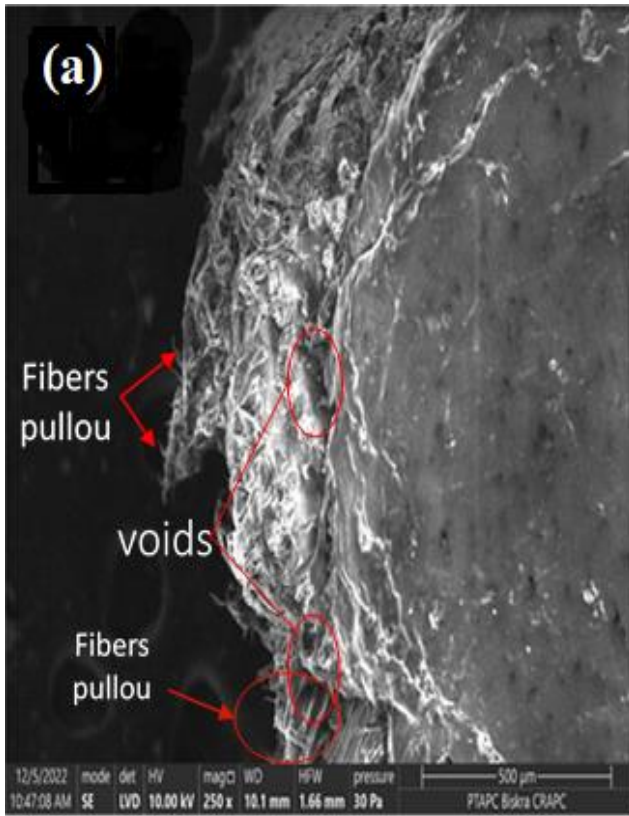
free surfaces of the hydrophilic filler and the hydrophobic polymer; it is also discovered that impurities on the palm surface reduce interfacial bonding with the matrix [2].

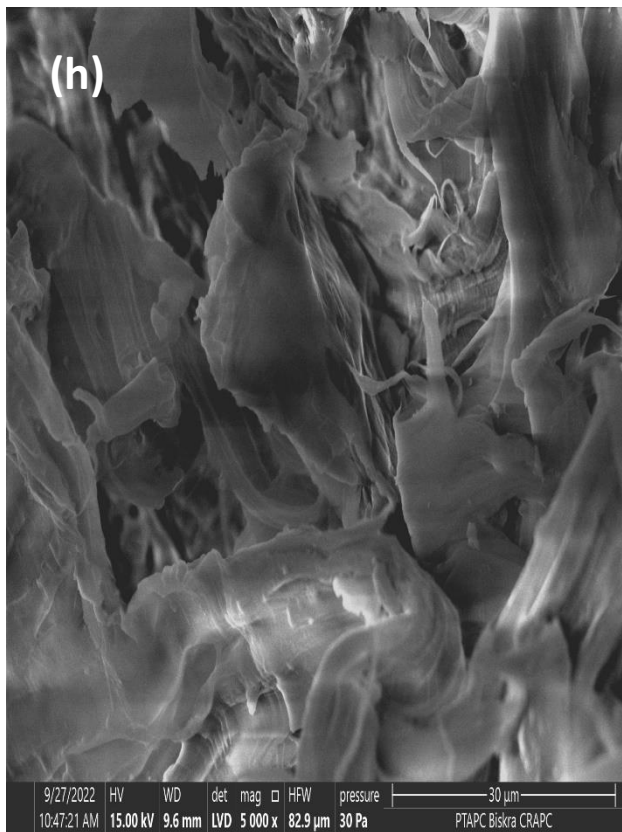
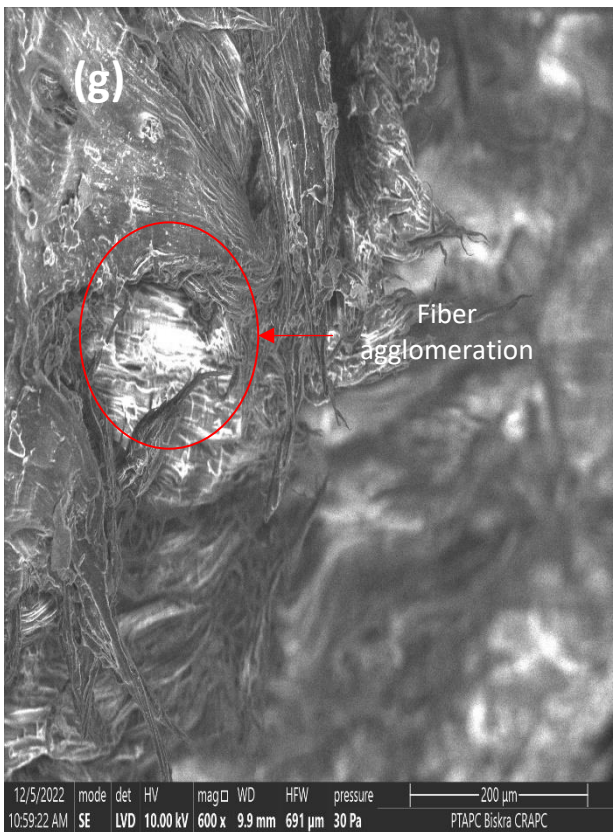
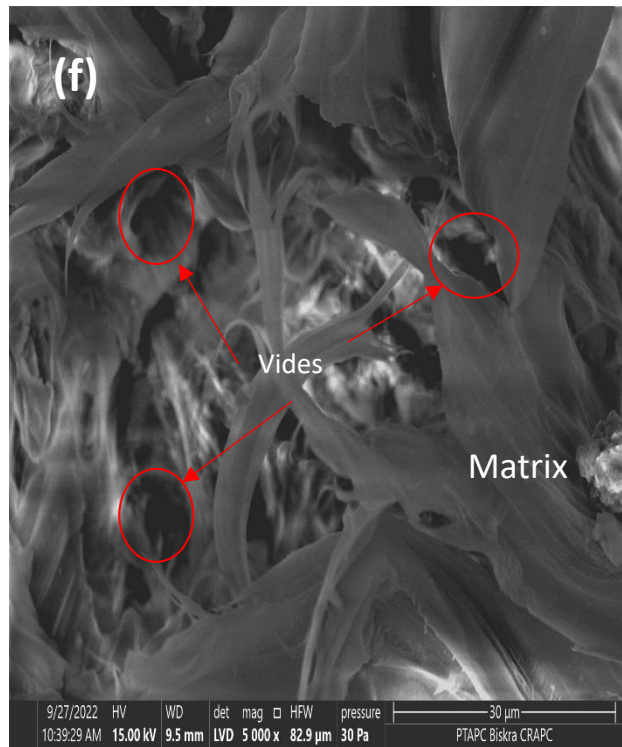
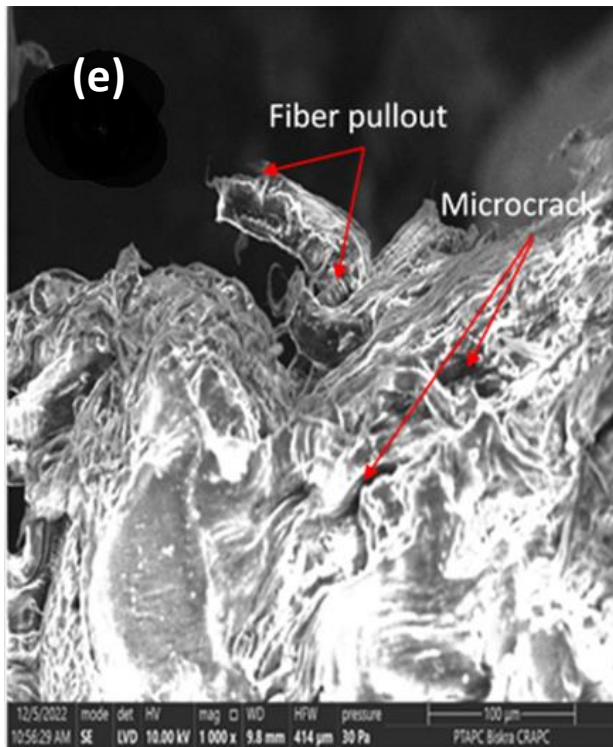
b. Treatment effect

Fig. II.2 (a-k) shows the SEM images of the fractured cross sections of tensile testing samples of the composite reinforced with treated and untreated fibers. The fig. II.2 shows rough surfaces on the all composites due to the presence of certain agglomerates and aggregates of filler particles distributed throughout the polymeric matrix. Fig II.2 (a,b) shows how the fibers are distributed in the matrix and how some microcracks and fiber pullout can be observed on the surface of the composites LLDPE/FU 15-25%. Fig II.2 (a,b) also shows that the middle area of the composite is poorly distributed and the microrovoid is also observable, which is due to the presence of the untreated fibers.

Alkaline treatment roughened the surfaces of the fibers on account of the removal of lignin and hemicelluloses. As a result, as shown in Fig II.2 (c,d), the load transfer between fiber and matrix in the LLDPE/FN 15-25% composites has improved, which shows a more homogeneous surface compared to untreated composites with smaller microvoids.

The alkaline peroxide treatment improved the adhesion characteristics between the fibers and the polymer matrix. Fig II.2 (e,f) clearly indicates the relatively clean surface of the composites LLDPE/FNH 15-25% as a result of the removal of the impurities on the surface and the formation of microvoids in the fibers during the treatment process. The presence of microvoids is important in promoting the adhesion between the fibers and the polymer via a mechanical interlocking mechanism. This may also explain why the LLDPE/FNH composite had better mechanical properties than the LLDPE/FN composite. Fig II.2 (g,h) demonstrates that the acetylation of palm petiole fiber surfaces has reduced microvoids around the fibers. The surface roughness of the LLDPE/FNA 15-25% composites after acetylation treatment is lower than that of untreated composites. LLDPE/FNA and FNHA created a smoother surface in the composite. This confirms the good interfacial adhesion between acetylated fibers and LLDPE. In the instance of the LLDPE/FNHA 15-25% samples, which showed the greatest interfacial bonding, the fibers have cracked in the fracture plane, proving the efficacy of the surface modification technique used in Fig II.2. (j,k). In the same way, the surface of the fibers that had been bleached LLDPE/FNH or bleached and acetylated LLDPE/FNHA was smoother than that of the FN and FNA samples because amorphous layers had been removed from the surface of the fibers [3].





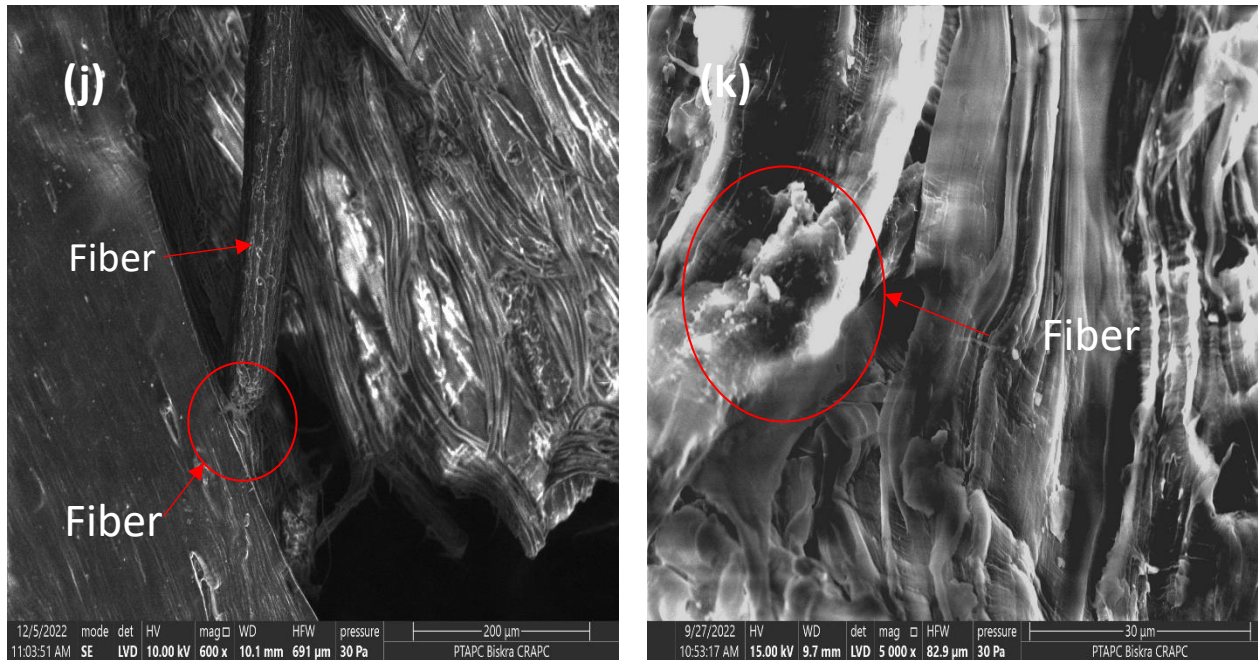


Figure II.2: SEM micrographs of treated and untreated composite (a-b) LLDPE/FU 15-25%, (c-d) LLDPE/FN 15-25%, (e-f) LLDPE/FNH 15-25%, (g-h) LLDPE/FNA 15-25%, (j-k) LLDPE/FNHA 15-25%

II.2. Thermogravimetric analysis (ATG/DTG)

a. Load Effect

Fig. II.3 and II.4 represents the TG and DTG thermograms of the neat LLDPE and various composites produced with 15-25% of untreated fiber. It can be seen that the incorporation of the untreated petiole fibers into the LLDPE matrix reduces the temperature of decomposition, and this reduction is all the more significant as the rate of petiole fibers increases. It is estimated at 356.2 °C for virgin LLDPE, 229 and 233°C for untreated composites FU 15% and FU 25%, respectively. This decrease is attributed to the presence of the three main constituents (cellulose, hemicellulose, and lignin) of the fibers [4, 5]. Cellulose fiber degrades between 200 and 350 °C. At the same time, our polymer degrades at temperatures above 400 °C. Consequently, the thermal behavior of the composite represents the sum of the individual behaviors of these two fiber and matrix constituents. In the vicinity of 490 °C, a plateau of stability is recorded, attributed to the formation of cinder.

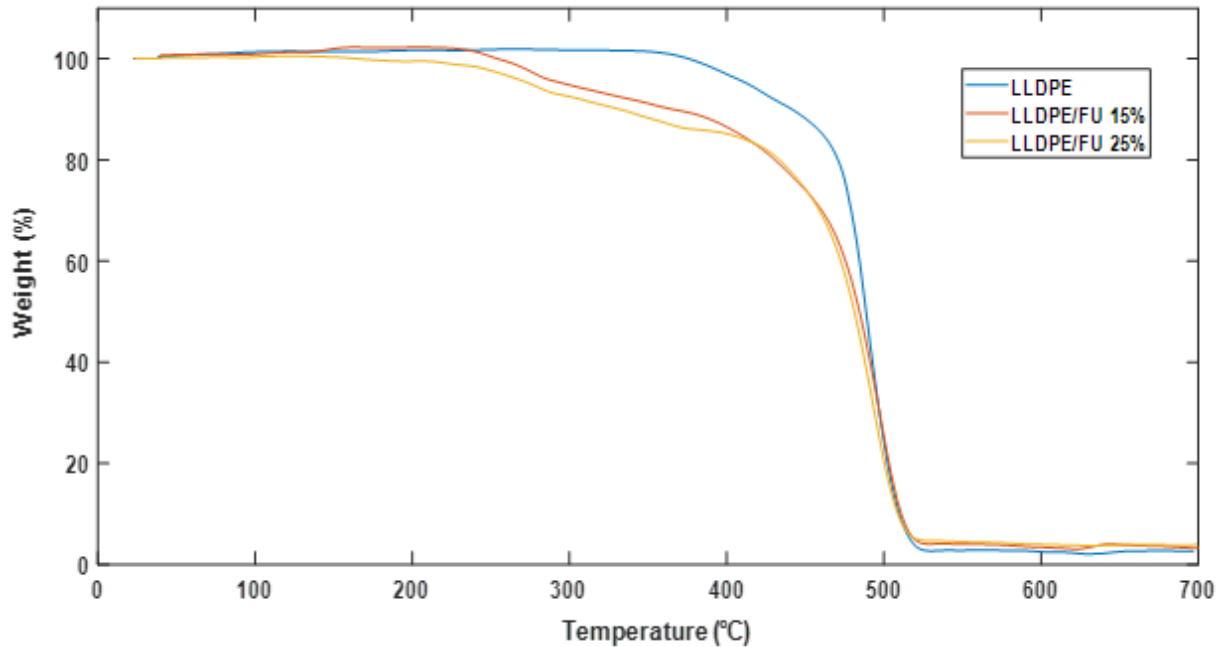


Figure II.3: TGA curves of neat LLDPE and untreated composite LLDPE/FU 15-25%

On the DTG thermograms Fig II.4, we notice the appearance of different peaks.

A first peak appears around 100 – 120 °C, corresponding to the evaporation of the water physically adsorbed on the surface of the particles of the petiole fibers for the untreated composites. This phenomenon can be attributed to the hydrophilic nature of the fibers, which can absorb more water molecules. On the other hand, in the same temperature range, LLDPE does not record any peak, a signature of the hydrophobic nature of the polymer. A second peak corresponding to the thermal degradation of hemicellulose and cellulose is 213 and 304 °C. More precisely, the thermal decomposition of cellulose occurs essentially at a temperature of 310 °C and is done by depolymerization [6]. Indeed, when subjected to very high temperatures, it absorbs enough energy to cause the breaking of the glycosidic bond. Depolymerization can also be accompanied by the dehydration of sugars, giving rise to unsaturated compounds and a variety of volatile compounds. Hemicelluloses are less thermally stable than cellulose and generally degrade at temperatures between 200 and 260 °C. Although they represent a smaller fraction in the fiber than cellulose, they can nevertheless significantly affect the thermal behavior of the composite because of their structural association with the other constituents. In a study on Leaf and Kenaf fiber and its components [7] they attribute this process to the pyrolysis of the hemicellulose fraction.

Around 350 °C, a third peak appears; it corresponds to the decomposition of lignin. This process can be explained by the cleavage of carbon-carbon bonds between the structural units of lignin and dehydration reactions [8]. Above 300 °C, the aliphatic chains of the aromatic ring begin to break to produce phenolic

derivatives. Similar results were reported by [9]. A broad and intense peak appears between 450°C and 520°C, corresponding to the decomposition of the polyethylene matrix. It is noted that the introduction of the untreated fiber petiole leads to a decrease in the maximum decomposition rate. We also note a slight shift in the maximum decomposition temperatures towards high temperatures, indicating better stability. Above 520° C, a plateau of stability is recorded, corresponding to the residue's formation.

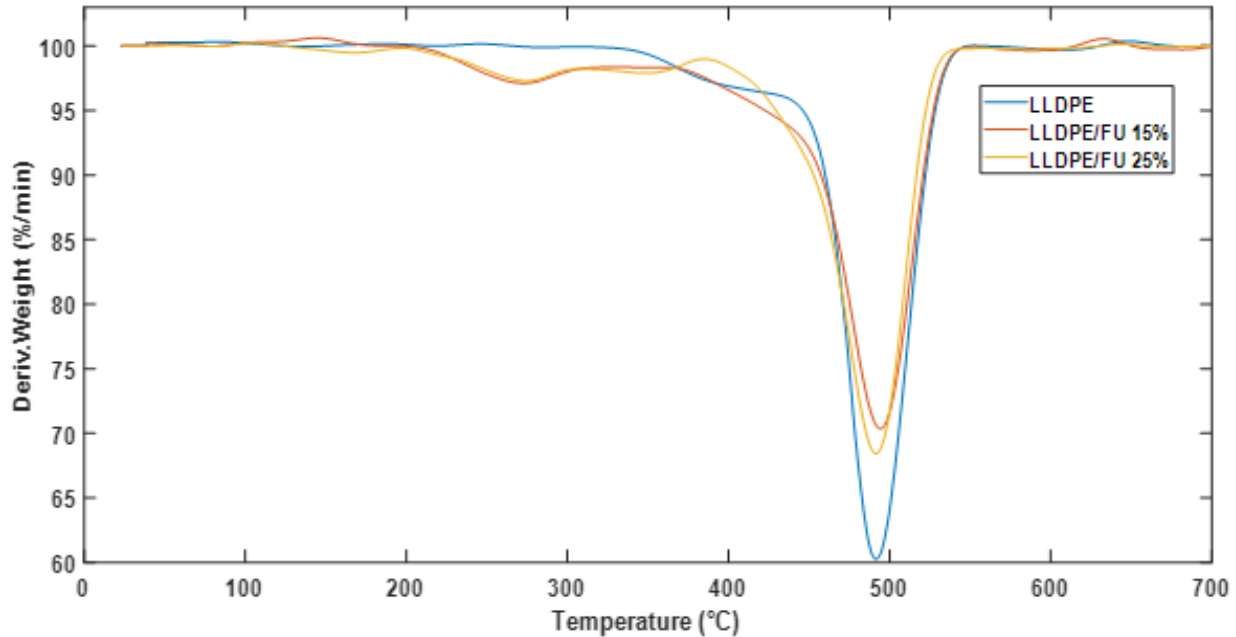


Figure II.4: DTG curves of neat LLDPE and untreated composite LLDPE/FU 15-25%

b. Treatment effect

Fig II.5 and II.6 represents the ATG thermograms of the different untreated and treated composites with different loading 15% and 25%, respectively. Through these thermograms shown in Fig II.5 and II.6, the NaOH and NaOH/H₂O₂ treatments of natural fibers improve their thermal stability. The start of decomposition temperatures for the composites increases 260-274.6 °C and 252.4-275.4 °C for the LLDPE/FN 15-25% and LLDPE/FNH 15-25% composites, compared to that of the composites with untreated LLDPE/FU 15-25%, which is 229-233 °C. This result is probably due to the removal of some amorphous components from the fiber, such as hemicelluloses and lignin, and increasing the crystallinity of fiber [4]. Thermogravimetric data for the LLDPE/FNA composite as shown in Fig II.5 and II.6 indicate that acetylation reduces their thermal stability compared to LLDPE/FN, which results in a decrease in the temperature at which degradation begins and a shift in mass losses to lower temperatures. This behavior may be related to the disruption of the crystal structure of the fibers caused by the substitution of hydroxyl groups by more significant and less polar acetyl groups [10].

On the other side, we see the onset of thermal degradation for LLDPE/FNHA composite with 263.3-268.5 °C is higher than LLDPE/FNA composites. The acetylated fibers are more stable after mercerization alkali and oxidation. The acetyl groups on the fiber surface make it more hydrophobic and less susceptible to moisture absorption [11]. Moisture absorption can accelerate the thermal degradation of natural fibers. The LLDPE matrix also plays a role in the thermal degradation of the composite. LLDPE is a relatively thermally stable polymer that will still degrade at high temperatures. The degradation of the LLDPE matrix can release free radicals, accelerating the degradation of the acetylated fibers.

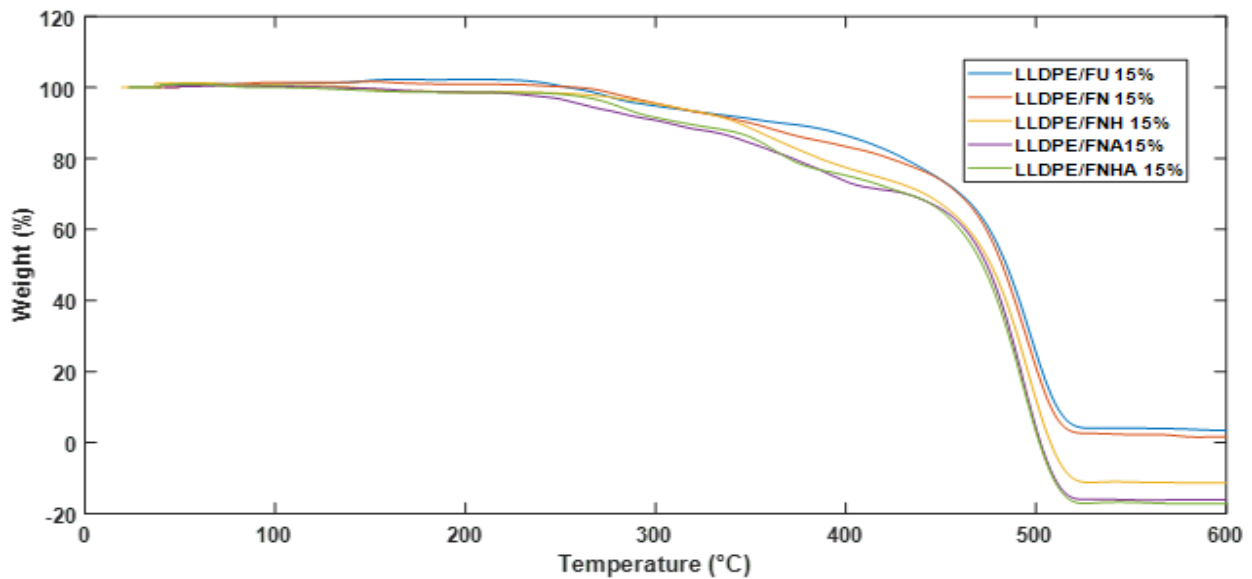


Figure II.5: ATG curves of treated and untreated composite 15%

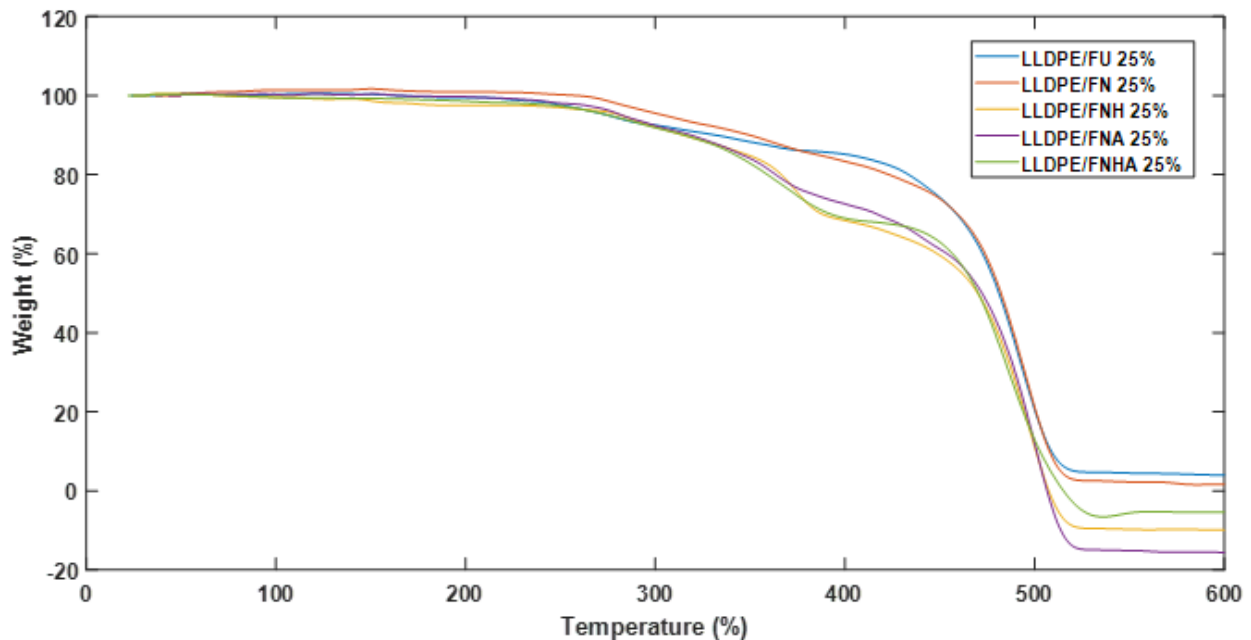


Figure II.6: ATG curves of treated and untreated composite 25%

Fig II.7 and II.8 represents the mass differentials (DTG curves) of the treated and untreated composites (15-25%).

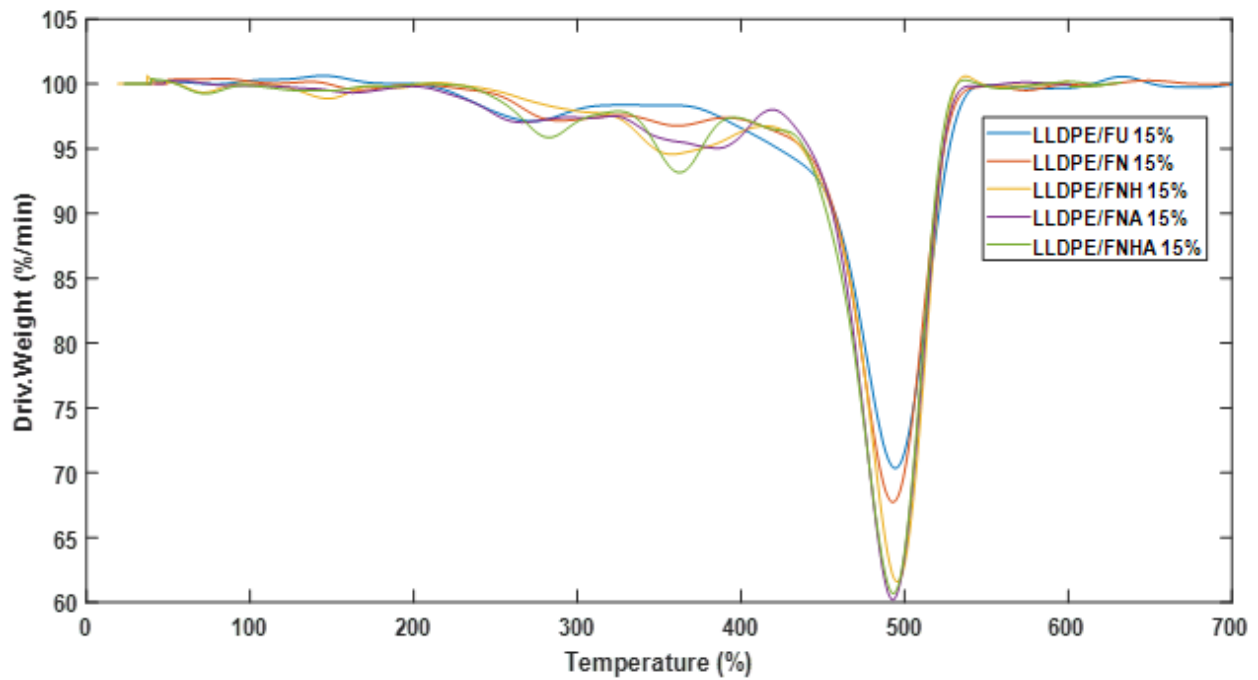


Figure II.7: DTG curves of treated and untreated composite 15%

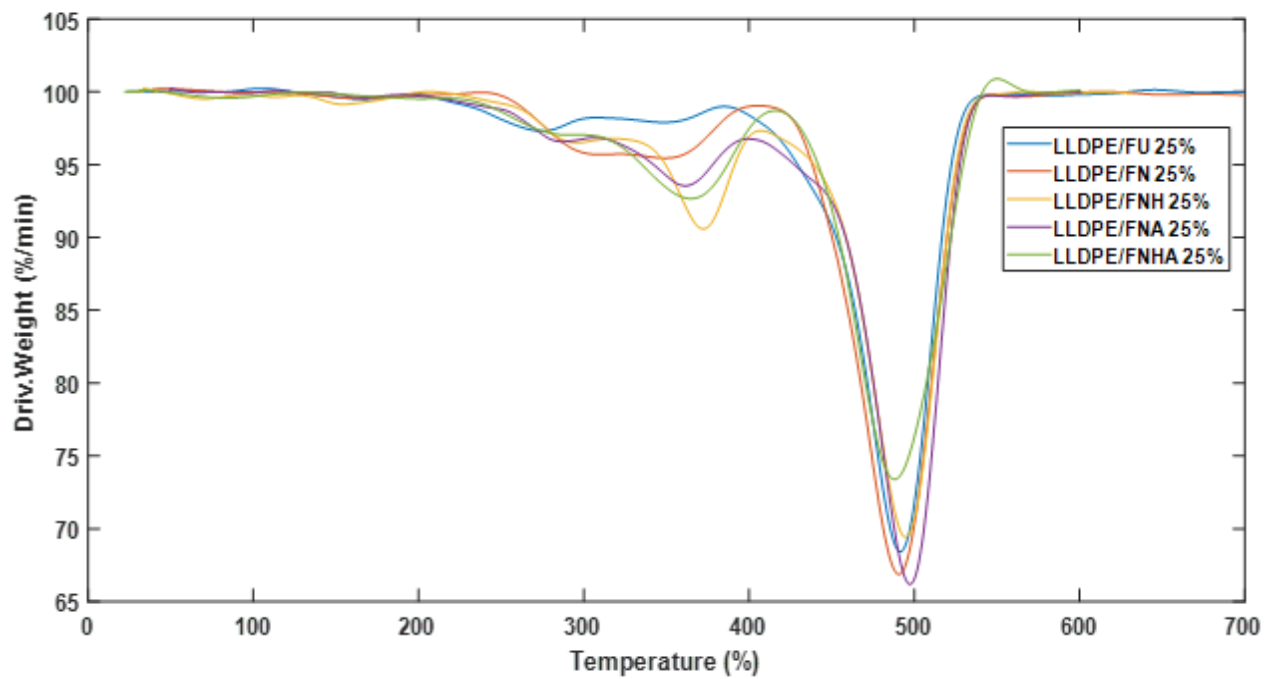


Figure II.8: DTG curves of treated and untreated composite 25%

Exploiting the TG-DTG thermograms of the various untreated and treated composites allows us to determine the temperatures at the start of the composition, and the residue content. The details of these results are reported in Table II.1.

Table II.1: Thermal parameters of neat LLDPE, treated and untreated composites (15-25%)

Sample	IDT (°C)	MDR (%/min)	MDT (°C)	Residue (%)
LLDPE	356.2	60.25	448.9	2.66
LLDPE/FU 15%	229	70.35	480	3.197
LLDPE/FU 25%	233	68.42	488	3.947
LLDPE/FN 15%	260	67.73	491.7	1.734
LLDPE/FN 25%	274.6	66.86	487.8	2.01
LLDPE/FNH 15%	252.4	61.6	490.1	/
LLDPE/FNH 25%	275.4	69.42	489.8	/
LLDPE/FNA 15%	243	60.21	486.5	/
LLDPE/FNA 25%	253.2	66.19	492.2	/
LLDPE/FNHA 15%	263.3	60.7	492.2	/
LLDPE/FNHA 25%	268.5	73.39	485.1	/

IDT: initial decomposition temperature, **MDR:** Maximum degradation rate, **MDT:** Maximum decomposition temperature.

The results in Table II.1. allow us to draw the following conclusions:

Same observation as previously, around 100°C, there is a slight variation in mass, which characterizes the evaporation of water. Between 200° and 360°C, hemicellulose, cellulose, and lignin degradation occurs. Pure polyethylene (LLDPE) is more thermally stable than untreated composites. It begins to decompose at a temperature of 356.2 °C and reaches a maximum decomposition rate of 60.25 %/min at 488.9 °C.

The introduction of untreated petiole fiber (15-25%) leads to a reduction in the temperature at which degradation begins 229-233 °C and increase in the maximum speed of decomposition 70.35-68.42 %/min. The residue level increases as untreated petiole fiber (FU) is added to the LLDPE matrix with 3.197% of LLDPE/FU 15% and 3.947% of LLDPE/FU 25%.

All Treatments increase the temperature of decomposition in comparison to LLDPE/FU. This is explained by eliminating contaminants, wax, and hemicellulose from the surface of the fibers. These constituents coat the cellulose, which retards its decomposition. Cellulose represents the high percentage of material that forms the fibers [12].

In summary, we can claim that the composite containing 25% untreated and treated fibers has more excellent thermal stability than the neat LLDPE and LLDPE/PPF 15%, with a bit of an advantage for the untreated sample over the treated sample, considered residues. While 15% integration of treated and untreated fibers does not significantly alter the thermal stability of the composite, it is observed that the curves are somewhat overlapping due to the tiny amount of fibers. The extreme thermal deterioration of composites occurs at temperatures above 210 °C, which cannot be achieved during the production process or when utilizing these composite materials [13].

II.3. Mechanical Properties

II.3.1. Tensile testing

II.3.1.1. Tensile strength

a. Load Effect

The evolution of the tensile strength of untreated composites as a function of a load of palm petiole fibers is illustrated in Fig II.9. We note a decrease in the tensile strength of composites loaded with FU compared with that of the virgin LLDPE matrix. This reduction is estimated at 35.66% and 43.82% for the formulations LLDPE/FU 15% and LLDPE/FU 25%, respectively. This decrease is attributed to the decrease in the bond strength between fiber and matrix, which obstructs the propagation of stress [14]; this can be explained by the tendency of the particles of the fibers to form agglomerates, which induce heterogeneities and it may be due to the less amount of fibers unable to distribute homogeneously in matrix cause poor stress transfer from matrix to fibers [15].

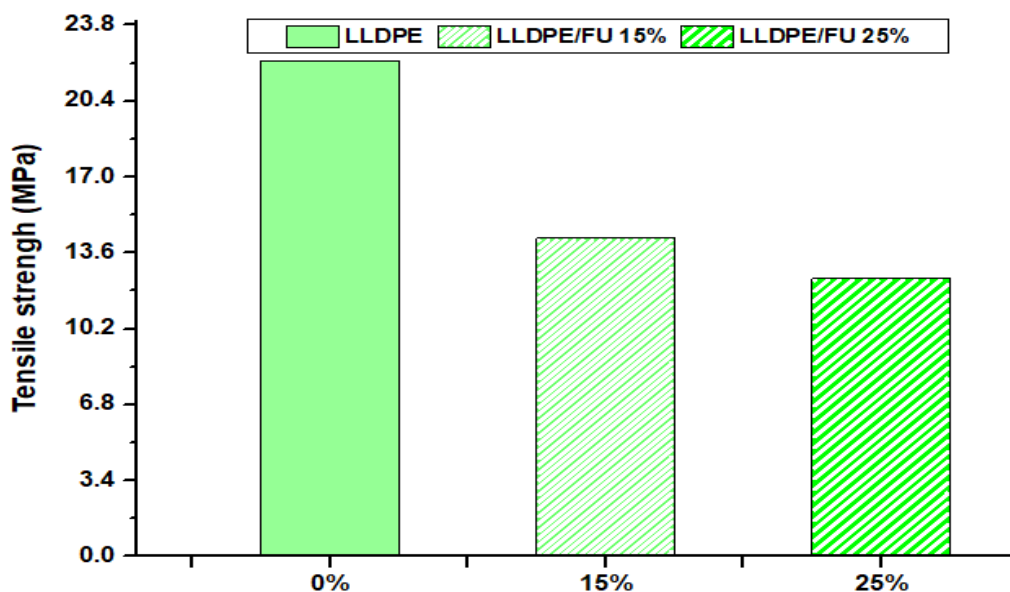


Figure II.9: Tensile strength of neat LLDPE and untreated composites 15-25%.

b. Treatment effect

Fig II.10 and II.11 shows the variations in tensile strength of treated and untreated LLDPE/Palm petiole fiber composites (15-25%). The tensile strength decreased by 51.55% and 43.81% by adding 15 and 25 % wt untreated fibers to the composite. The meager particulate size of fibers (35 μm) acts as stress concentration points if not appropriately dispersed, leading to the failure of the composite [16, 17]. Also, the character hydrophilic fibers and the character hydrophobic LLDPE matrix lead to poor adhesion interfacial.

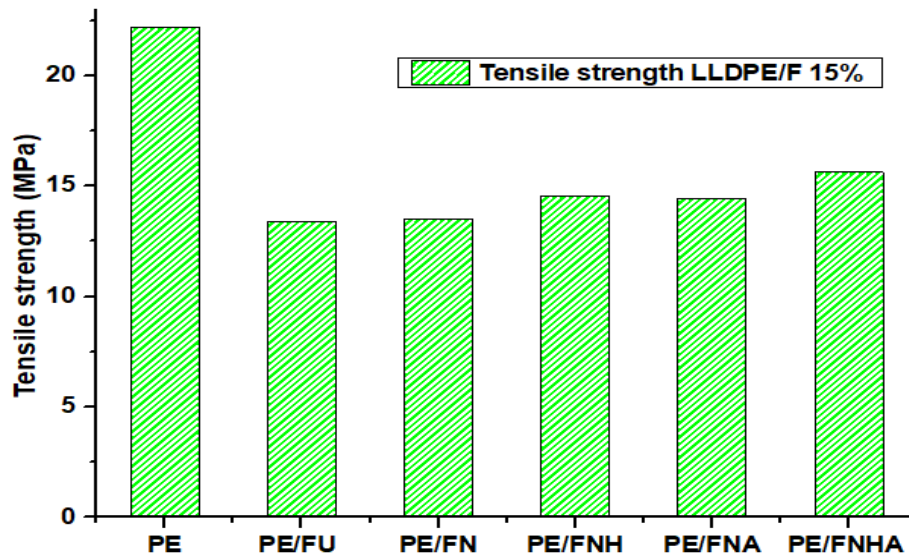


Figure II.10: Tensile strength of neat LLDPE, treated and untreated composites 15%.

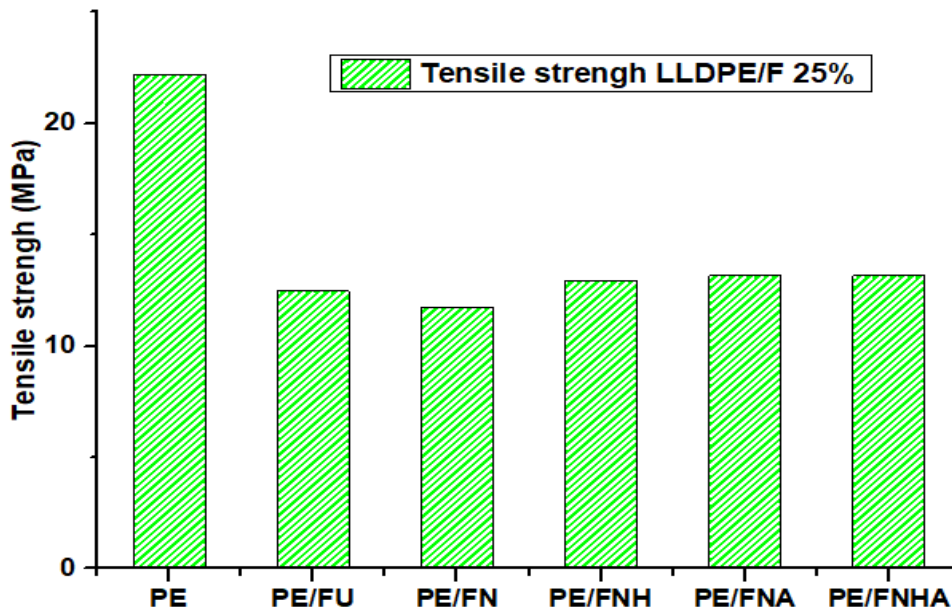


Figure II.11: Tensile strength of neat LLDPE, treated and untreated composites 25%.

However, using chemical treatments like alkali treatment and hydrogen peroxide to reduce lignin and hemicellulose increases the surface area of the fiber. It makes exposing OH-groups on the fiber surface easier for acetylation treatment. This usually results in good physical effective interactions and improves interfacial adhesion region, enhances the stiffness imparted by the fibers to the composites [3], and increases the tensile strength of treated composites LLDPE/FN with 13.56 MPa, LLDPE/FNH 14.61 MPa, LLDPE/FNA 14.49 MPa, LLDPE/FNHA 15.64 MPa compared to the untreated composite LLDPE/FU 13.39 MPa. The tensile strength of LLDPE/acetylated palm fiber composites (LLDPE/FNA and LLDPE/FNHA) improved as fiber loading increased, from 13.39 MPa for LLDPE/FU to 14.49 MPa for LLDPE/FNA and 15.64 MPa for LLDPE/FNHA. The increase in tensile strength could be attributed to several factors, including removing lignin and extractable substances, a slight rise in cellulose content, and converting a small portion of hemicellulose into acetylated hemicellulose.

The acetylation process involves replacing the hydrogen atoms of the hydroxyl groups in the fiber cell membrane with acetyl groups, which reduces the fiber's polarity. This process removes waxy material from the fiber surface, leading to better adhesion between the fiber and the matrix in composite materials. Additionally, acetylation increases the surface free energy, which helps to enhance composite properties and we see a reduction in tensile strength in treated and untreated LLDPE/F 25% composite due to the higher loading of fibers [18].

II.3.1.2. Young's modulus

a. Load Effect

Fig II.12 represents the evolution of Young's modulus of untreated composites as a function of a load of palm petiole fibers. Adding untreated petiole palm fibers to the LLDPE matrix increases the material's rigidity. In other words, Young's modulus increases by 503.78 MPa for the virgin LLDPE to reach the values of 651.59 MPa and 756.30 MPa for the composites containing 15 and 25% of the FU, which is an increase of approximately 28.89% and 50.12%, respectively, due to good dispersion of palm petiole fibers in composites [19]. In the LLDPE/FU 25% composite, the tensile strength decreased but the tensile modulus increased. Tensile strength may have decreased due to a higher proportion of fibers that are unable to mix properly with the matrix.

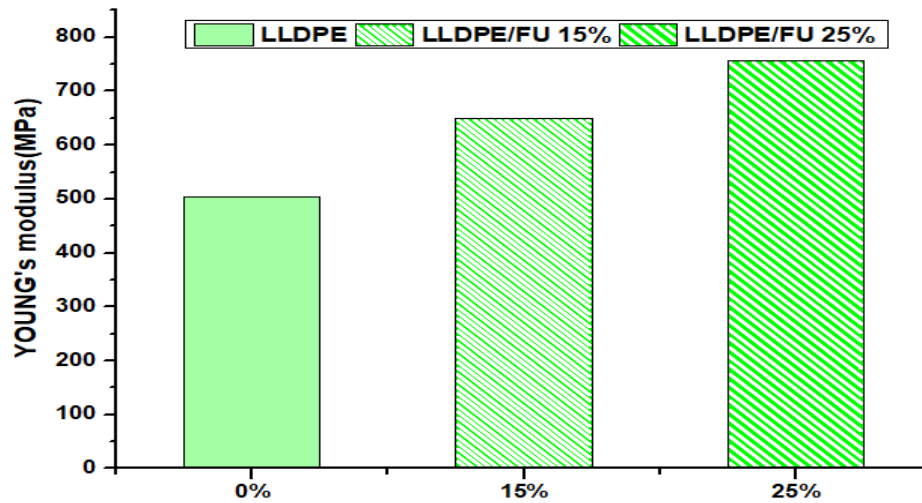


Figure II.12: Young's modulus of neat LLDPE and untreated composites 15-25%.

b. Treatment effect

Young's modulus of LLDPE/palm petiole fiber composites reinforced with treated and untreated fibers is higher than that of polyethylene matrix, as shown in Fig II.13 and II.14. Adding 15-25% palm petioles fibers to the LLDPE matrix made the composites stiffer without changing their strength. These results are the same as those found in [20]. It was shown that composites made of LLDPE/FU 15% had Young's modulus of 598 MPa, LLDPE/FN 15% of 465 MPa, LLDPE/FNH 15% of 490 MPa, LLDPE/FNA 15% of 420 MPa, and LLDPE/FNHA 15% of 422 MPa and composites made of LLDPE/FU 25% had Young's modulus of 756.61 MPa, LLDPE/FN 25% of 522.58 MPa, LLDPE/FNH 25% of 532.91 MPa, LLDPE/FNA 25% of 544.82 MPa, and LLDPE/FNHA 25% of 542.20 MPa. During mercerization, NaOH reacts with the hydroxyl groups of the material hemicellulose. This causes the cell structure to become tangled and the fibers to break. By breaking down the hemicellulose, the space between the cells should become less thick and stiff. This may facilitate the fibers' ability to reorganize themselves. This results in a more efficient packing of cellulose chains [21], and it was found that the fibers being bleached with H_2O_2 have more interactions with the polymer matrix, which leads to good dispersion in the composite. This results in stiffness enhancements from the fibers to the composites.

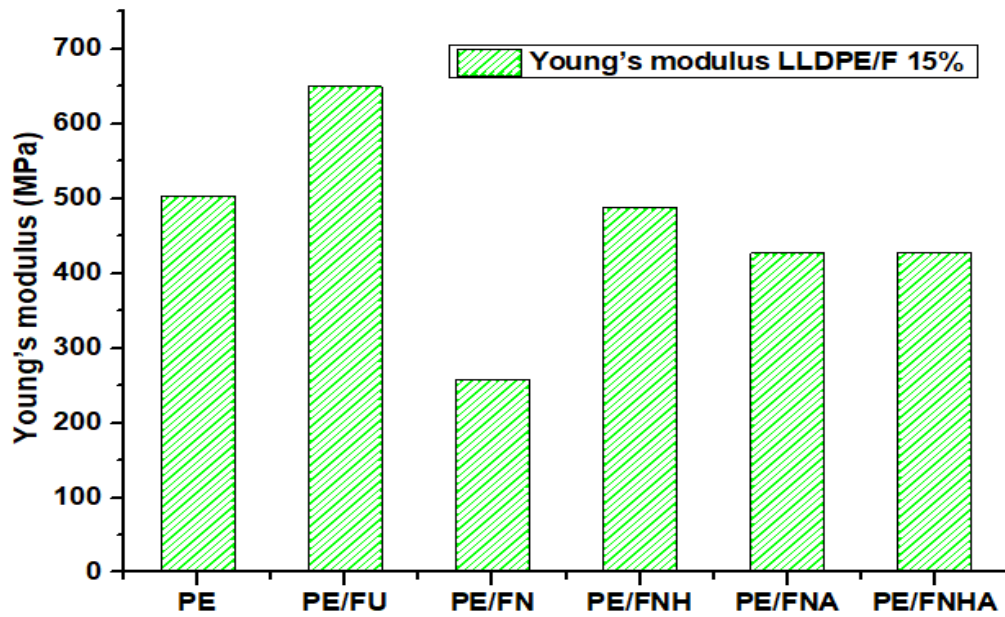


Figure II.13: Young's modulus of neat LLDPE, treated and untreated composites 15%.

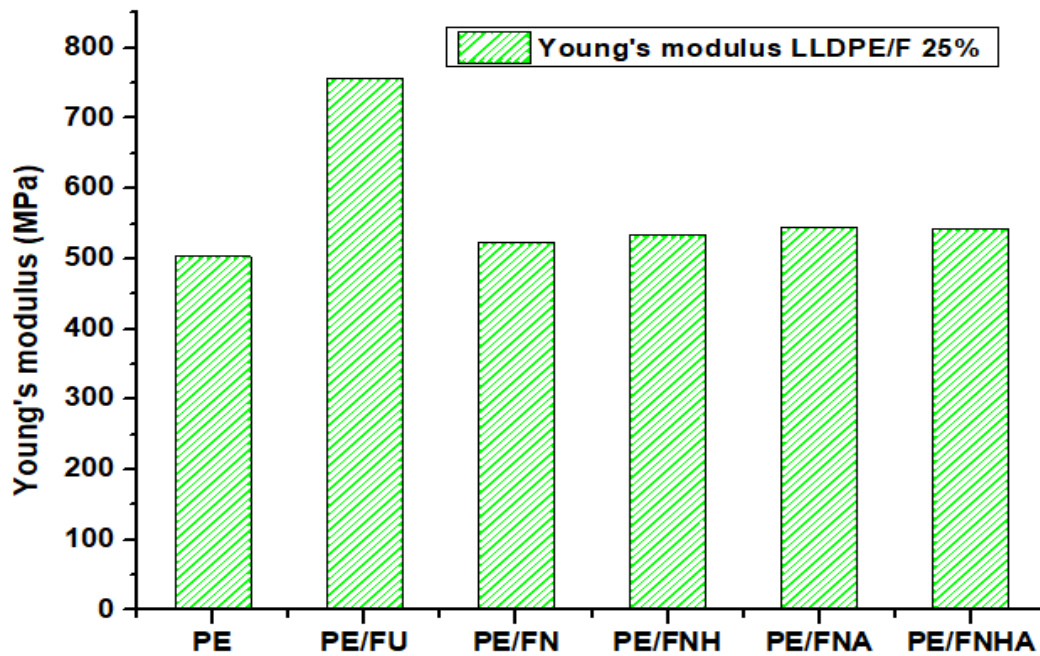


Figure II.14: Young's modulus of neat LLDPE, treated and untreated composites 25%.

II.3.2. Flexural testing

II.3.2.1. Flexural strength

a. Load Effect

The evolution of the flexural strength of untreated composites as a function of a load of palm petiole fibers is illustrated in Fig II.15. We note an increase in the flexural stress of the composites filled with untreated fibers compared to the unfilled LLDPE. This increase is evaluated at 15.56 and 16.04 MPa for the LLDPE/FU 15% and LLDPE/FU 25%, respectively. This increase increases as the fiber rate increases due to the increase in the bond strength between the fiber and the matrix. After adding 25% of FU, the flexural strength was improved. The flexural properties improve with increasing the fiber loading up to the critical loading point; afterward, it declines. Some researchers [22, 23] found that flexural properties increased with the fiber loading increase but decreased from 50 to 60% of loading.

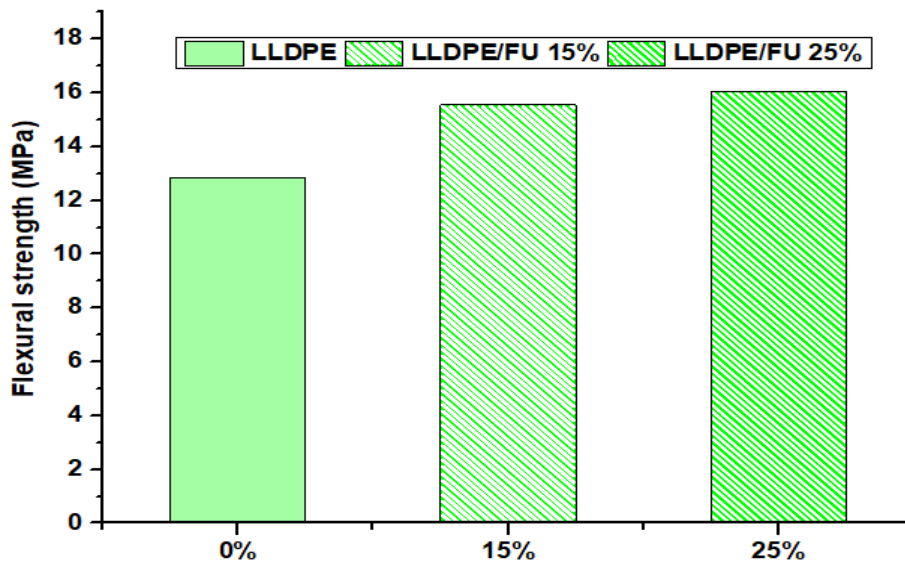


Figure II.15: Flexural strength of neat LLDPE and untreated composites 15-25%

b. Treatment effect

Fig II.16 and II.17. shows the variations in flexural strength for neat LLDPE and LLDPE composites reinforced with (15-25%) of treated and untreated palm petiole fiber. The flexural strength improved by 22.51%, 24.88% by adding 15-25% untreated and treated fibers to the composite compared to virgin LLDPE. This rise due to reinforced composites with treated fibers improved the fiber-matrix interaction under compressive loads during bending and greater transfer capacity at the fiber-matrix interface in reinforced composites treated fibers. However, in LLDPE/FNH 15% and LLDPE/FNH 25% it is noted that there is a decrease of 0.89 MPa and 0.165 MPa in flexural stress compared to LLDPE/FN 15% and LLDPE/FN 25% composites due to poor adhesion between the fiber and matrix phase. Several references

[24, 25] have also reported that fiber agglomerations could cause reduced flexural strength for LLDPE/FNH composites in the matrix, fiber moisture absorption, and interfacial defects, which limited the stress transfer from LLDPE to palm petiole fibers during bending tests. It is worth noting that the adhesion between the fibers-matrix is enhanced when the fiber's surface is pretreated with an alkaline solution [26]. The composites LLDPE/FU, LLDPE/FN, LLDPE/FNA and LLDPE/FNHA showed higher flexural stress at (15.56, 16.17, and 15.94 for LLDPE/F 15%) and (16.05, 17.23, 17.023 and 17.025 MPa for LLDPE/F 25%) respectively, due to a higher lignin content in FU, FN, and FNA, FNHA than in FNH, which is responsible for the rigidity of fibers [27].

The H_2O_2 interacts with lignin components during the bleaching of fibers in peroxide solution, removing lignin from the fiber. It also interacts with the hydroxyl groups of hemicelluloses to eliminate humidity from the fiber and increase its hydrophobicity. Following delignification, fibers become more flexible and exhibit reduced stiffness. Acetylated palm fiber composites LLDPE/FNA have been found to exhibit greater flexural strength compared to LLDPE/FNH composites. This improved strength can be attributed to the alkaline pretreatment, which removes hemicellulose and extractives from the fiber, thus improving its surface characteristics. Furthermore, acetylation reduces polarity by covering hydroxyl groups in the fiber cell wall, replacing hydrogen atoms with acetyl groups [28].

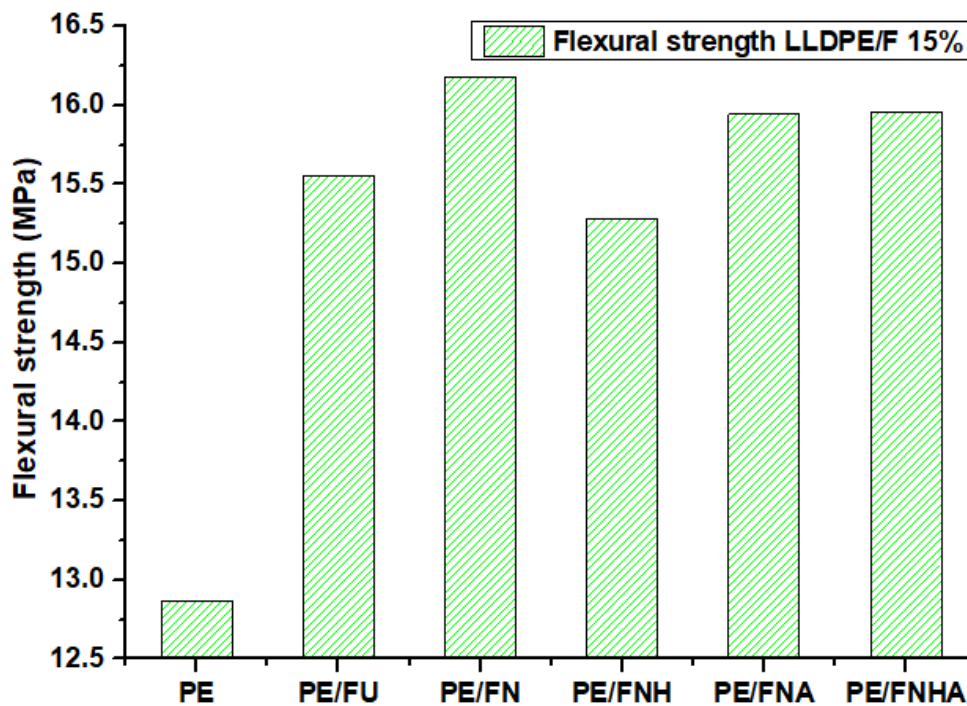


Figure II.16: Flexural strength of neat LLDPE, treated and untreated composites 15%.

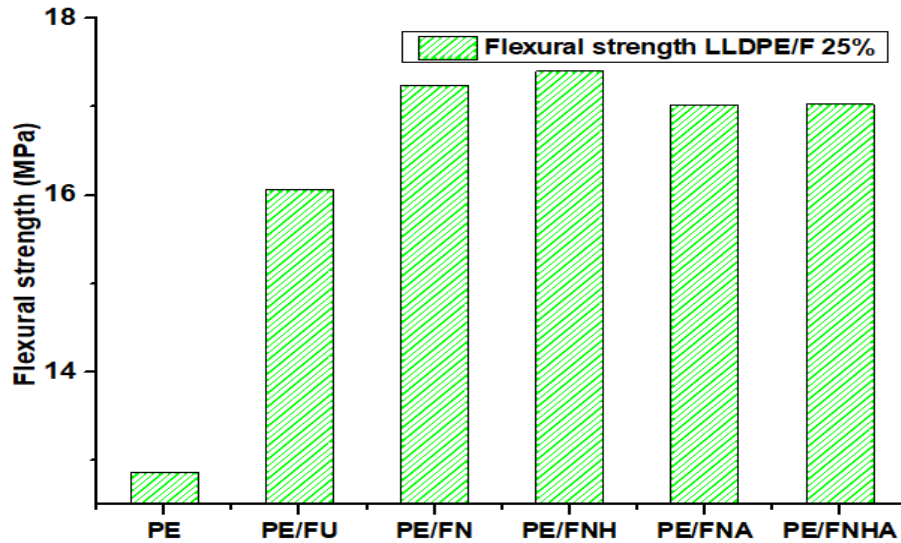


Figure II.17: Flexural strength of neat LLDPE, treated and untreated composites 25%.

II.3.2.2. Flexural modulus

a. Load Effect

The fig II.18 presents the variations of flexural modulus for the composites studied as a function of the palm petiole fiber content (15-25%). It was found that neat LLDPE has an excellent modulus compared to LLDPE/FU composites. After using 15% of the loading, LLDPE/FU composites decreased flexural modulus. The reduced properties may be due to a lower amount of reinforcement materials distributed in the sample unevenly that cannot transfer stress from the matrix. flexural modulus increases by adding 25% of FU with 1.49% more than virgin LLDPE [8]. These mechanical results indicate good adhesion between the LLDPE matrix and the petiole fiber.

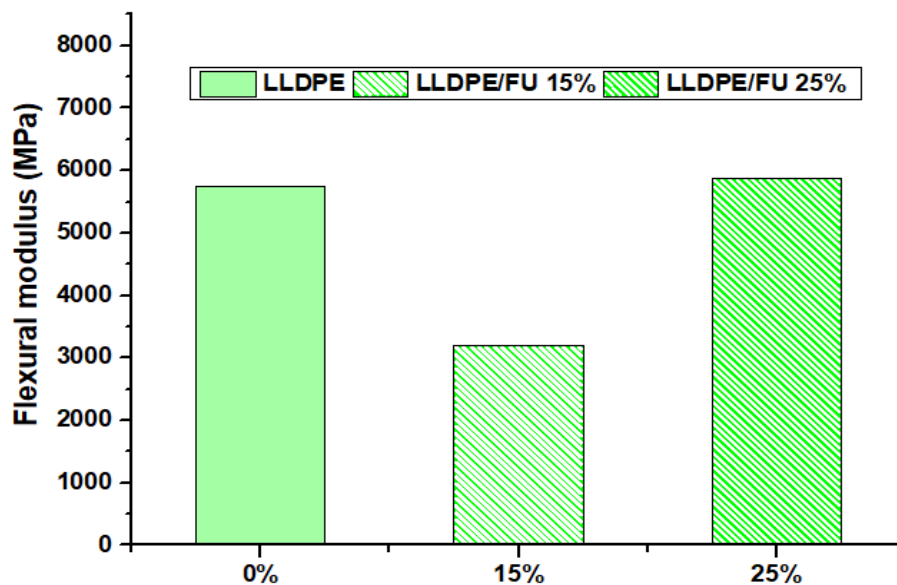


Figure II.18: Flexural modulus of neat LLDPE and untreated composites 15-25%.

b. Treatment effect

As shown in fig II.19 and II.20, the flexural modulus shows a wiggle after adding fibers into the LLDPE matrix. A similar trend was also found by [29]. After treatment, The LLDPE/FN 15-25 % and LLDPE/FNHA 15-25 % composites show the most significant improvement (6728 MPa, 7693 MPa for 15%) and (4870 MPa, 5173 MPa for 25%), respectively, in flexural modulus; this is due to fiber bundles being broken and uniformly distributed, resulting in a better flexural modulus. In contrast, The LLDPE/FNH 15% and LLDPE/FNA 15% composites revealed a slight reduction in flexural modulus (2257 MPa 1465 MPa), respectively, compared to the LLDPE/FN 15% sample, which is likely due to partial deterioration of the structure of the FNH and FNA fibers. [3].

Compared to the untreated and treated composites, the acetylated composite LLDPE/FNHA 15-25% has a high flexural modulus. Researchers hypothesized that the fiber's low polarity and high surface roughness treated successively with alkali, peroxide, and acetylation improved the compatibility of the fiber with the polymer matrix, resulting in excellent interaction between the two and even distribution of the fibers throughout the matrix [30].

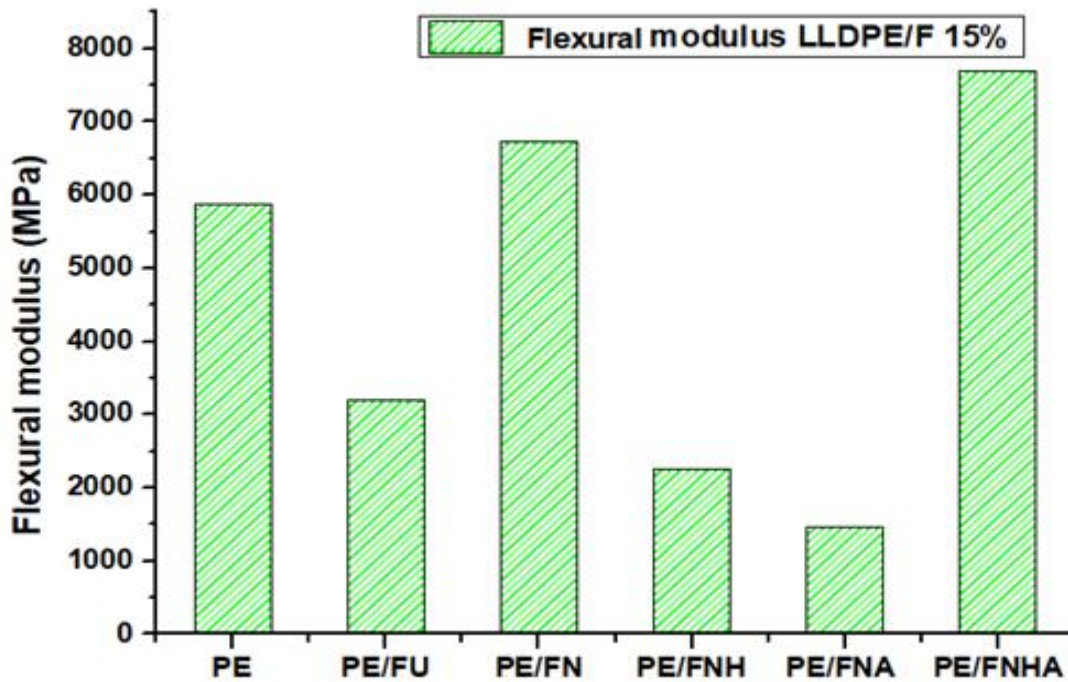


Figure II.19: Flexural modulus of neat LLDPE, treated and untreated composites 15%.

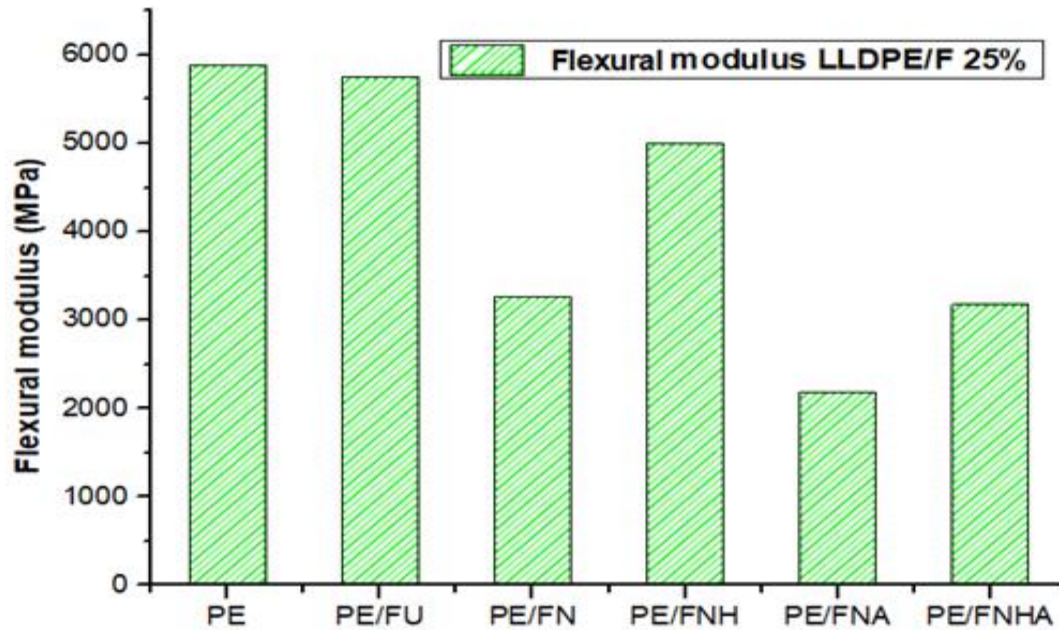


Figure II.20: Flexural modulus of neat LLDPE, treated and untreated composites 25%.

II.4. Dynamic mechanical analysis (DMA)

II.4.1. Storage modulus (E')

a. Load Effect

The variation of storage modulus of the untreated palm petiole fiber loadings (FU 15-25 %) reinforced LLDPE composites, and neat LLDPE composites are shown in Fig II.21.

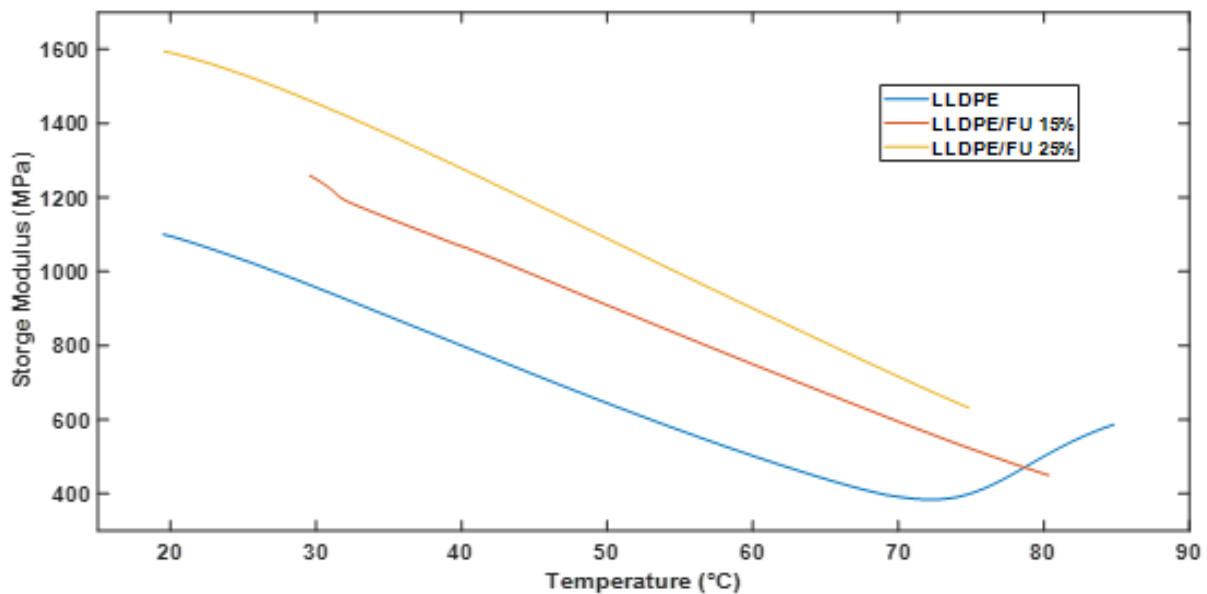


Figure II.21: Storage modulus of neat LLDPE and untreated composites 15-25%.

It can be seen that the storage modulus of fiber composites increases with increasing the content in the LLDPE matrix, and the curve falls with increasing temperature. In the case of the pure LLDPE sample, there is the lowest storage modulus. It is due to the increased molecular mobility of the polymer chains above [31]. The allocation of FU particles can be attributed to two essential factors; The first is the excellent dispersion of these particles in the LLDPE matrix, and the second is the good interaction between the particles of the fibers and the matrix.

b. Treatment effect

The storage modulus (E') indicates the quantity of energy a material can store during one oscillation cycle [32]. It exhibits the temperature-dependent stiffness behavior and load-bearing capacities of composite materials. Fig II.22 and II.23. shows the storage modulus curves of LLDPE composites with 15-25 % of palm petiole fiber, treated and untreated, recorded at 1 Hz from 20°C to 80°C. At 20°C, pure LLDPE is less stiff, with a lower value of E' at 1100 MPa, and more flexible [33] compared to LLDPE composites such as LLDPE/FU, LLDPE/FN, LLDPE/FNH, LLDPE/FNA, and LLDPE/FNHA (1259, 1272, 1200, 1331 and 1252 MPa for 15%) and (1594, 1508, 1510, 1539 and 1570 MPa for 25%) in the range of temperature 29–34°C. The incorporation of fibers has been found to improve (E') and decrease with an increase in temperature [34]. The stiff fibers reduce the molecular mobility of LLDPE, making the material more rigid. Higher values of E' indicate greater energy storage capacity and excellent interfacial adhesion between the matrix and fiber, as demonstrated by research [35]. The composites containing more lignin in fibers FU, FN, and FNA have higher E' due to considerable stress transfer at the fiber-matrix interface, reducing molecular mobility according to S. Shinoj et al [36].

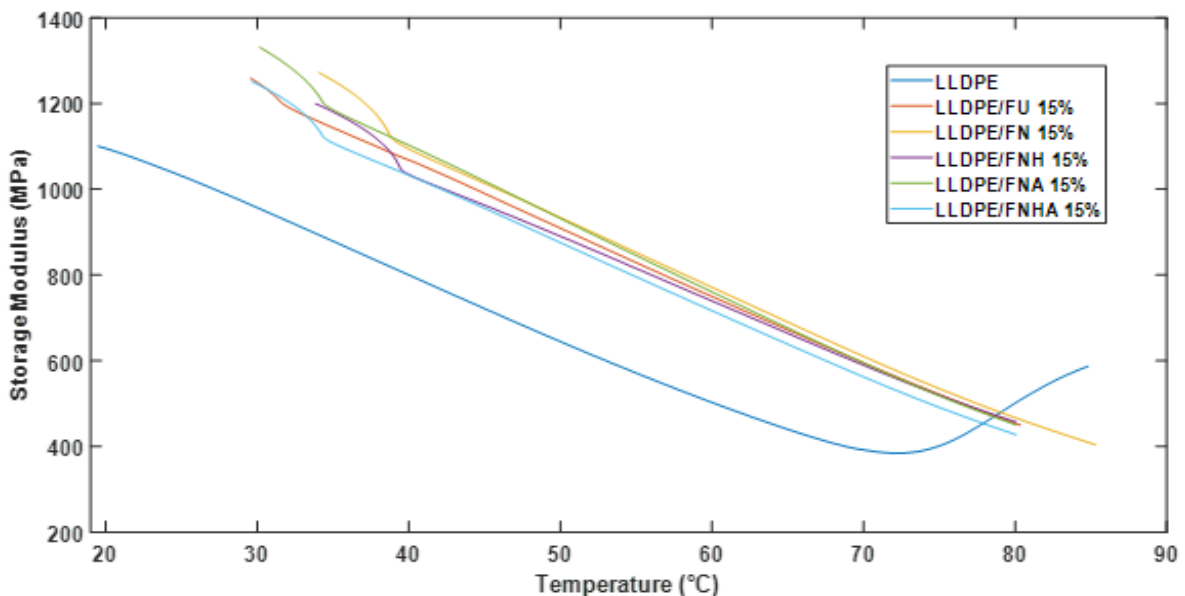


Figure II.22: Storage modulus of neat LLDPE, treated and untreated composites 15%.

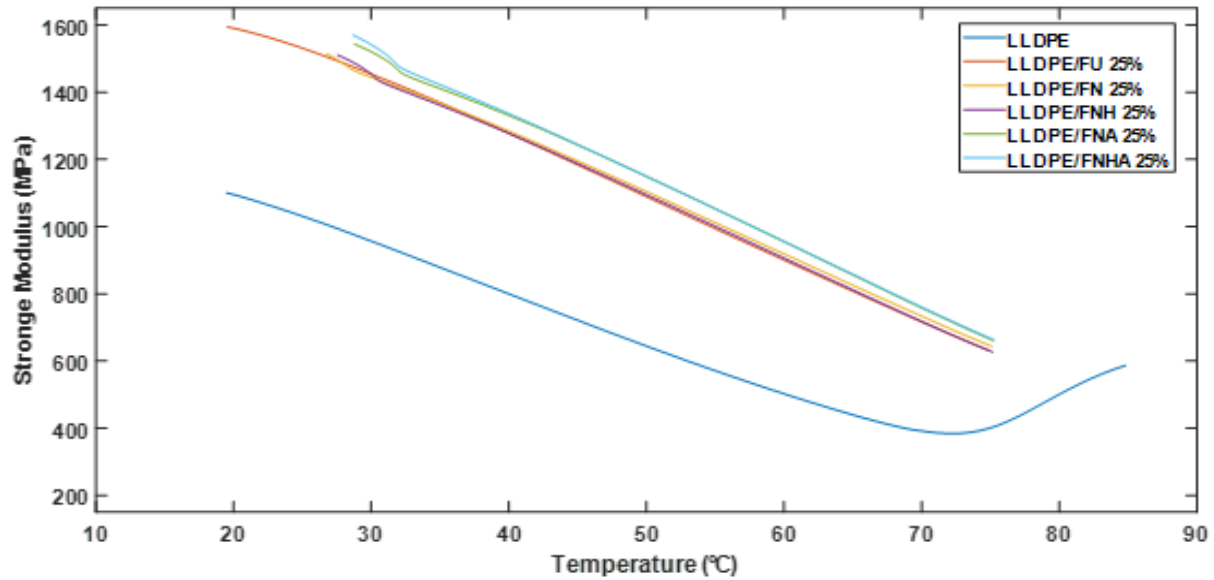


Figure II.23: Storage modulus of neat LLDPE, treated and untreated composites 25%.

II.4.2. Loss modulus (E'')

a. Load Effect

Fig II.24 shows the effect of loadings of palm petiole fiber on the loss modulus of the LLDPE/FU composite.

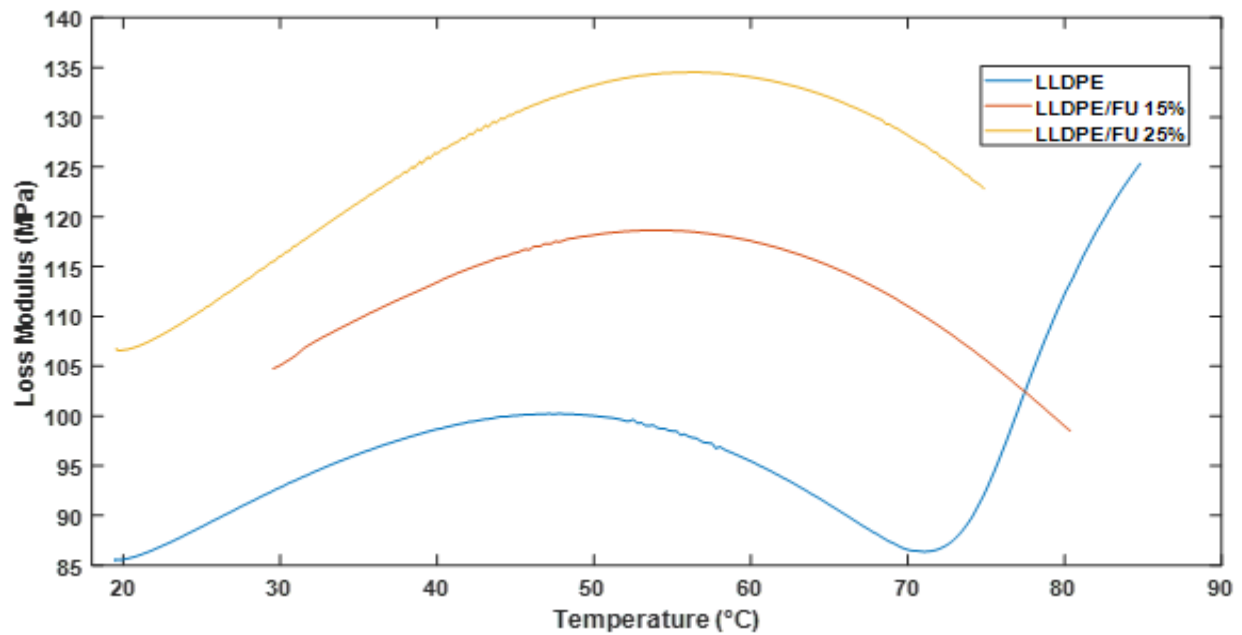


Figure II.24: Loss modulus of neat LLDPE and untreated composites 15-25%.

It can be observed that the loss modulus E'' increases with the increase in temperature until it reaches a maximum value at a temperature equal to 49 °C for neat LLDPE, then decreases with the increase in temperature due to a reduction in the friction of the polymer chains. The relaxation peak broadened after incorporating FU, and the loss modulus of all composites is higher than neat LLDPE due to the internal friction in composites that enhances the dissipation of energy where LLDPE/FU 25% composite showed the highest loss modulus [19], perhaps due to the higher percentage of natural fibers enhanced internal friction.

b. Treatment effect

The loss modulus (E'') represents the dissipated thermal energy of composites under applied energy [37]. Fig II.25 and II.26. shows that the E'' value of pure LLDPE (100 MPa at 49 °C) was lower than that of composites reinforced with 15-25% of palm petiole fibers.

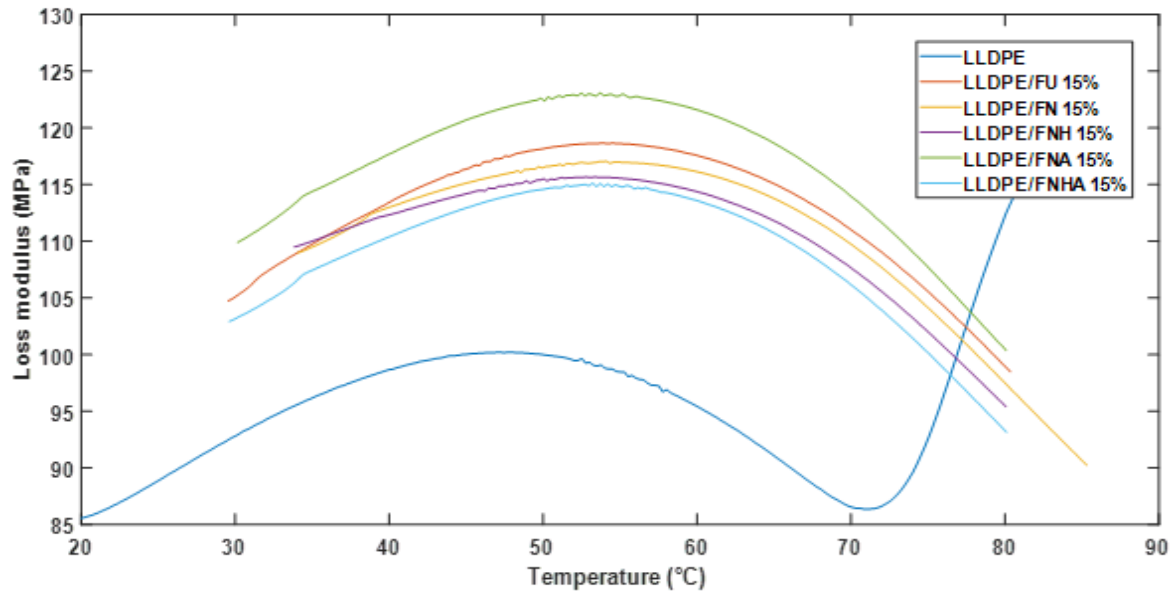


Figure II.25: Loss modulus of neat LLDPE, treated and untreated composites 15%.

The E'' values increased with the addition of FN, FNH, and FNA fibers due to the decreased mobility of the matrix chains. This is consistent with findings from other studies on OPF-LLDPE and OPF-sisal fiber-natural rubber-reinforced composites [36, 38]. Among the composites, the loss modulus of the LLDPE/FNA 15% composite had the highest value of 123 MPa, followed by LLDPE/FU 15% with 118 MPa and LLDPE/FN 15% with 117 MPa at a temperature range of 52–55 °C. This could result from the enhanced adhesion between the fibers and the LLDPE matrix [39]. The E'' curves of all composites peaked and fell as the temperature increased, indicating that most of the energy was dissipated due to the free

mobility of the polymer chains [40]. At elevated temperatures, the E'' of the LLDPE/FNHA composite decreased slightly to 115 MPa at 54 °C, possibly because the fiber prevented the polymer chains from moving freely [41]. Interestingly, for the internal fractions in composites that increase energy dissipation, the loss modulus of all composites was significantly better than that of plain LLDPE. But in LLDPE/FNH 25%, we show a decrease of loss modulus due to a higher proportion of fibers that cannot mix properly with the matrix.

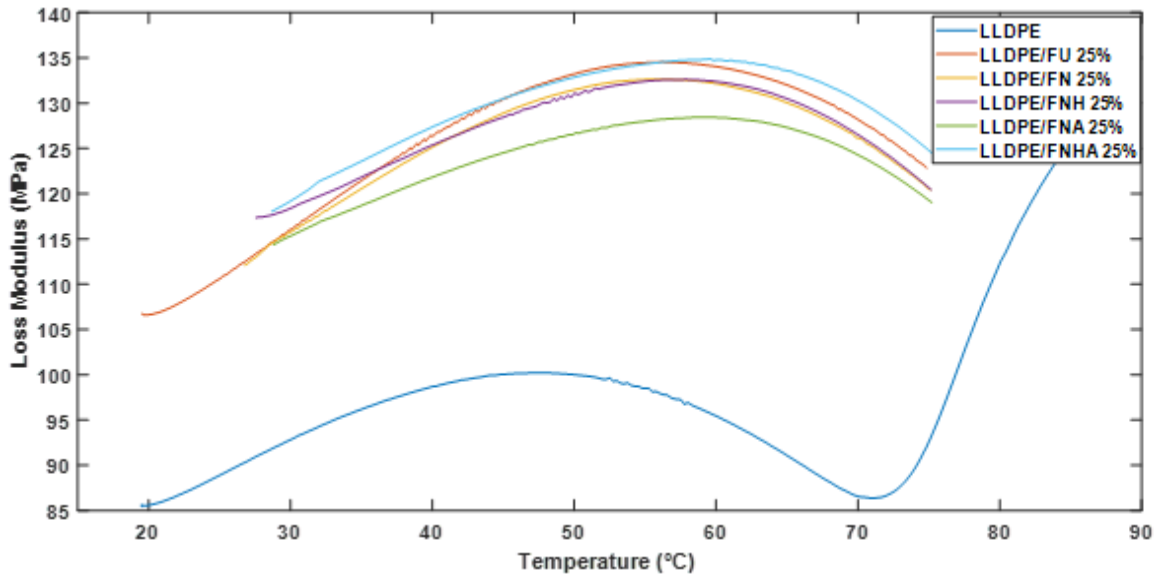


Figure II.26: Loss modulus of neat LLDPE, treated and untreated composites 25%.

II.4.3. Tan Delta

a. Load Effect

The $\tan \delta$ temperature curve of LLDPE and untreated composites with different fiber loading is presented in Fig II.27. It was observed that $\tan \delta$ increased at higher temperatures. In the $\tan \delta$ value of LLDPE/FU composites at various fiber loadings, Only one peak was observed for all the composite samples, which indicates better interaction between fiber and matrix due to decreased heterogeneity in the composite. Higher $\tan \delta$ was observed for unfilled LLDPE except between temperatures of 20 to 80 °C, which indicates a higher degree of molecular mobility [42]. It can be summarized that heterogeneous fiber allows the temperature to infiltrate polymers. However, if the polymer and fibers are homogeneous and have strong bonding, then the polymer holds fibers and also protects from high temperatures, and maintains thermal stability.

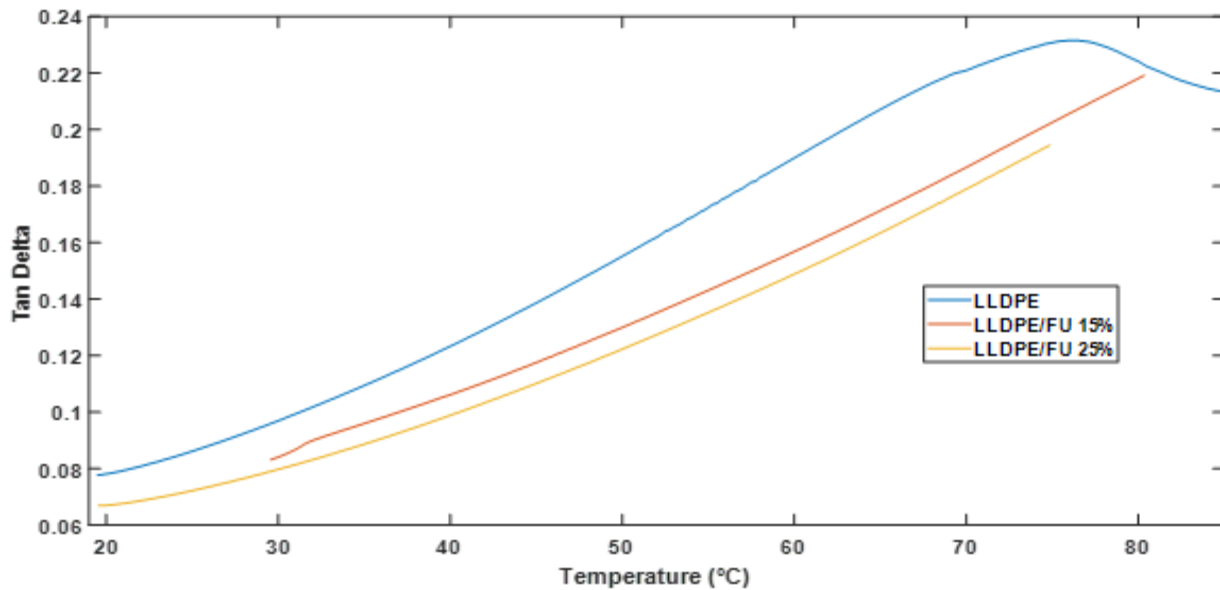


Figure II.27: Tan Delta of neat LLDPE and untreated composites 15-25%

b. Treatment effect

Tan δ measures the frictional behavior of fibers and the molecular mobility of polymers in composite materials [31]. Fig. 11. shows the change in the value of tan δ as a function of temperature for treated and untreated palm petiole fiber reinforced LLDPE composites with 15-25% fiber loading, which were measured at 1 Hz in the range of 20°C to 80°C. At a temperature of 75°C, pure LLDPE exhibited a higher tan δ value of 0.2315; similar results were discovered by [36] higher tan δ was observed for pure LLDPE except between temperatures of 100 °C and 25 °C. As shown in Figure 7, the energy dissipation coefficients for the reinforced LLDPE/F 15-25% composites (FU, FN, FNH, FNA, and FNHA) were found to be lower than that of pure LLDPE, with values of (0.2192, 0.2236, 0.2089, 0.223, and 0.2182 for 15%) and (0.1945, 0.1877, 0.1923, 0.1801, 0.1877 for 25%), respectively, in the range of temperature 80-85°C. This shows excellent contact between the palm petiole fibers and the matrix, resulting in reduced composite damping due to the polymeric chains connecting to the petiole fibers [7], which reduces their mobility and friction, as suggested in reference [43]. Saba et al. [44] found that fiber agglomeration is another factor contributing to the reduced tan δ value, resulting from less polymer by volume in the composites. The drop in tan δ observed after chemical modification of the fibers was attributed to enhanced interaction between the treated fibers and LLDPE. This trend is similar to the observations of Aziz et al. [45] on long kenaf polyester composites.

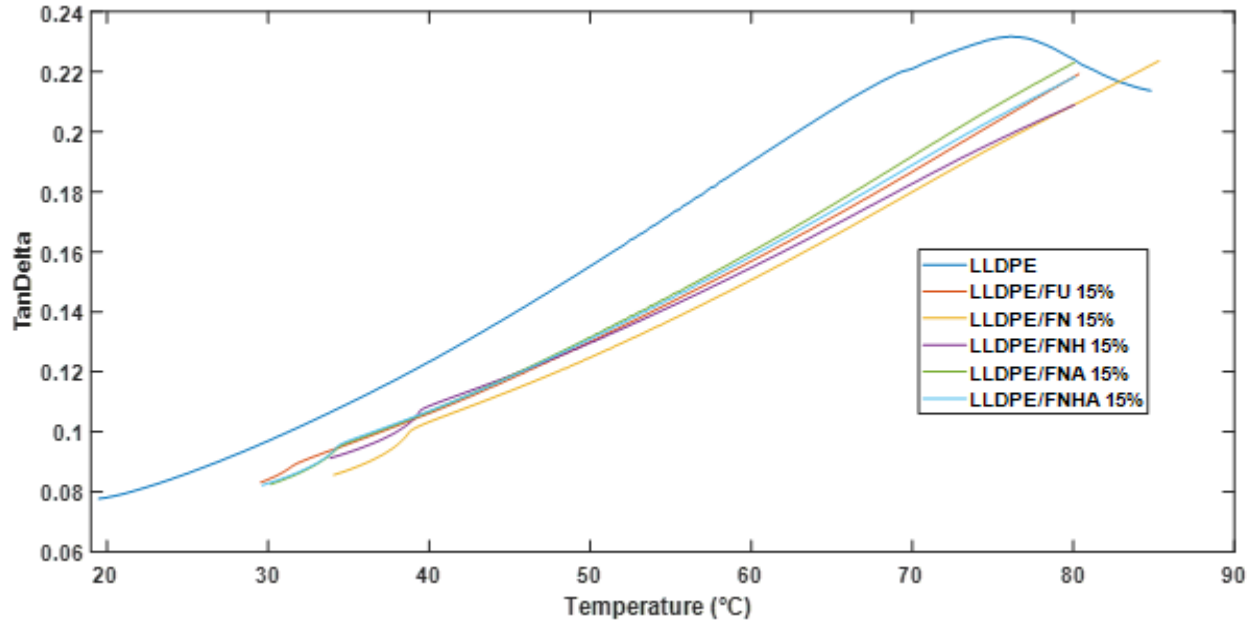


Figure II.28: Tan Delta of neat LLDPE, treated and untreated composites 15%.

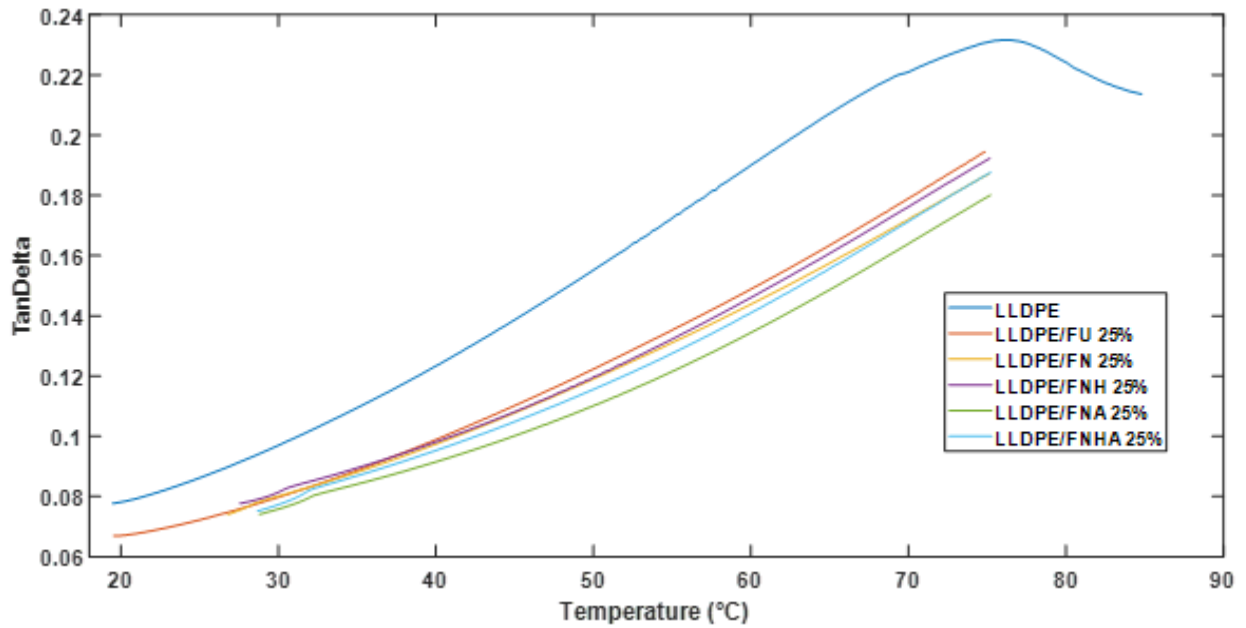


Figure II.29: Tan Delta of neat LLDPE, treated and untreated composites 25%.

II.5. Hardness

a. Load Effect

Material hardness is material resistance to penetration. The principle used to measure Shore A hardness is based on the strength of needle resistance that penetrates the material. The results of this test are used to compare the hardness of composite materials. The measurement is done at one point of material and repeated at another end at a distance of 1 cm. In one data sample, 6 points were taken. Fig II.30 shows the effect of fiber loading on the hardness of composites. The curves clearly show the significant increase in hardness with the incorporation of untreated palm petiole fiber. This increase is all the more significant as the rate of fibers is high [12]. These results are predictable insofar as the palm petiole fiber has a hard character which increases the hardness of the LLDPE/FU 15-25% composites. this result indicates the decrease in flexibility and the increase in rigidity hardness values are a measure of resistance to wear and abrasion since hard materials are more resistant to friction.

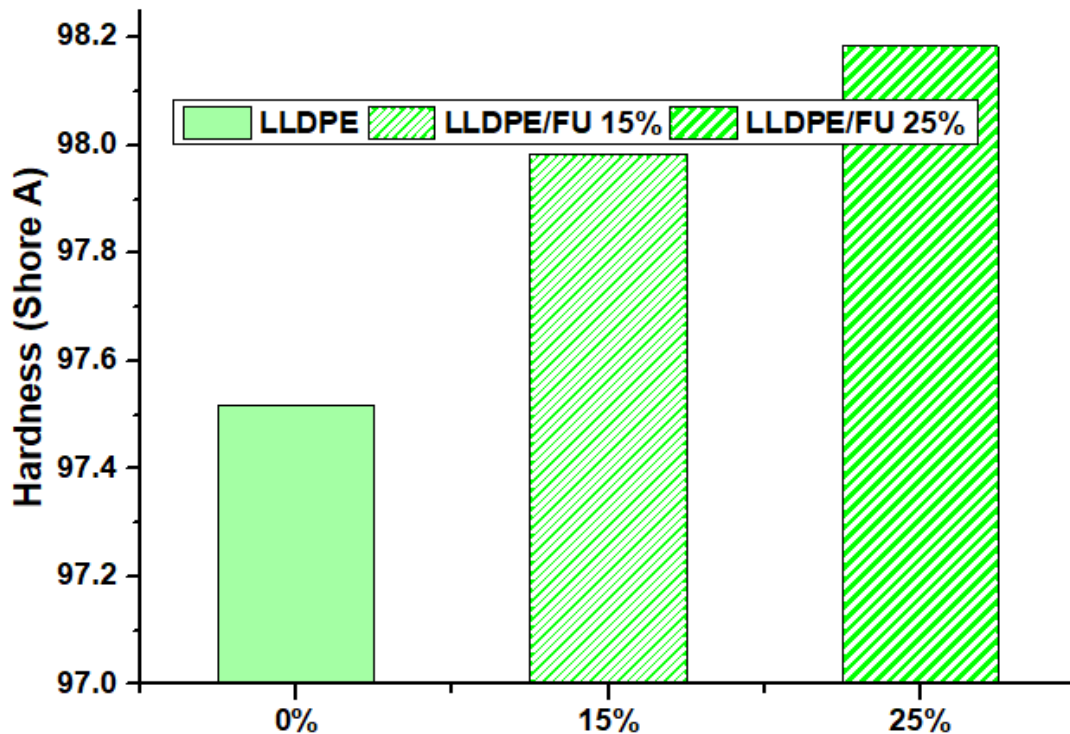


Figure II.30: Hardness shore A of neat LLDPE and untreated composites 15-25%.

b. Treatment effect

After successive treatments, it can be seen in the Fig II.31 and II.32 that has increased with the addition of fiber in polyethylene from 15 to 25%. The fiber is very influential on the hardness of composite materials due to the higher the strength of the fiber and higher the content. The hardness of composite materials is affected by fibers treated with a 10% NaOH solution. The fibers' adhesion to the matrix material in the composite LLDPE/FN 25% increased by increasing the surface roughness of the fiber through NaOH treatment. The uniform distribution of the fibers throughout the composite results from enhanced adhesion between the fibers and the matrix, increasing the material's overall stiffness and strength. The NaOH/H₂O₂ solution alters the surface properties, eliminates the lignin and hemicellulose that play a role in the hardness of the fibers, and makes the surface roughness, wettability, and chemical composition different. This decreases the adhesion between the fibers and the matrix and reduces the hardness of the LLDPE/FNH by 97.3 composites compared to LLDPE/FU by 97.9.

After double pretreatment, the NaOH and acetylation processes substantially impact the hardness of composite materials. The chemical modification technique of acetylation makes petiole fiber more reactive on the surface and more compatible with LLDPE matrices. Acetylated fiber can create a more influential band with the surrounding matrix when employed in composite materials, which leads to improved mechanical qualities such as raised hardness, stiffness, and strength [46]. The acetylation procedure also increases the fibers' dimensional stability and water resistance, increasing the composite material's overall durability. The adhesion between fibers and the matrix material in LLDPE/FNHA composites was improved by treating fiber with NaOH/ H₂O₂ and acetic anhydride solutions; this enhanced adhesion and increased mechanical properties, such as hardness. Removing the impurities and altering the surface chemistry of fibers with NaOH/ H₂O₂ results in a cleaner and more reactive surface. Encouraging chemical bonding between the two materials increases adhesion. The matrix material and these acetyl groups may react, improving adhesion and increasing hardness [47].

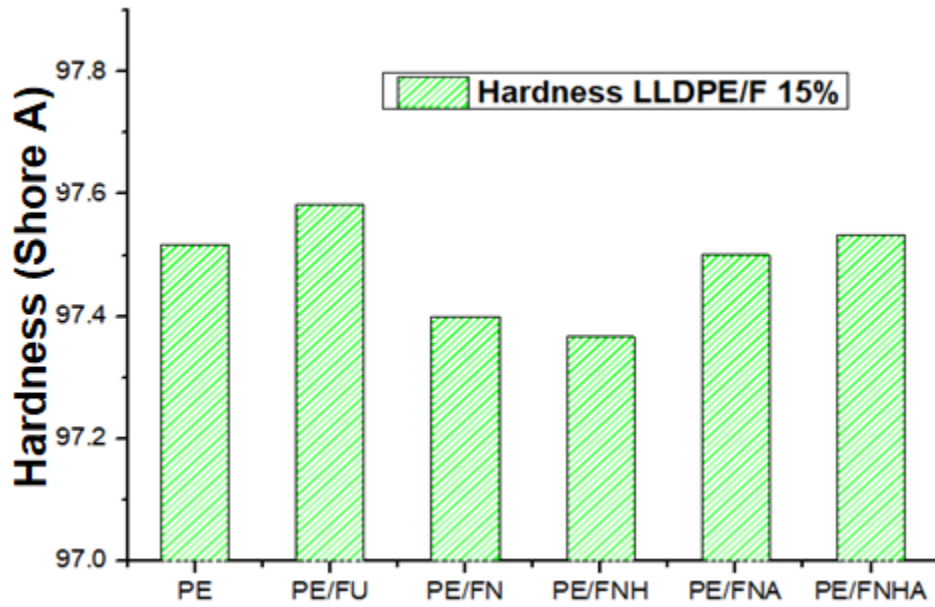


Figure II.31: Hardness Shore A of neat LLDPE, treated and untreated composites 15%.

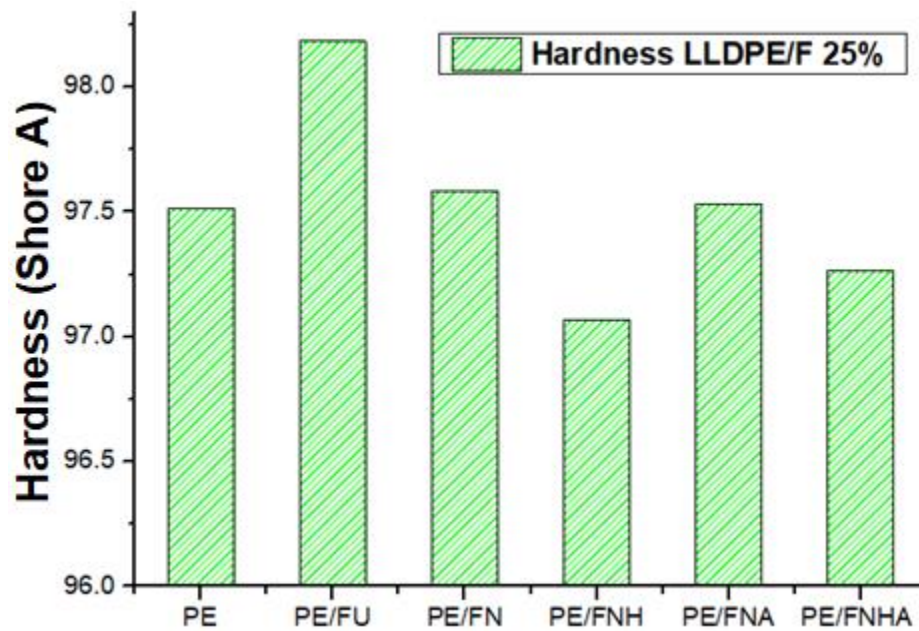


Figure II.32: Hardness Shore A of neat LLDPE, treated and untreated composites 25%.

Reference

- [1] X. Li, L. G. Tabil, and S. Panigrahi, "Chemical treatments of natural fiber for use in natural fiber-reinforced composites: a review," *Journal of Polymers and the Environment*, vol. 15, pp. 25-33, 2007.
- [2] D. Jones, G. O. Ormondroyd, S. F. Curling, C. M. Popescu, and M. C. Popescu, "2 - Chemical compositions of natural fibres," in *Advanced High Strength Natural Fibre Composites in Construction*, M. Fan and F. Fu, Eds., ed: Woodhead Publishing, 2017, pp. 23-58.
- [3] M. Barczewski, D. Matykiewicz, and M. Szostak, "The effect of two-step surface treatment by hydrogen peroxide and silanization of flax/cotton fabrics on epoxy-based laminates thermomechanical properties and structure," *J. Mater. Res. Technol.*, vol. 9, pp. 13813-13824, 2020.
- [4] S. N. Sarmin, M. Jawaid, A. Ismail, M. Hashem, H. Fouad, M. Midani, *et al.*, "Effect of chitosan filler on the thermal and viscoelasticity properties of bio-epoxy/date palm fiber composites," *Sustainable Chemistry and Pharmacy*, vol. 36, p. 101275, 09/24 2023.
- [5] B. Safieddine, A. Belaadi, A. Makhoulf, H. Alshahrani, M. Khan, and M. Jawaid, "Effect of Fiber Loading on Thermal Properties of Cellulosic Washingtonia Reinforced HDPE Biocomposites," *Polymers*, vol. 15, p. 2910, 07/01 2023.
- [6] M. Asim, M. T. Paridah, N. Saba, M. Jawaid, O. Y. Alothman, M. Nasir, *et al.*, "Thermal, physical properties and flammability of silane treated kenaf/pineapple leaf fibres phenolic hybrid composites," *Composite Structures*, vol. 202, pp. 1330-1338, 2018/10/15/ 2018.
- [7] M. Asim, M. Jawaid, M. Nasir, and N. Saba, "Effect of fiber loadings and treatment on dynamic mechanical, thermal and flammability properties of pineapple leaf fiber and kenaf phenolic composites," *Journal of Renewable Materials*, vol. 6, p. 383, 2018.
- [8] E. V. Torres-Tello, J. R. Robledo-Ortíz, Y. González-García, A. A. Pérez-Fonseca, C. F. Jasso-Gastinel, and E. Mendizábal, "Effect of agave fiber content in the thermal and mechanical properties of green composites based on polyhydroxybutyrate or poly(hydroxybutyrate-co-hydroxyvalerate)," *Industrial Crops and Products*, vol. 99, pp. 117-125, 2017/05/01/ 2017.

- [9] A. p. V.R and R. A, "Thermo-mechanical characterization of siliconized E-glass fiber/hematite particles reinforced epoxy resin hybrid composite," *Applied Surface Science*, vol. 384, pp. 99-106, 2016/10/30/ 2016.
- [10] M. Alshammari, A. Ahmad, M. Jawaid, and S. Awad, "Thermal and Dynamic Performance of Kenaf/Washingtonia Fibre-Based Hybrid Composites," *Journal of Materials Research and Technology*, vol. 25, 06/01 2023.
- [11] C. Muthukumar, S. Krishnasamy, M. Jawaid, S. Alamery, H. Fouad, and M. Midani, "Tensile, Thermal and Physical Properties of Washightonia Trunk Fibres/Pineapple Fibre Biophenolic Hybrid Composites," *Journal of Polymers and the Environment*, vol. 30, 07/15 2022.
- [12] S. Awad, M. Jawaid, H. Fouad, N. Saba, H. Dhakal, O. Alothman, *et al.*, "A comparative assessment of chemical, mechanical, and thermal characteristics of treated oil palm/pineapple fiber/bio phenolic composites," *Polymer Composites*, vol. 43, 02/08 2022.
- [13] O. Alothman, H. Shaikh, B. Alshammari, and M. Jawaid, "Structural, Morphological and Thermal Properties of Nano Filler Produced from Date Palm-Based Micro Fibers (*Phoenix dactylifera L.*)," *Journal of Polymers and the Environment*, vol. 30, pp. 1-9, 02/01 2022.
- [14] B. Bax and J. Müssig, "Impact and tensile properties of PLA/Cordenka and PLA/flax composites," *Composites Science and Technology*, vol. 68, pp. 1601-1607, 2008/06/01/ 2008.
- [15] V. Manikandan, J. T. Winowlin Jappes, S. M. Suresh Kumar, and P. Amuthakkannan, "Investigation of the effect of surface modifications on the mechanical properties of basalt fibre reinforced polymer composites," *Composites Part B: Engineering*, vol. 43, pp. 812-818, 2012/03/01/ 2012.
- [16] K. S. Chun, C. M. Yeng, S. Husseinsyah, M. M. Pang, and A. Ismail, "Effect of eco-degradant on properties of low density polyethylene/corn stalk eco-composites," *J. Eng. Sci. Technol*, vol. 12, pp. 1165-77, 2017.
- [17] J. J. Joglekar, Y. Munde, A. Jadhav, D. Bhutada, S. Radhakrishnan, and M. Kulkarni, "Mechanical and morphological properties of Citrus Maxima waste powder filled Low-Density polyethylene composites," *Mater. Today: Proc.*, vol. 47, pp. 5640-5645, 2021.

- [18] H. U. Zaman and R. A. Khan, "Acetylation used for natural fiber/polymer composites," *J. Thermoplast. Compos. Mater.*, vol. 34, pp. 3-23, 2021.
- [19] M. Jawaid, H. P. S. Abdul Khalil, A. Hassan, R. Dungani, and A. Hadiyane, "Effect of jute fibre loading on tensile and dynamic mechanical properties of oil palm epoxy composites," *Composites Part B: Engineering*, vol. 45, pp. 619-624, 2013/02/01/ 2013.
- [20] M. A. AlMaadeed, Z. Nógellová, I. Janigová, and I. Krupa, "Improved mechanical properties of recycled linear low-density polyethylene composites filled with date palm wood powder," *Materials & Design*, vol. 58, pp. 209-216, 2014.
- [21] Y. Cao, S. Shibata, and I. Fukumoto, "Mechanical properties of biodegradable composites reinforced with bagasse fibre before and after alkali treatments," *Composites part A: Applied science and Manufacturing*, vol. 37, pp. 423-429, 2006.
- [22] N. Saba, M. T. Paridah, and M. Jawaid, "Mechanical properties of kenaf fibre reinforced polymer composite: A review," *Construction and Building Materials*, vol. 76, pp. 87-96, 2015/02/01/ 2015.
- [23] H. Anuar and A. Zuraida, "Improvement in mechanical properties of reinforced thermoplastic elastomer composite with kenaf bast fibre," *Composites Part B: Engineering*, vol. 42, pp. 462-465, 2011/04/01/ 2011.
- [24] N. Venkateshwaran, A. E. Perumal, and D. Arunsundaranayagam, "Fiber surface treatment and its effect on mechanical and visco-elastic behaviour of banana/epoxy composite," *Materials & Design*, vol. 47, pp. 151-159, 2013.
- [25] M. Li, Y. Pu, V. M. Thomas, C. G. Yoo, S. Ozcan, Y. Deng, *et al.*, "Recent advancements of plant-based natural fiber-reinforced composites and their applications," *Composites Part B: Engineering*, vol. 200, p. 108254, 2020.
- [26] K. Gulati, S. Lal, S. Kumar, and S. Arora, "Effect of gamma irradiation on thermal, mechanical and water absorption behavior of LLDPE hybrid composites reinforced with date pit (*Phoenix dactylifera*) and glass fiber," *Polymer Bulletin*, vol. 78, pp. 7019-7038, 2021.
- [27] T. Nampitch, "Mechanical, thermal and morphological properties of polylactic acid/natural rubber/bagasse fiber composite foams," *Results in Materials*, vol. 12, p. 100225, 2021.

- [28] M. Kabir, H. Wang, K. Lau, and F. Cardona, "Chemical treatments on plant-based natural fibre reinforced polymer composites: An overview," *Composites Part B: Engineering*, vol. 43, pp. 2883-2892, 2012.
- [29] J. Sahari, S. Sapuan, E. Zainudin, and M. A. Maleque, "Mechanical and thermal properties of environmentally friendly composites derived from sugar palm tree," *Materials & Design*, vol. 49, pp. 285-289, 2013.
- [30] A. Bledzki, A. Mamun, M. Lucka-Gabor, and V. Gutowski, "The effects of acetylation on properties of flax fibre and its polypropylene composites," *Express Polymer Letters*, vol. 2, pp. 413-422, 2008.
- [31] N. Saba, M. Jawaid, O. Y. Alothman, and M. Paridah, "A review on dynamic mechanical properties of natural fibre reinforced polymer composites," *Constr Build Mater.*, vol. 106, pp. 149-159, 2016.
- [32] T. J. Elappunkal, R. Mathew, P. Thomas, S. Thomas, and K. Joseph, "Dynamic mechanical properties of cotton/polypropylene commingled composite systems," *J. Appl. Polym. Sci.*, vol. 114, pp. 2624-2631, 2009.
- [33] M. Faker, M. R. Aghjeh, M. Ghaffari, and S. Seyyedi, "Rheology, morphology and mechanical properties of polyethylene/ethylene vinyl acetate copolymer (PE/EVA) blends," *European Polymer Journal*, vol. 44, pp. 1834-1842, 2008.
- [34] H. Faria, N. Cordeiro, M. N. Belgacem, and A. Dufresne, "Dwarf Cavendish as a Source of Natural Fibers in Poly (propylene)-Based Composites," *Macromolecular Materials and Engineering*, vol. 291, pp. 16-26, 2006.
- [35] H. A. Khonakdar, "Dynamic mechanical analysis and thermal properties of LLDPE/EVA/modified silica nanocomposites," *Composites Part B: Engineering*, vol. 76, pp. 343-353, 2015.
- [36] S. Shinoj, R. Visvanathan, S. Panigrahi, and N. Varadharaju, "Dynamic mechanical properties of oil palm fibre (OPF)-linear low density polyethylene (LLDPE) biocomposites and study of fibre-matrix interactions," *Biosystems engineering*, vol. 109, pp. 99-107, 2011.
- [37] M. Asim, M. Jawaid, H. Fouad, and O. Alothman, "Effect of surface modified date palm fibre loading on mechanical, thermal properties of date palm reinforced phenolic composites," *Composite Structures*, vol. 267, p. 113913, 2021.

- [38] M. Jacob, B. Francis, S. Thomas, and K. Varughese, "Dynamical mechanical analysis of sisal/oil palm hybrid fiber-reinforced natural rubber composites," *Polymer Composites*, vol. 27, pp. 671-680, 2006.
- [39] S. Abhilash and D. Lenin Singaravelu, "A comparative study of mechanical, dynamic mechanical and morphological characterization of tampico and coir fibre-reinforced LLDPE processed by rotational moulding," *Journal of Industrial Textiles*, vol. 51, pp. 285S-310S, 2022.
- [40] T. Singh, B. Gangil, A. Patnaik, S. Kumar, A. Rishiraj, and G. Fekete, "Physico-mechanical, thermal and dynamic mechanical behaviour of natural-synthetic fiber reinforced vinylester based homogenous and functionally graded composites," *Materials Research Express*, vol. 6, p. 025704, 2018.
- [41] R. M. Shahroze, M. R. Ishak, M. S. Salit, Z. Leman, M. Chandrasekar, N. S. Munawar, *et al.*, "Sugar palm fiber/polyester nanocomposites: Influence of adding nanoclay fillers on thermal, dynamic mechanical, and physical properties," *J. Vinyl Addit. Technol.*, vol. 26, pp. 236-243, 2020.
- [42] A. Etaati, S. Pather, Z. Fang, and H. Wang, "The study of fibre/matrix bond strength in short hemp polypropylene composites from dynamic mechanical analysis," *Composites Part B: Engineering*, vol. 62, pp. 19-28, 2014/06/01/ 2014.
- [43] A. Martínez-Hernández, C. Velasco-Santos, M. De-Icaza, and V. M. Castano, "Dynamical-mechanical and thermal analysis of polymeric composites reinforced with keratin biofibers from chicken feathers," *Composites Part B: Engineering*, vol. 38, pp. 405-410, 2007.
- [44] N. Saba, M. Paridah, K. Abdan, and N. A. Ibrahim, "Dynamic mechanical properties of oil palm nano filler/kenaf/epoxy hybrid nanocomposites," *Construction and Building Materials*, vol. 124, pp. 133-138, 2016.
- [45] S. H. Aziz and M. P. Ansell, "The effect of alkalization and fibre alignment on the mechanical and thermal properties of kenaf and hemp bast fibre composites: Part 1-polyester resin matrix," *Composites science and technology*, vol. 64, pp. 1219-1230, 2004.
- [46] M. Al-Otaibi, O. Alothman, M. Alrashed, A. Anis, N. Jesuarockiam, and M. Jawaid, "Characterization of Date Palm Fiber-Reinforced Different Polypropylene Matrices," *Polymers*, vol. 12, p. 597, 03/05 2020.

- [47] R. Siakeng, M. Jawaid, H. Ariffin, S. M. Sapuan, M. Asim, and N. Saba, "Natural fiber reinforced polylactic acid composites: A review," *Polymer Composites*, vol. 40, pp. 446-463, 2019.

Chapter III
Characterization of
Composite After
Natural Weathering

Chapter III : Characterization of Composite After Natural Weathering

This chapter focuses on the behavior of LLDPE matrix composites reinforced with 15% of Palm petiole fibers after natural weathering (PPFw). The effects of aging will be evaluated by determining the exposed samples' morphological, physico-chemical, and mechanical properties.

III.1. Effect of natural weathering on the visual appearance (color)

The color change is the first indication of the natural degradation of polymers and the composite. Fig III.1 represents the color change evolution of the samples during natural aging after 360 days. We notice that the models have changed color compared to the reference sample (0 days).

Natural weathering causes significant color changes in biocomposite materials. There are main factors responsible for color change. UV radiation from the sun breaks down the chemical bonds in the polymers and fibers, leading to discoloration. Moisture, oxygen, the type of fibers, and the processing conditions affect the degree of color change during natural weathering. As shown in Fig III.1, LLDPE neat was not significantly influenced by aging. The bleaching kinetics of LLDPE/FUw, LLDPE/FNw, and LLDPE/FNAw were more likely to discolor than LLDPE/FNHw and LLDPE/FNHaw cellulose-rich. This color variation is due to a decomposition of the lignocellulosic constituents sensitive to solar radiation and rain. Furthermore, lignin looks reactive to UV rays and degrades more easily than polysaccharides [1]. Indeed, it presents chromophoric groups, structures susceptible to light. Photochemical decomposition takes place in two steps:

- The formation of paraquinone compounds following oxidation of the polymer chains of lignin manifests itself by a yellowing of the material. The reactions involved are lignin chain scission and demethoxylation. This last decomposition process is evidenced by a decrease in the level of methoxy - OCH₃ groups after exposure to ultraviolet light.
- Reduction of paraquinones to hydroquinones causing surface whitening.

Thus, chromophoric and moisture-sensitive compounds of lignocellulosic nature and present in natural fibers induce changes in the color and clarity of biocomposites through structural change and can affect their brightness during their life cycle [2].



Figure III.1: Color change evolution of neat LLDPE, treated and untreated composite after 1 year of natural weathering

III.2. Effect of natural weathering on weight loss

Weight losses of LLDPE/PPF upon weathering could be assumed as an indicator of biodegradation in the natural environment and depend on many factors, including the type of fiber, the amount of fiber loading, the thickness of the composite, and the exposure conditions.

Fig III.2 illustrates the variation in the weight of treated and untreated LLDPE/PPF composites as a function of exposure for 6-12 months; after recovery, the samples were washed, dried, and weighed. We can see that the mass loss increases as the aging time increases. This increase is more pronounced for composites treated than untreated composites and LLDPE. The porous structures enhance the accessibility of water, oxygen, and microorganisms into the polymer matrix and cause fractures in the LLDPE chains. Cellulosic materials were also degraded into a lower molecular weight compound [3]. The exposed surfaces permit moisture penetration that promotes microbial attack on the fiber and hydrolysis of the matrix component. These might contribute to the leaching out of the components to the outer surface and result in overall weight loss [4].

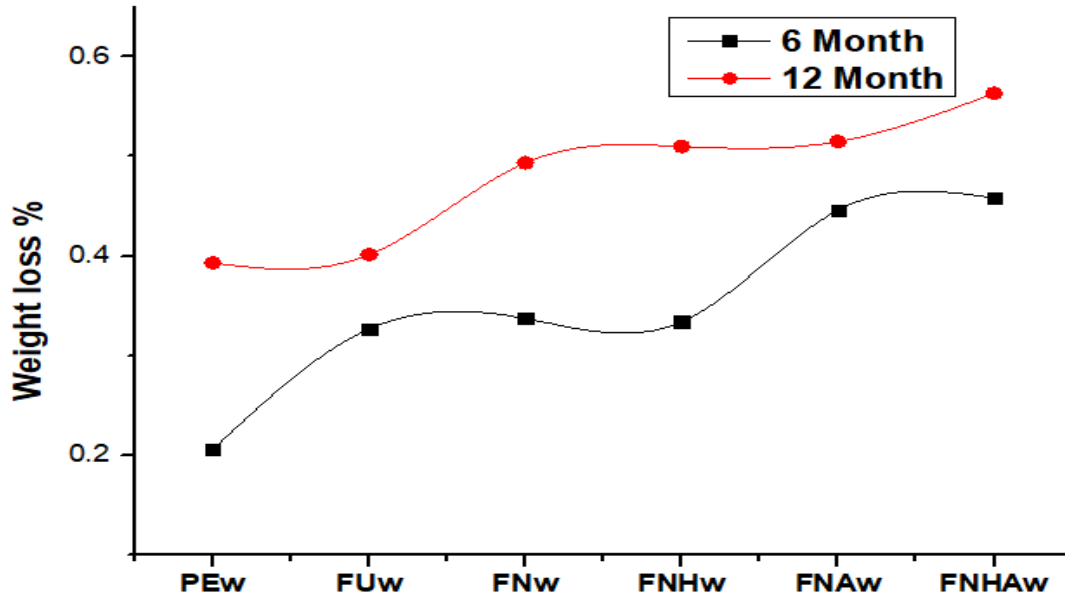


Figure III.2: Weight loss of neat LLDPE, treated and untreated composite after 6 and 12 months of natural weathering

III.3. Effect of natural weathering on the morphological structure (SEM)

The effect of natural aging was studied by examining the fractured surfaces of tensile testing samples of pure LLDPEw and treated and untreated composite after weathering with the scanning electron microscope (SEM). The obtained micrographs are shown in Figure III.3 (a, b, c, d, e, f), respectively.

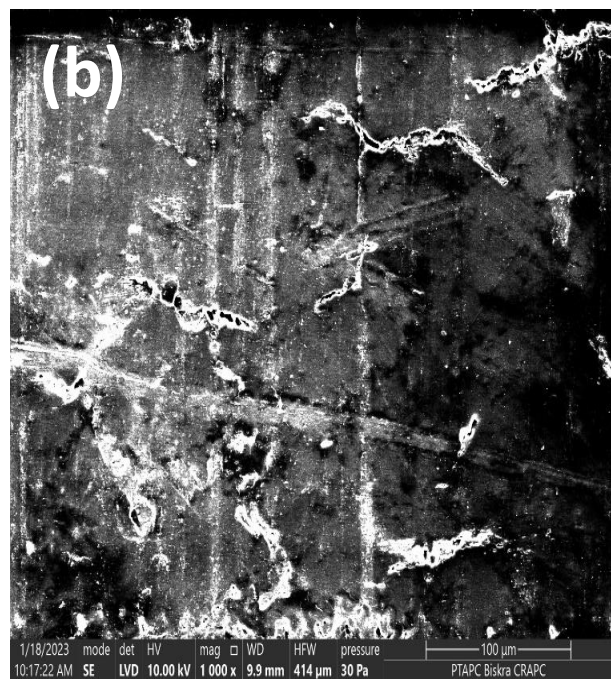
Fig III.3 (a) represents the SEM images of pure LLDPE after 360 days of weathering. The virgin LLDPEw presents a rough surface of the degraded sample. This is due to the formation of cracks and pits on the surface, which are the combined effects of UV radiation, oxygen, and water. Surface roughening increases dirt and grime adhesion, further accelerating the weathering process [5]. After the incorporation of 15% of fibers, Fig III.3 (b) shows the effect of natural weathering on the morphology of LLDPE/FUw. The micrograph shows a rough surface of the composite after 360 days and the formation of cracks, pits, and voids; it is worth noting that as the content of the fibers increased, more fungus colonized the surface of the samples, and larger pores were observed which can weaken the fiber and reduce its mechanical properties [6].

Natural weathering affects the morphological properties of LLDPE reinforced with FN and FNH shown in Fig III.3 (c) and 3 (d). The LLDPE/FNw and LLDPE/FNHw composites present more rough surfaces than the LLDPE/FUw composite, revealing that the surface cracks exposed the embedded fibers to the surface upon weathering [7]. The hygroscopic nature of PPF increased moisture absorption. It thus facilitated the formation of severe cracks in the composites. Thus, the fibers were easily seen, and the

detachment of PPF from the matrix proved that they had undergone degradation leading to poor fiber-matrix interactions.

The fibers treated with NaOH and Hydrogen peroxide also accelerate the degradation process of the composite due to a decrease in fiber diameter and an increase in surface roughness. These changes can weaken the fiber and make it more likely to break [8].

After one year of natural weathering exposure, the LLDPE/FNAw and LLDPE/FNHAw composites' appeared some small cracks on the surface, Fig III.3 (e), 3 (f). The extreme daily changes in temperature and humidity cause surface cracking on the composites. As can be seen, cracks can be found throughout the blend surface, indicating the occurrence of photo and thermal degradation. Generally, biodegradation of the composites is believed to result from a microbial attack on polymer chains in amorphous regions; weight loss then begins, followed by a deeper microbial invasion along with humidity leading to the extensive degradation of the material [8].



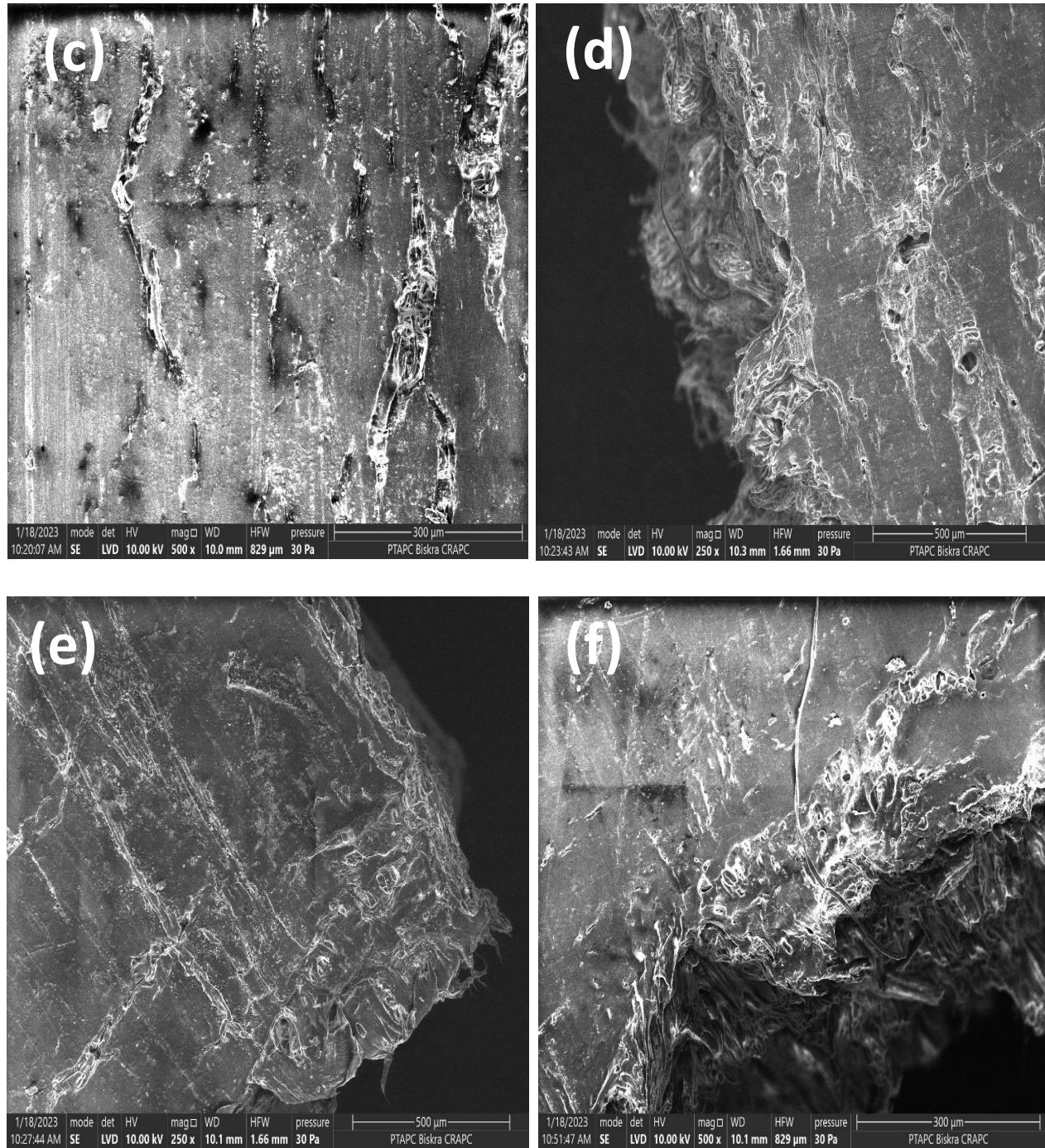


Figure III.3: SEM micrographs of neat LLDPE, treated and untreated composite (a) LLDPEw, (b) LLDPE/FUw, (c) LLDPE/FNw, (d) LLDPE/FNHw, (e) LLDPE/FNAw and (f) LLDPE/FNHAw

III.4. FTIR Spectroscopy

FTIR spectroscopy is a powerful tool for studying the degradation of composites. It can be used to track the changes in the functional groups of the composite as it degrades, which can provide insights into the degradation mechanism. The FTIR spectra of the pure linear low-density polyethylene LLDPE, treated and untreated LLDPE/PPF composites before and after one year of natural weathering aging are shown in Figure III.4. and III.5, respectively.

Generally, shows characteristic peaks at $3468\text{--}3093\text{ cm}^{-1}$ (stretching of hydroxyl groups OH), $2921\text{--}2852\text{ cm}^{-1}$ (stretching of CH and CH_2 groups), 1738 cm^{-1} (carbonyl group), 1650 cm^{-1} (hydroxyl groups of adsorbed water), 1472 cm^{-1} (bending of CH_2 groups), $1370\text{--}1329\text{ cm}^{-1}$ (bending vibration of CH and C-O groups), 1263 cm^{-1} (stretching of C-O groups), 1166 cm^{-1} (stretching vibration of C-O-C groups), $1045\text{--}1020\text{ cm}^{-1}$ (vinyl group), and $730\text{--}619\text{ cm}^{-1}$ (stretching vibration of CH and CH_2 groups).

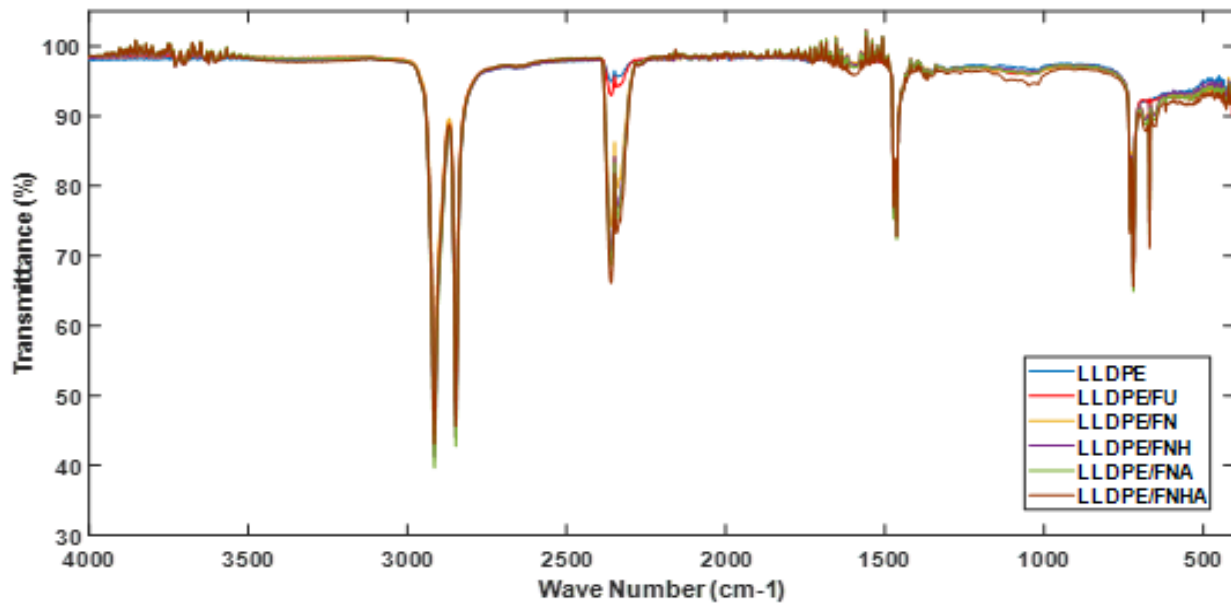


Figure III.4: FTIR spectra of neat LLDPE, treated and untreated composite before natural weathering

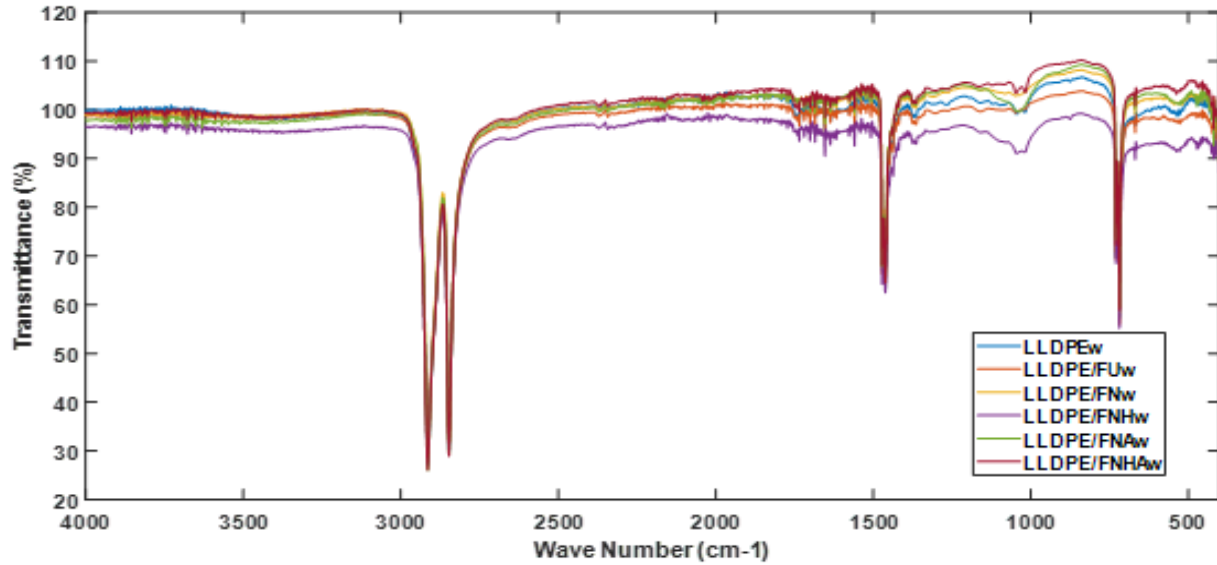


Figure III.5: FTIR spectra of neat LLDPE, treated and untreated composite after natural weathering

In other words, the FTIR spectra show that the pure LLDPE, treated, and untreated LLDPE/PPF composites all contain the same functional groups characteristic of these materials. Before weathering exposure, the spectra of the composites show some changes, but the characteristic peaks remain. The presence of these absorption bands in the composite spectrum indicates that the filler material is interacting with the LLDPE matrix. This interaction can improve the properties of the composite, such as its strength, stiffness, and toughness [9].

Figures III.6 (a, b), 7 (a, b) and 8 (a, b) represent the FTIR spectra of the composites recorded in regions $3600\text{--}3100\text{ cm}^{-1}$, $1800\text{--}1500\text{ cm}^{-1}$, and $1400\text{--}900\text{ cm}^{-1}$ before and after natural aging.

- In the $3600\text{--}3100\text{ cm}^{-1}$ region described in Figure III.6 (a) and 6 (b):

The O-H stretching peak in Fig III.6 (b) is higher than in Fig III.6 (a). This is likely due to hydroxyl groups produced when hydroperoxide and hydroxyl species are generated [10]. UV radiation is known to shorten the chain length of composites and form groups such as carbonyl, carboxyl, and hydroxyl. The appearance of the hydroxyl region in Fig III.6 (b) may be due to the O-H stretching of PPE exposed on the weathered composite surface [11].

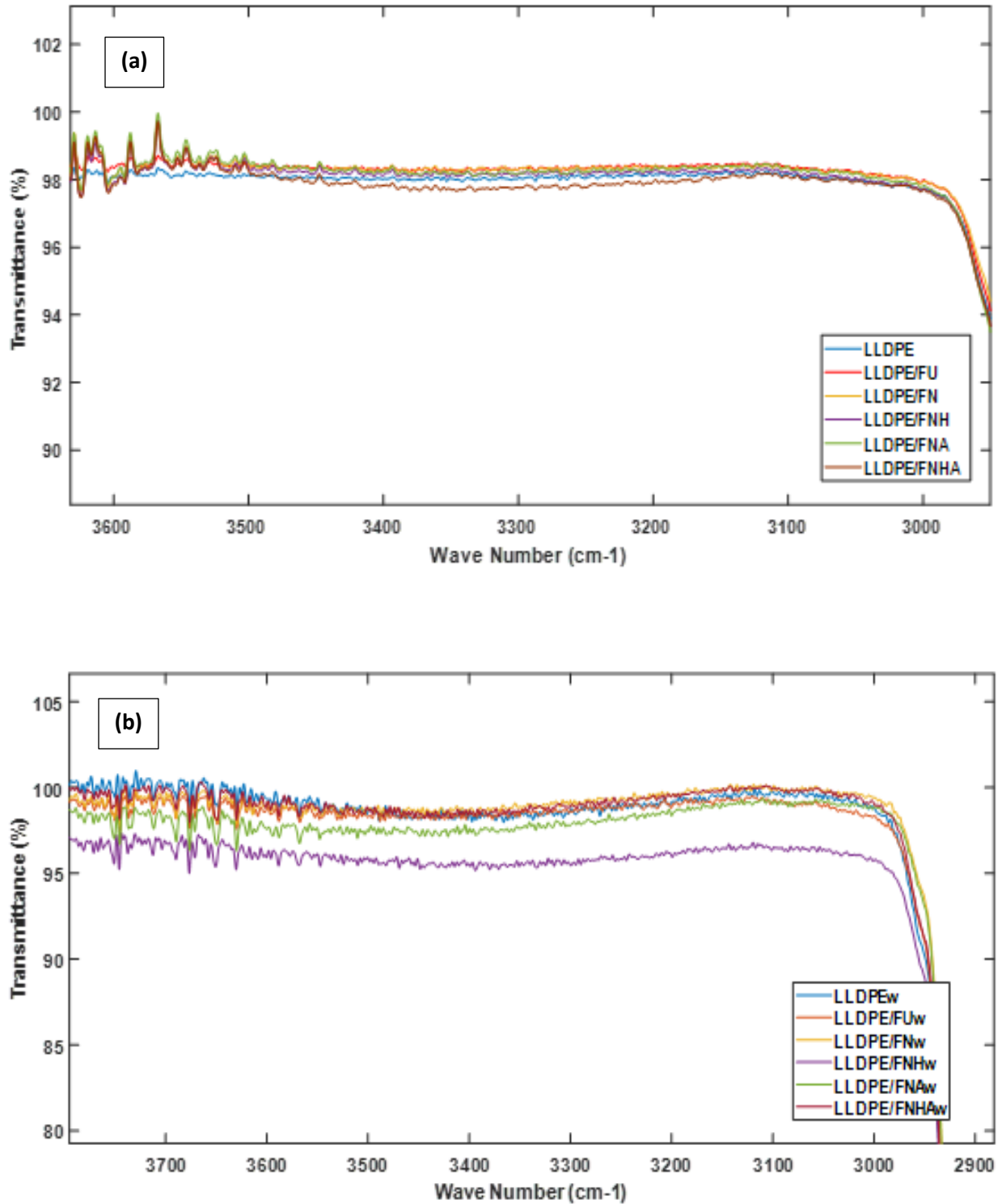


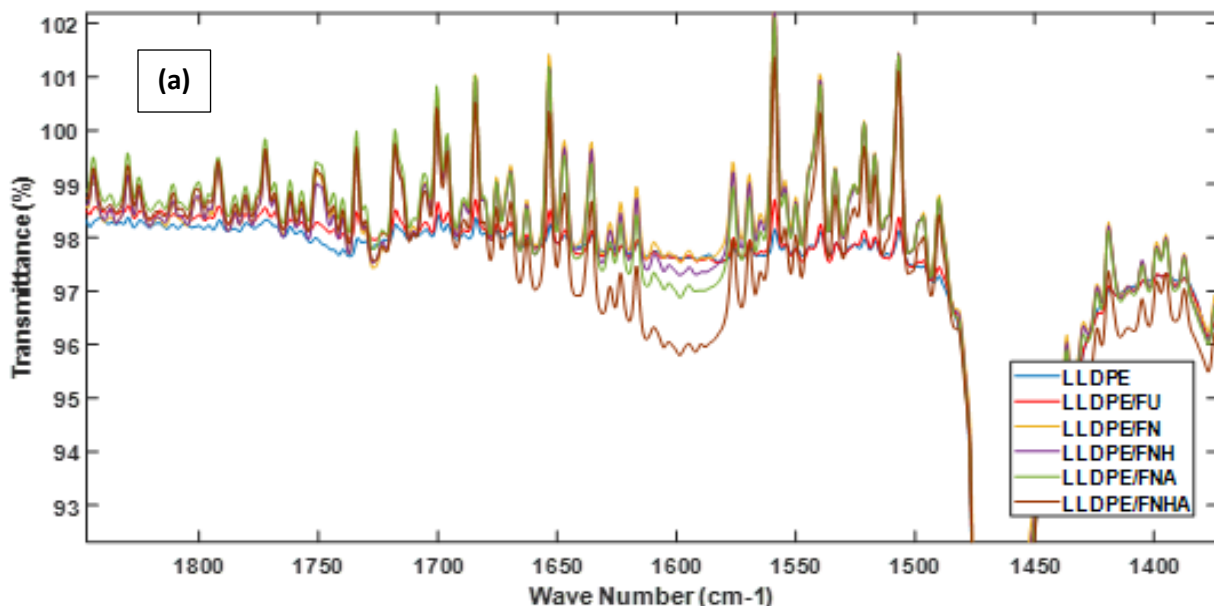
Figure III.6 : FTIR spectra of neat LLDPE, treated and untreated composite (a) before natural weathering and (b) after natural weathering in the 3600-3100 cm⁻¹ region

- In the 1800-1500 cm^{-1} region described in Figure III.7 (a) and 7 (b):

We notice in Fig III.7 (a) a reduction of the peaks in the stretching vibration of the C=O bond in carbonyl groups of hemicellulose and stretching vibration of the C=O bond stretching vibration of the C=C bond in aromatic lignin compounds. This peak is present in the spectra of treated and untreated LLDPE composites. However, the intensity of this peak is reduced in the spectra of treated composites LLDPE/FN and LLDPE/FNH. Also, we notice an augmentation of C=O peaks of acetyl groups in the composite LLDPE/FNA and LLDPE/FNHA.

As seen in Fig III.7 (b) after weathering, the peak intensity of the C=O carbonyl group increased in LLDPE/FUw and LLDPE/FNHw composite due to the oxidation of the surface [12]. In addition, it is evident that the characteristic peaks of cellulose, hemicellulose, or lignin of PPF decreased with prolonged weathering is probably attributed to PPF being detached from the exposed composite surfaces, as shown in the later surface morphology micrographs.

The formation of carbonyl groups after weathering confirms that photo-degradation took place and that the chemical structure of the composite was changed. As seen in Fig III.7 (b) compared to Fig III.7 (a), upon exposure to natural weathering, the band at 1738 cm^{-1} , attributed to C=O vibration, the intensities of the functional groups seem to be slightly higher, indicating more deterioration of the system. This is probably due to the presence of PPF in the composites, which increases the carbonyl functionality and makes the composites more susceptible to degradation [12, 13]. It is also worth noting that the band associated with C=O stretching vibrations resulted from carboxyl groups in the xylan components of hemicelluloses and the chemical groups of lignin.



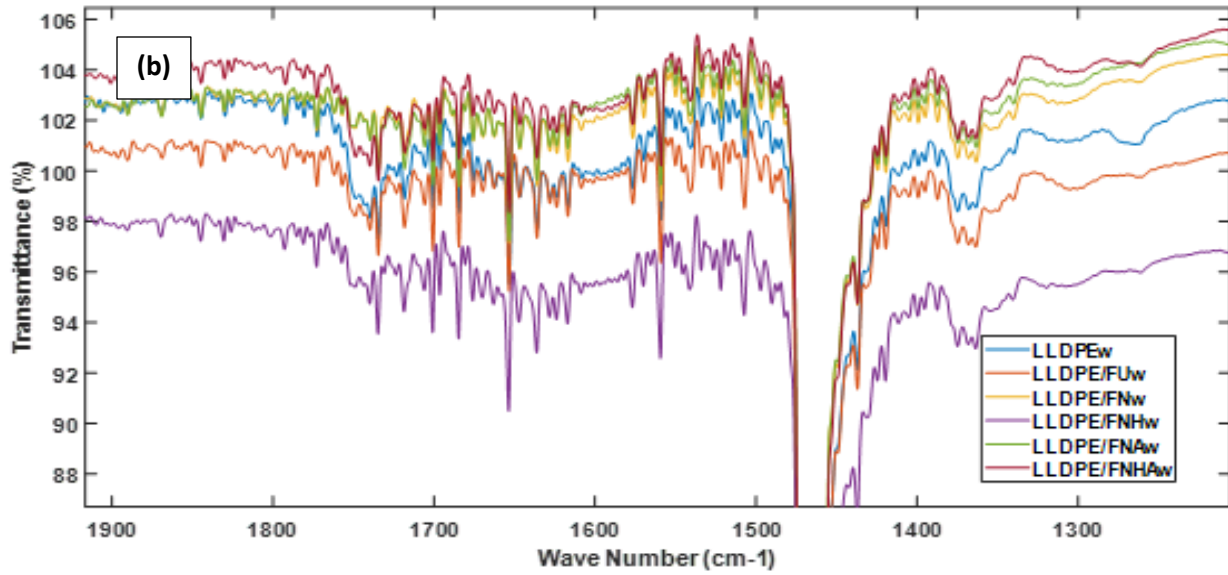


Figure III.7 : FTIR spectra of neat LLDPE, treated and untreated composite (a) before natural weathering and (b) after natural weathering in the 1800-1500 cm^{-1} region

- In the 1400-900 cm^{-1} region described in Figure III.8 (a) and III.8 (b):

By comparison, it can be seen that the intensity of the peak appearing at 1370 cm^{-1} assigned to C-O stretching (cellulose, hemicellulose, and lignin) becomes broader and stronger upon exposure to natural weathering.

The peaks at 1045 and 1020 cm^{-1} , as shown in Figs III.8 (a) and III.8 (b), which correspond to the vinyl group, seem to increase with weathering. This is likely due to UV light's scission of the LLDPE chains. The increase in the vinyl group concentration indicates that carbonyl degradation has occurred. However, the degradation of LLDPE/PPF composites may not be directly caused by the chain scission of the LLDPE matrix. It could also be due to the degradation of the PPF constituents. Parameswaranpillai et al [3] found that the formation of the vinyl group upon weathering results from carbonyl degradation due to polymer chain scission in both the matrix and the natural fiber. The formation of the vinyl group is usually delayed in the early stage of natural weathering. Still, it increases steeply as weathering time increases due to the degradation of the polymer matrix [14].

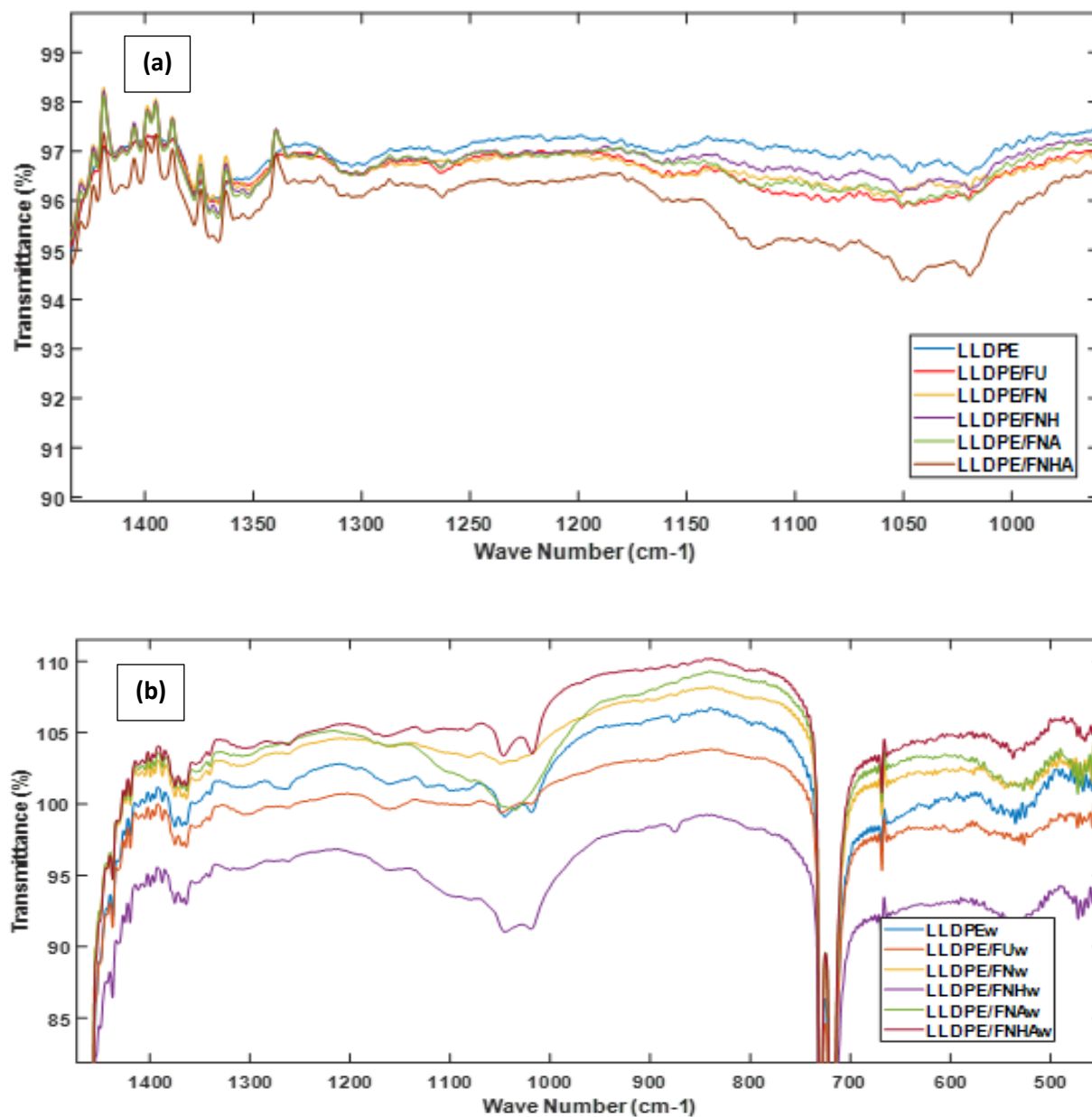


Figure III.8 : FTIR spectra of neat LLDPE, treated and untreated composite (a) before natural weathering and (b) after natural weathering in the 1400-900 cm⁻¹ region

In conclusion, the FTIR spectra of the treated composites are similar to those of the untreated samples, with the same absorption bands but different intensities. This suggests that both treated and untreated composites undergo the exact degradation mechanism. Therefore, it can be inferred that the treatment accelerates the degradation process.

III.5. Effect of natural weathering visual on the mechanical Properties

III.5.1. Tensile testing

III.5.1.1. Tensile strength

The evolution of the tensile strength of pure LLDPE, treated and untreated composites before and after one year of natural weathering is illustrated in Fig III.9. Which was reduced by 10% due to UV radiation and oxygen causing chain scission in the LLDPE molecules, decreasing tensile strength. Moisture also degrades the tensile strength of LLDPE by making it more susceptible to chain scission [15].

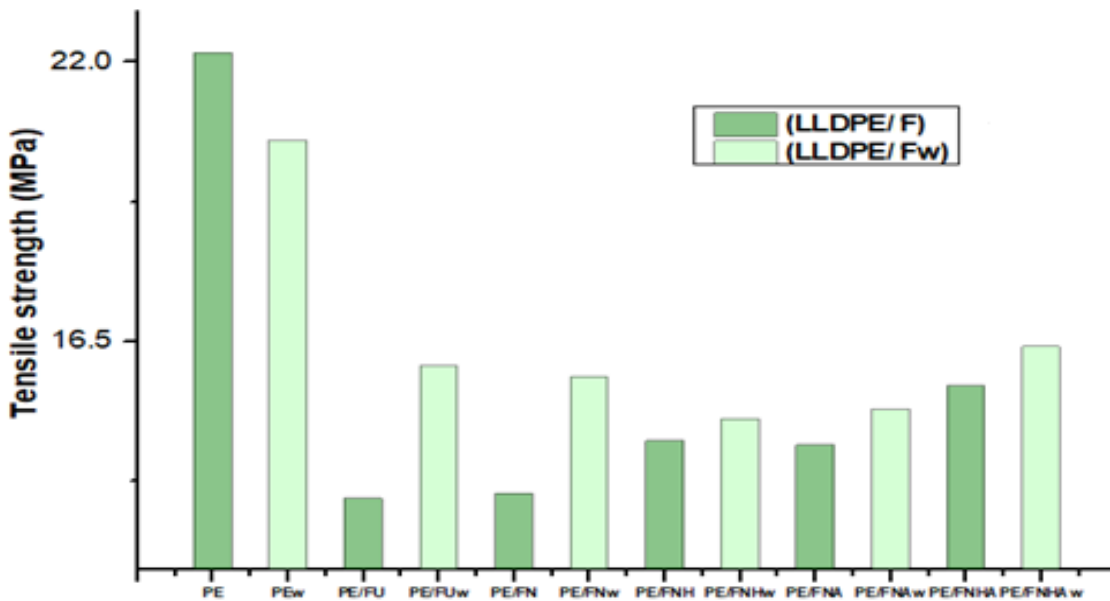


Figure III.9: Tensile strength of neat LLDPE and untreated composites before and after natural weathering

As described in the literature, natural fiber-reinforced composite materials show a faster loss of strength than other materials. However, this research showed an increase in the tensile strength of treated and untreated composite after one year of aging compared to composite before aging. The weathering process, which includes UV radiation and moisture, induces changes in a composite material's polymer matrix and fibers [16]. These changes affect the material's properties, such as its tensile strength. UV radiation causes the polymer matrix to undergo cross-linking, a chemical reaction that creates stronger bonds between the polymer chains. This cross-linking increases the tensile strength of the composite. The fibers also undergo fibrillation, which is the splitting of the fibers into smaller fibers. This also increases the composite's strength, as the smaller fibers have a higher surface area-to-volume ratio and better interlock with the polymer matrix. Weathering causes the natural fibers in the composite to recrystallize, which is a process that rearranges the fiber's molecular structure [17]. This recrystallization increases the tensile strength of the

fiber. It is important to note that the increase in tensile strength after one year of weathering is only sometimes observed. The extent of the increase will depend on several factors, including the type of natural fibers used, the type of polymer matrix used, and the weathering conditions [18].

Overall, the effect of weathering on the tensile strength of composite-reinforced natural fibers is complex and depends on some factors. In some cases, the tensile strength can increase after one year of weathering, while in others, it decreases.

III.5.1.2. Young's modulus

The evolution of Young's modulus of pure LLDPE, treated and untreated composites before and after one year of aging is illustrated in Figure III.10. It is noted that the modulus increases in pure LLDPE_w, LLDPE/FN_w, LLDPE/FNA_w, and LLDPE/FNHA_w with (506.327, 653.6785, 619.9423, 498.4601, 566.3519, and 584.1809 MPa), respectively; this increase is due to the increase in crystallinity analysis. According to [19, 20], The fibers and matrix in a composite material are typically held together by weak van der Waals forces. However, when the composite material is exposed to water and oxygen, these forces can be replaced by stronger chemical bonds. This will also increase the stiffness of the composite material. Chemical degradation would be manifested by chain breaks leading to increased crystallinity, increasing Young's modulus.

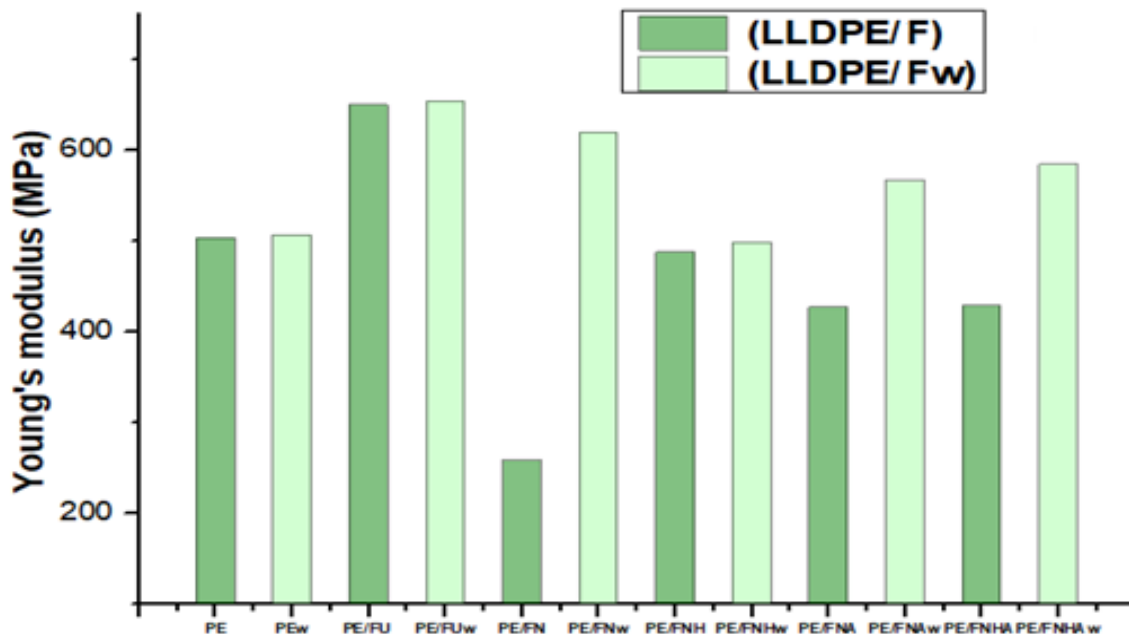


Figure III.10 : Young's modulus of neat LLDPE and untreated composites before and after natural weathering

Reference

- [1] B. Alshammari, O. Alothman, A. Alhamidi, M. Jawaid, and H. Shaikh, "Effect of Accelerated Weathering on the Thermal, Tensile, and Morphological Characteristics of Polypropylene/Date Nanofiller Composites," *Materials*, vol. 15, p. 6053, 09/01 2022.
- [2] C. Ganesan, M. Chandrasekar, M. Nisha, and S. Subha, "Effect of Compatibilizer on the Aging and Degradation Mechanism of the Natural Fiber-Reinforced Thermoplastic Composites," in *Aging Effects on Natural Fiber-Reinforced Polymer Composites: Durability and Life Prediction*, ed: Springer, 2022, pp. 51-61.
- [3] J. Parameswaranpillai, J. Jacob, M. Dominic CD, C. Muthukumar, S. M. K. Thiagamani, A. Jayakumar, *et al.*, "Effect of Water Absorption on the Tensile, Flexural, Fracture Toughness and Impact Properties of Biocomposites," *Aging Effects on Natural Fiber-Reinforced Polymer Composites: Durability and Life Prediction*, pp. 35-50, 2022.
- [4] M. Ramesh, L. Rajeshkumar, D. Balaji, and V. Bhuvaneswari, "Influence of Moisture Absorption on Mechanical properties of Biocomposites reinforced Surface Modified Natural Fibers," in *Aging Effects on Natural Fiber-Reinforced Polymer Composites: Durability and Life Prediction*, ed: Springer, 2022, pp. 17-34.
- [5] A. Vedralnam, D. Gunwant, H. Verma, and K. Kalauni, "Effect of Aging and UV Exposure on Mechanical Properties of Natural Fiber Composites," *Aging Effects on Natural Fiber-Reinforced Polymer Composites: Durability and Life Prediction*, pp. 189-217, 2022.
- [6] M. Ramesh, M. Tamil Selvan, and K. Niranjana, "Hygrothermal Aging, Kinetics of Moisture Absorption, Degradation Mechanism and Their Influence on Performance of the Natural Fibre Reinforced Composites," in *Aging Effects on Natural Fiber-Reinforced Polymer Composites: Durability and Life Prediction*, ed: Springer, 2022, pp. 257-277.

- [7] J. J. Andrew and H. Dhakal, "Influence of Seawater Ageing on the Physical and Mechanical Properties of the Natural Fiber-Reinforced Composites," in *Aging Effects on Natural Fiber-Reinforced Polymer Composites: Durability and Life Prediction*, ed: Springer, 2022, pp. 335-355.
- [8] T. Akderya, C. Bilir, and B. O. Baba, "Effects of Natural Weathering on Aesthetics, Thermal and Mechanical Properties of the Bio-composites," in *Aging Effects on Natural Fiber-Reinforced Polymer Composites: Durability and Life Prediction*, ed: Springer, 2022, pp. 137-157.
- [9] A. E.-A. A. El-Wakil, H. Moustafa, and A. M. Youssef, "Antimicrobial low-density polyethylene/low-density polyethylene-grafted acrylic acid biocomposites based on rice bran with tea tree oil for food packaging applications," *Journal of Thermoplastic Composite Materials*, vol. 35, pp. 938-956, 2022.
- [10] A. Fairbrother, H.-C. Hsueh, J. H. Kim, D. Jacobs, L. Perry, D. Goodwin, *et al.*, "Temperature and light intensity effects on photodegradation of high-density polyethylene," *Polymer Degradation and Stability*, vol. 165, pp. 153-160, 2019/07/01/ 2019.
- [11] G. Grause, M.-F. Chien, and C. Inoue, "Changes during the weathering of polyolefins," *Polymer Degradation and Stability*, vol. 181, p. 109364, 2020/11/01/ 2020.
- [12] C. Ihamouchen, H. Djidjelli, A. Boukerrou, S. Krim, M. Kaci, and J. Martinez, "Effect of surface treatment on the physicomechanical and thermal properties of high-density polyethylene/olive husk flour composites," *Journal of applied polymer Science*, vol. 123, pp. 1310-1319, 2012.
- [13] N. Nurazzi, M. Asyraf, M. Rayung, M. Norrrahim, S. Shazleen, M. Rani, *et al.*, "Thermogravimetric analysis properties of cellulosic natural fiber polymer composites: A review on influence of chemical treatments," *Polymers*, vol. 13, p. 2710, 2021.
- [14] N. A. M. Nasharudin, N. F. Sulaiman, N. A. Mohammad, W. N. R. WAN JAAFAR, and S. N. Surip, "The Effect of Heat Treatment and Chemical Treatment on Natural Fibre to The Durability of Wood Plastic Composites—A Review," *Journal of Materials Exploration and Findings (JMEF)*, vol. 2, p. 1.
- [15] A. Joseph, V. Mahesh, V. Mahesh, D. Harursampath, and M. Loja, "Effects of Hygrothermal Aging on the Mechanical Properties of the Biocomposites," in *Aging Effects on Natural Fiber-Reinforced Polymer Composites: Durability and Life Prediction*, ed: Springer, 2022, pp. 63-83.

- [16] J. B. Moreira, S. G. Kuntzler, C. K. da Silva, J. A. V. Costa, and M. G. de Morais, "Degradation Effects on the Mechanical and Thermal Properties of the Bio-Composites Due to Accelerated Weathering," in *Aging Effects on Natural Fiber-Reinforced Polymer Composites: Durability and Life Prediction*, ed: Springer, 2022, pp. 159-172.
- [17] M. Tuasikal, O. Alothman, M. Luqman, S. al-zahrani, and M. Jawaid, "Influence of Natural and Accelerated Weathering on the Mechanical Properties of Low-Density Polyethylene Films," *International Journal of Polymer Analysis and Characterization*, vol. 19, 04/03 2014.
- [18] H. Demir, D. Balköse, and S. Ülkü, "Influence of surface modification of fillers and polymer on flammability and tensile behaviour of polypropylene-composites," *Polymer Degradation and Stability*, vol. 91, pp. 1079-1085, 2006.
- [19] C. M. Chan, S. Pratt, and B. Laycock, "Effects of Natural Weathering on Aesthetics, Thermal and Mechanical Properties of Completely Biodegradable Composites," in *Aging Effects on Natural Fiber-Reinforced Polymer Composites: Durability and Life Prediction*, ed: Springer, 2022, pp. 173-188.
- [20] T. Ratanawilai and K. Taneerat, "Alternative polymeric matrices for wood-plastic composites: Effects on mechanical properties and resistance to natural weathering," *Construction and Building Materials*, vol. 172, pp. 349-357, 2018.

General Conclusion

General Conclusion

Recent decades have been marked in the field of materials by the remarkable evolution of composites based on natural fibers, which are increasingly used in exterior and structural applications, particularly in construction, covering, and packaging. This doctoral project is part of a broad theme aimed at developing biocomposites reinforced by lignocellulosic fibers produced when the palm is present in significant quantities. The extraction of these bio-reinforcements or surface modifications remains essential. Thus, one of the priority challenges to be met currently is to find environmentally irreproachable ways and means for these purposes while controlling the cost of production.

The main goal of this thesis was to set up a process for successive treatment of palm petiole fiber for surface modification of these fibers. More specifically, it was a question of:

How do the NaOH and hydrogen peroxide treatments and acetylation treatment affect the properties of palm petiole fibers and their interaction with LLDPE? And can these composites withstand external environmental factors?

linear low-density polyethylene /petiole fiber composite mixtures (15 and 25%) were prepared by mono-screw extrusion. Firstly, we were particularly interested in the adhesion problem to the fiber/matrix interface. We were particularly interested in the adhesion problem to the fiber/matrix interface. Furthermore, we chose three modes of successive treatment. The first treatment consists of modifying the petiole fibers by mercerization, the second is blanching by hydrogen peroxide, and the final treatment is acylated with acetic anhydride. Several characterization techniques collected as much information as possible on the treated and untreated petiole fiber and processed on the different composites developed and studied the effect of natural weathering on the properties of LLDPE composite reinforced with palm petiole fibers.

The results of FTIR spectroscopy of treated and untreated palm petiole fiber reveal that the mercerization reaction was confirmed by the decrease in the absorption band of the OH groups located at 3340 cm^{-1} . The disappearance of the absorption bands at 1723 cm^{-1} and 1224 cm^{-1} corresponds to the C=O and C-O bonds of the acetyl group of hemicelluloses and the C-O-C bond of lignin, respectively. FTIR spectra revealed that the two-step modification method (alkaline and blanching) in palm petiole fibers (FN, FNH) has a more critical ability to remove non-cellulosic materials, particularly lignin. For petiole fiber treated with acetic anhydride, the results of the IRTF analysis made it possible to confirm the acetylation reaction, confirmed by the pairing of a band absorption in the region between 1723 and 1238 cm^{-1} , characteristic of axial deformation of (C=O)-O and C=O from acetyl groups.

General Conclusion

The SEM results show that the alkaline treatment removes impurities such as hemicellulose, lignin, and pectin, which enhances adhesion to the polymer matrix. It also causes the fiber to swell and become more flexible, increasing its surface area and flexibility. Hydrogen peroxide treatment removes the cuticle (waxy layer) from the fiber surface and opens the fiber lumen, allowing water and other molecules to penetrate the fibers. This results in decreased fiber diameter and a change in the fiber surface morphology. Acetylation treatment replaces the hydrogen atoms in the hydroxyl groups of the fiber cell membrane with acetyl groups. This reduces the fiber's polarity, removes waxy material from the surface, and causes the fiber diameter to increase slightly. It also reduces the roughness of the fiber surface and increases the fiber's crystallinity.

The ATG, DTG, and DSC thermograms show that treated petiole fibers are more thermally stable than untreated fiber. These surface modifications play a major role in the bond between the matrix and the filler during the development of composite materials.

SEM images confirmed the behavior of untreated and treated fibers in composites. The interfacial interaction between the fibers-matrix was improved after treatment. The LLDPE/FNHA composite had better interfacial bonding, homogeneity, and fiber distribution than the other fiber composites, which resulted from removing the amorphous material from the fiber surface after chemical treatments.

The thermal analysis showed that incorporating the fiber into the LLDPE matrix augments the temperature at which decomposition begins, and the successive treatment of fiber makes a composite more stable and more biodegradable.

The treated fibers substantially impact the composite's hardness by adding stiffness to the polymer. usually results in an improvement in the mechanical properties, which was observed in LLDPE/FNA and LLDPE/FNHA composites, which provided 108% and 116% increases in tensile strength, respectively, in comparison to other composites. The higher stiffness and good fiber-matrix bonding of the composite decreased the molecular mobility of LLDPE, indicating a greater capacity to store energy, resulting in a high storage modulus in treated composites LLDPE/FN and LLDPE/FNA. At elevated temperatures, the loss modulus of the LLDPE/FNHA composite was slow due to the fiber preventing the polymer from free mobility. The higher $\tan \delta$ was found for pure LLDPE, and reinforced composites have lower energy dissipation coefficients; composite damping has been significantly reduced due to polymeric chains connected to the petiole fibers.

The molecular structure, mechanical properties, and shape of LLDPE/PPFw composites changed after exposure to natural weathering for one year. SEM images clearly show that the degradation is severe with aging and characterized by significant damage. Furthermore, by FTIR spectroscopy analysis, we noticed the formation of various oxidation products, mainly in the hydroperoxide and carbonyl regions. Young's

General Conclusion

modulus would increase if the crystallinity rate went up because the amorphous parts of the LLDPEw would rearrange themselves as it breaks down in chain scission reactions.

Finally, this study suggests that palm petiole fibers reinforce linear low-density polyethylene (LLDPE). Using natural fiber-reinforced composites in engineering is intelligent because they have the same mechanical properties as synthetic fibers and lower environmental effects. The scientific researcher must also do more to stimulate and support using natural fibers improved in polymeric materials, which may be employed with a high potential for several applications. NFC is currently being employed in electronics and sports equipment in ways that will help them gain a significant market share.

Appendices

Mechanical analysis

a. Tensile testing

Sample	Tensile strength	Young's modulus
LLDPE	22.18094	503.3858
LLDPE/FU 15%	13.4	649.80247
LLDPE/FN 15%	13.50483	258.33
LLDPE/FNH 15%	14.54246	487.62963
LLDPE/FNA 15%	14.45742	426.90693
LLDPE/FNHA 15%	15.6179	428.46914
LLDPE/FU 25%	12.46311	756.61728
LLDPE/FN 25%	11.74641	522.58333
LLDPE/FNH 25%	12.91832	532.9188
LLDPE/FNA 25%	13.15885	544.82716
LLDPE/FNHA 25%	13.14871	542.20133

Sample	Tensile strength	Young's modulus
LLDPE _w	20.45001	506.327
LLDPE/FU _w 15%	16.00541	627.6785
LLDPE/FN _w 15%	15.79848	619.9423
LLDPE/FNH _w 15%	14.97147	468.4601
LLDPE/FNA _w 15%	15.15567	566.3519
LLDPE/FNHA _w 15%	16.39186	584.1809

b. Flexural testing

Sample	Flexural strength	Flexural modulus
LLDPE	12.8639	5882.556
LLDPE/FU 15%	15.556	3198.889
LLDPE/FN 15%	16.17834	6723.389
LLDPE/FNH 15%	15.28147	2256
LLDPE/FNA 15%	15.94595	1472
LLDPE/FNHA 15%	15.95739	7690.333
LLDPE/FU 25%	16.05716	4749.833
LLDPE/FN 25%	17.23641	4870.889
LLDPE/FNH 25%	17.40191	3999.667
LLDPE/FNA 25%	17.02352	2188.556
LLDPE/FNHA 25%	17.02592	5173.889

c. Hardness

Sample	D1	D2	D3	D4	D5	D6	Average
LLDPE	98.2	96.9	96.7	98.2	97.9	99.6	97.91667
LLDPE/FU 15%	95.3	97.1	98.6	97.9	98.1	95.5	97.08333
LLDPE/FN 15%	96.9	95.8	98.9	97.8	96.3	98.7	97.4
LLDPE/FNH 15%	95.6	98.5	96.2	98.9	96.3	98.7	97.36667
LLDPE/FNA 15%	96.5	97	97.9	98.9	96	98.7	97.5
LLDPE/FNHA 15%	97.2	96.2	98.2	98.1	97.7	97.8	97.53333
LLDPE/FU 25%	97.3	98	98.7	97.5	98.8	98.8	98.18333
LLDPE/FN 25%	97	97.6	97.8	97.7	96.6	98.8	97.58333
LLDPE/FNH 25%	94.5	95.3	97.3	98.3	97.9	98.5	96.96667
LLDPE/FNA 25%	97.4	97.3	98.6	95.2	96.2	96.8	96.91667
LLDPE/FNHA 25%	96.9	96.4	98.1	97.9	97.8	96.5	97.26667